THE IMPACT OF FDG-PET/CT ON TREATMENT INDIVIDUALISATION IN NSCLC

EDWIN USMANIJ

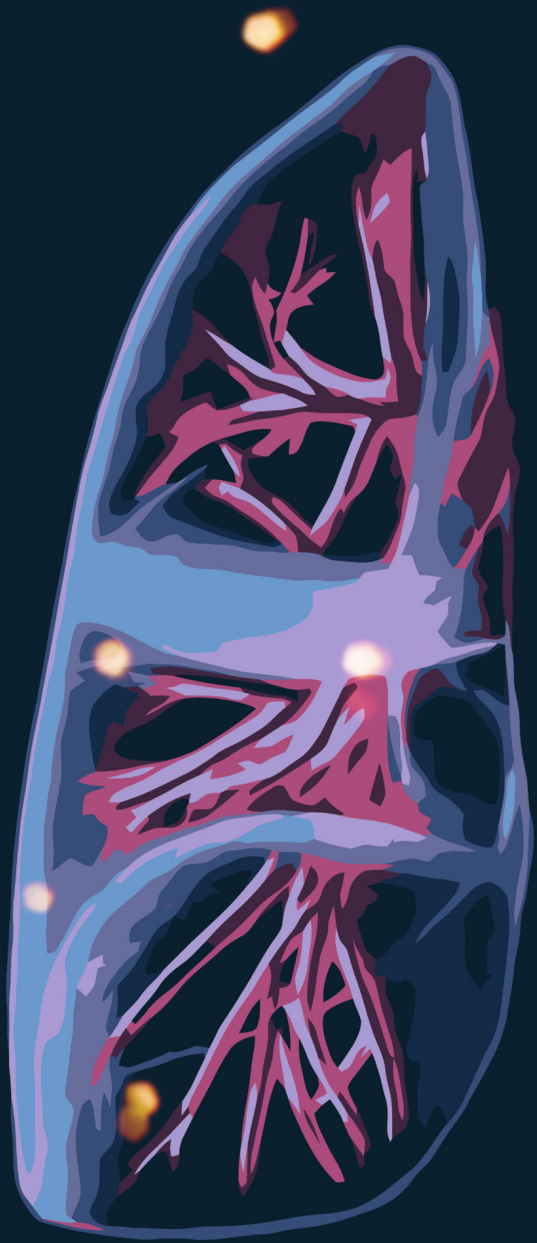

The impact of FDG-PET/CT on treatment individualisation in NSCLC

Edwin Usmanij

The impact of FDG-PET/CT on treatment individualisation in NSCLC

Colofon

The research presented in this thesis was conducted at the Institute of Health Sciences of the Radboud University Medical Centre Nijmegen. Printing of this thesis was financially supported by Radboud University Medical Centre Nijmegen. Due to consistency reasons, the language (British-English) has been standardised throughout the text of this thesis and therefore may slightly differ in respect to the text in the published articles.

ISBN: 978-94-028-1614-3
Cover design: E.A. Usmanij
Printing: Ipskamp Printing BV, Enschede

The impact of FDG-PET/CT on treatment individualisation in NSCLC

Proefschrift

ter verkrijging van
de graad van doctor aan de Radboud Universiteit Nijmegen
op het gezag van de rector magnificus
prof. dr. J.H.J.M. van Krieken,
volgens besluit van het college van decanen
in het openbaar te verdedigen op vrijdag 4 oktober 2019 om 10:30 uur precies

door

Edwin Arthur Usmanij
geboren op 29 juni 1988 te Tiel

Promotoren:

Prof. dr. L.F. de Geus-Oei (Universiteit Leiden)

Prof. dr. J. Bussink

Prof. dr. W.J.G. Oyen

Manuscriptcommissie:

Prof. dr. C.M.L. van Herpen

Prof. dr. E.F.I. Comans (Amsterdam UMC)

Prof. dr. M. van den Heuvel

The impact of FDG-PET/CT on treatment individualisation in NSCLC

Doctoral Thesis

to obtain the degree of doctor
from Radboud University Nijmegen
on the authority of the Rector Magnificus prof. dr. J.H.J.M. van Krieken,
according to the decision of the Council of Deans
to be defended in public on Friday, October 4, 2019
at 10.30 hours

by

Edwin Arthur Usmanij
born on June 29, 1988 in Tiel (the Netherlands)

Supervisors:

Prof. dr. L.F. de Geus-Oei (Leiden University)
Prof. dr. J. Bussink
Prof. dr. W.J.G. Oyen

Doctoral Thesis Committee:

Prof. dr. C.M.L. van Herpen
Prof. dr. E.F.I. Comans (Amsterdam UMC)
Prof. dr. M. van den Heuvel

to my parents

TABLE OF CONTENTS

CHAPTER I

General introduction and thesis outline

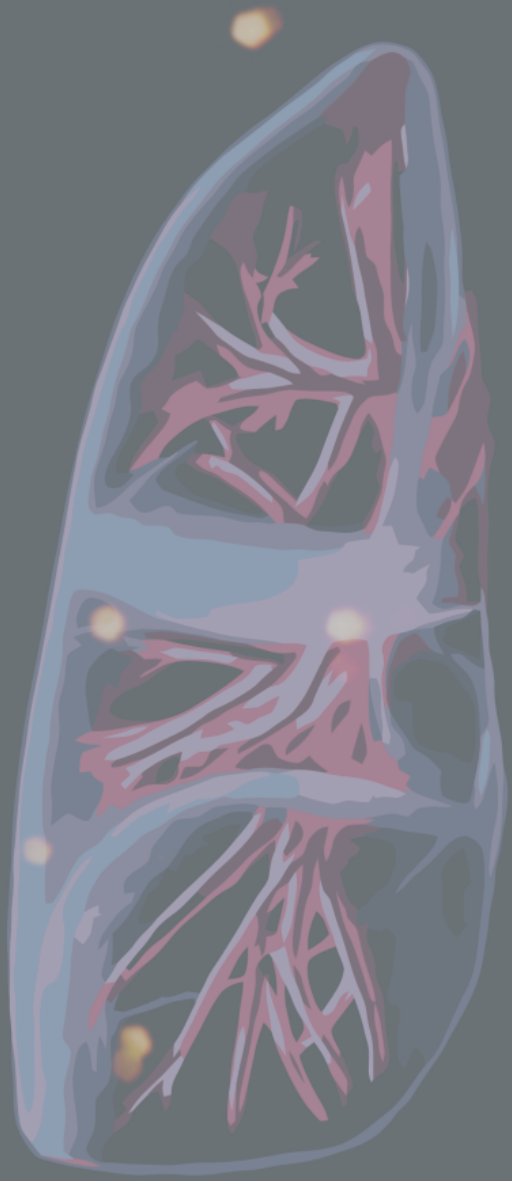

1

Lung cancer, a global health concern

Cancer poses a major burden to society worldwide. Due to significant improvements in the treatment and prevention of cardiovascular diseases, cancer has become the number one cause of death in Europe and the USA. Lung cancer is a common type of cancer and with nearly 2.09 million new cases of lung cancer worldwide, showing a high case fatality and the highest absolute mortality of all cancer types (1). Non-small cell lung cancer (NSCLC) is the most common histological type of lung cancer and accounts for 87% of all lung cancers. When fit for surgery, patients with early-stage NSCLC (stage I and stage II) can be treated with curative surgery as the initial modality with a 5-year survival rate of 80%. However, a substantial number of patients (~78%) present with advanced (stage III) or metastatic disease (stage IV) with a dismal prognosis. For locally advanced NSCLC the standard of care is concurrent platinum-based chemotherapy and radiotherapy up to 60–66 Gy, with the recent addition of adjuvant immunotherapy (2). In stage IV disease palliative chemotherapy is the cornerstone of treatment. For a significant number of patients, the treatment is unlikely to succeed and is associated with low survival rates (5-y) of less than 10%.

Personalised medicine in NSCLC

In the past, the treatment of NSCLC followed a 'one size fits all' approach deriving treatment options from tumour stage and performance score. However, it is increasingly recognised that NSCLC is a heterogeneous and complex disease, being subdivided into histological type to optimise chemotherapeutic strategies. With targeted therapies focused on oncogenes (i.e., epidermal growth factor receptor, anaplastic lymphoma kinase) the treatment options for subgroups of NSCLC have expanded considerably (3-9), but they benefit only a minority of patients. It remains challenging to identify patients who may benefit from radiotherapy, chemotherapy or immunotherapy. Currently, with overall low response rates of 40% in all NSCLC patients, most patients will eventually relapse. Due to an initial intrinsic resistance or resistance after initial treatment, the prescribed treatment will fail to either induce disease regression or slow down disease progression. Possibly, a significant number of patients will undergo toxic side effects without a benefit from treatment. As treatment becomes more individualised, early identification of responders and non-responders is increasingly important to optimise treatment and to minimise the toxicity of ineffective treatment in patients. This drives the need for identification of predictive factors for tumour response at an early stage during therapy and this is fundamental for cancer treatment adaptation and individualisation. Identification of early, in-treatment predictive factors would enable faster adaptation of therapy. This could

improve patient management by avoiding unnecessary side effects and could reduce the costs of ineffective treatment. Traditionally, the evaluation of the effectiveness of treatment is performed by imaging after the treatment has been given, when potentially ineffective treatment is already completed. The implementation of morphological measurements for response monitoring led to response criteria in solid tumours (RECIST) (10) and is often used to monitor the cytotoxic effects of therapy on malignancies. A therapy-induced reduction of tumour size is measured with computed tomography (CT) and is based on the percentage reduction in 'target lesions' and it includes a definition of complete response, partial response, stable disease and progressive disease. However, for early, in-treatment evaluation, tumour volume is an unreliable marker of response. One limitation is that non-malignant tissue components (e.g. atelectasis, fibrosis) contribute to the apparent tumour volume. Another limiting factor is the timing of CT, as response rates may vary and markedly CT evaluation is advised to be established as early as 6-8 weeks after the start of treatment (11). Since some targeted therapies may show a cytostatic rather than a cytoreductive response, especially in those cases, successful treatment may not result in a decrease of tumour size.

For optimal management of response to treatment, it is essential to have an evaluation as early as is feasible. For this purpose, instead of morphological imaging with CT, molecular imaging with ^{18}F-fluoro-deoxy-glucose positron emission tomography/computed tomography (FDG-PET/CT) could be used to evaluate therapy-induced changes in glucose metabolism during treatment (12).

For staging, the introduction of FDG-PET/CT has improved detection of lymph node metastases and distant metastases and has become part of the standard of care in lung cancer, as well as many other types of cancer. ^{18}F-Fluoro-2-Deoxy-2-D glucose is a glucose analogue radiolabelled with ^{18}F that is transported by glucose transporters (predominantly GLUT-1) over the cell membrane and is phosphorylated by hexokinase to FDG-6-phosphate. Since FDG-6-phosphate cannot be catabolised further intracellularly, it is trapped. Since cancer cells tend to favour metabolism via anaerobic glycolysis over oxidative phosphorylation (the Warburg effect), it results in higher net glycolysis. Based on this principle, with PET it is possible to characterise indeterminate lesions and to detect malignant lymph nodes and distant metastases.

The use of FDG-PET/CT is not only limited to initial staging and restaging but can also be used for (early) in-treatment response evaluation. One advantage is that change in cellular glucose metabolism may be faster during treatment than tumour size. Possibly the treatment evaluation can be brought forward to be performed before treatment is completed, even before any significant changes in size have occurred. With serial FDG-PET/CT studies it is possible to measure metabolic changes during treatment,

enabling analysis of subsequent treatment effects and ultimately capturing intrinsic mechanisms of resistance to treatment and treatment-induced resistance.

The feasibility of serial FDG-PET/CT for treatment response to chemotherapy has been widely evaluated (13) and has led to several initiatives for response monitoring studies with FDG-PET/CT. One benefit is that FDG-PET/CT provides an opportunity to investigate in a non-invasive way the biology of cancer in vivo, in a whole-body approach (and not only a single lesion). This holds true for patients with multiple metastases in whom pathological characterisation is limited to one or a few lesions. These harbours the inherent risk of sampling error, intra-tumour heterogeneity and inter-tumour heterogeneity.

The ability of FDG-PET/CT to indirectly assess the molecular mechanisms involved in the tumour process make it a valuable tool. The basis of metabolic imaging is that therapy response can be quantified due to an alteration in oncogenic signalling that (indirectly) affects glucose metabolism.

A decrease in glucose metabolism may reflect the cytotoxic effects and a loss of viable cells associated with effective treatment. On the other hand, a persistent increased FDG-uptake is associated with treatment resistance. Consequently, especially patients with metabolic disease progression may benefit from an early change of treatment to a more effective treatment. Therefore, FDG-PET/CT seems a suitable non-invasive tool for response evaluation and prediction of response and patient outcome.

Outline of the Thesis

FDG-PET/CT is considered as the standard of care in the work-up and management of NSCLC. In **Chapter II** the clinical impact of FDG-PET/CT on the guidance of invasive diagnostic procedures, staging and therapy selection is highlighted. The predictive performance of FDG-PET/CT of treatment response is discussed. For treatment personalisation **Chapter III** describes the predictive value of FDG-PET/CT in locally advanced NSCLC patients treated with concurrent chemoradiotherapy. Early, in-treatment evaluation performed after two weeks of treatment was correlated with the reduction of FDG-uptake expressed as total lesion glycolysis (TLG, the product of SUV and metabolic tumour volume). The predictive performance of FDG-PET/CT was further discussed in **Chapter IV**. In **Chapter V** FDG-PET/CT image derived indices are discussed and the different techniques for (automatic) image segmentation algorithms for segmentation of the metabolic active tumour volume. Also, the aggregation process of inclusion of the primary tumour alone versus a whole-body TLG approach (with affected lymph nodes) is evaluated. Apart from staging, FDG-PET/CT is frequently used in radiation oncology to optimise the radiation fields. In **Chapter VI**, early, in-treatment FDG-PET/CT is used to direct treatment to the more treatment-resistant subvolumes of the tumour, based on

persistent FDG-uptake. The feasibility of a stereotactic boost is evaluated in this planning study. In **Chapter VII** early in-treatment response monitoring with FDG-PET/CT was studied in inoperable stage III or stage IV patients treated with chemotherapy and bevacizumab. In **Chapter VIII** differences in histological subtype and gender differences, concerning metastatic patterns, are studied in a nationwide autopsy study in NSCLC. In **Chapter IX** the general discussion and future prospects are provided.

References

1. Siegel RL, Miller KD, Jemal A. Cancer statistics, 2019. CA: a cancer journal for clinicians. 2019;69(1):7-34.
2. Antonia SJ, Villegas A, Daniel D, Vicente D, Murakami S, Hui R, et al. Overall Survival with Durvalumab after Chemoradiotherapy in Stage III NSCLC. The New England journal of medicine. 2018;379(24):2342-50.
3. Brahmer J, Reckamp KL, Baas P, Crino L, Eberhardt WE, Poddubskaya E, et al. Nivolumab versus Docetaxel in Advanced Squamous-Cell Non-Small-Cell Lung Cancer. The New England journal of medicine. 2015;373(2):123-35.
4. Gandhi L, Rodriguez-Abreu D, Gadgeel S, Esteban E, Felip E, De Angelis F, et al. Pembrolizumab plus Chemotherapy in Metastatic Non-Small-Cell Lung Cancer. The New England journal of medicine. 2018;378(22):2078-92.
5. Hellmann MD, Ciuleanu TE, Pluzanski A, Lee JS, Otterson GA, Audigier-Valette C, et al. Nivolumab plus Ipilimumab in Lung Cancer with a High Tumor Mutational Burden. The New England journal of medicine. 2018;378(22):2093-104.
6. Shaw AT, Kim DW, Nakagawa K, Seto T, Crino L, Ahn MJ, et al. Crizotinib versus chemotherapy in advanced ALK-positive lung cancer. The New England journal of medicine. 2013;368(25):2385-94.
7. Solomon BJ, Mok T, Kim DW, Wu YL, Nakagawa K, Mekhail T, et al. First-line crizotinib versus chemotherapy in ALK-positive lung cancer. The New England journal of medicine. 2014;371(23):2167-77.
8. Soria JC, Ohe Y, Vansteenkiste J, Reungwetwattana T, Chewaskulyong B, Lee KH, et al. Osimertinib in Untreated EGFR-Mutated Advanced Non-Small-Cell Lung Cancer. The New England journal of medicine. 2018;378(2):113-25.
9. Reck M, Rodriguez-Abreu D, Robinson AG, Hui R, Csoszi T, Fulop A, et al. Pembrolizumab versus Chemotherapy for PD-L1-Positive Non-Small-Cell Lung Cancer. The New England journal of medicine. 2016;375(19):1823-33.
10. Nishino M, Jagannathan JP, Ramaiya NH, Van den Abbeele AD. Revised RECIST guideline version 1.1: What oncologists want to know and what radiologists need to know. AJR American journal of roentgenology. 2010;195(2):281-9.
11. Eisenhauer EA, Therasse P, Bogaerts J, Schwartz LH, Sargent D, Ford R, et al. New response evaluation criteria in solid tumours: revised RECIST guideline (version 1.1). Eur J Cancer. 2009;45(2):228-47.
12. Hicks RJ. Role of 18F-FDG PET in assessment of response in non-small cell lung cancer. Journal of nuclear medicine : official publication, Society of Nuclear Medicine. 2009;50 Suppl 1:31S-42S.

1

13. de Geus-Oei LF, van der Heijden HF, Visser EP, Hermsen R, van Hoorn BA, Timmer-Bonte JN, et al. Chemotherapy response evaluation with 18F-FDG PET in patients with non-small cell lung cancer. Journal of nuclear medicine : official publication, Society of Nuclear Medicine. 2007;48(10):1592-8.

1


Read online

CHAPTER II

The Role of FDG-PET/CT in Non-Small Cell Lung Cancer

Edwin A. Usmanij, Lioe-Fee de Geus-Oei, Johan Bussink, Wim J. G. Oyen

Adapted from: Current Opinion in Pulmonary Medicine. 2015 Jul;21(4):314-21

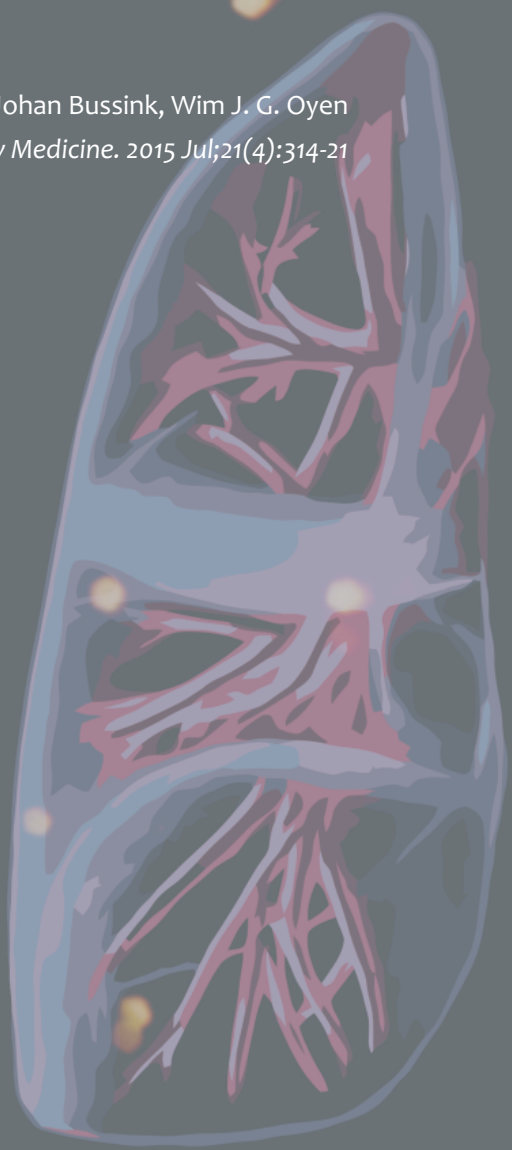

2

2

ABSTRACT

The aim of this review is to provide an outline of current evidence for the use of ^{18}F-fluoro-deoxy-glucose positron emission tomography/computed tomography (FDG-PET/CT) in non-small cell lung cancer (NSCLC) for diagnosis, staging, radiotherapy planning, response assessment and response monitoring.

Management of patients with non-small cell lung cancer requires a multimodality approach to diagnose and stage patients accurately. In this approach, FDG-PET/CT has become a standard staging instrument in lung cancer. FDG-PET/CT is, in addition to staging, also valuable for the characterisation of the solitary pulmonary nodule. Increased uptake in the nodule as compared to mediastinal blood pool is suspected of malignancy. In radiotherapy planning, FDG-PET/CT can assist the radiation oncologist for optimal dose delivery to the tumour, while sparing healthy tissues. Evidence of the prognostic and predictive implications of FDG-PET/CT is accumulating. Volumetric parameters of PET, such as metabolic active tumour volume and total lesion glycolysis, are promising predictive and prognostic biomarkers. However, for implementation of metabolic response parameters in clinical practice more randomised PET-based multicentre trails are necessary. The introduction of integrated PET and magnetic resonance imaging (PET/MR) scanners did not change the pivotal role of standard FDG-PET/CT yet, since with current technology PET/MR did not show superior performance in thoracic staging.

Keywords

non-small cell lung cancer, positron emission tomography, F-18-fluoro-deoxy-glucose, staging, prediction

INTRODUCTION

In the Western world, lung cancer is the leading cause of cancer-related death. Non-small cell lung cancer (NSCLC) accounts for 87% of all lung cancers (1). Adequate diagnosis and staging of NSCLC are of pivotal importance for clinical decision-making given that locoregional disease is treated with curative intent, while for disseminated disease the prognosis is dismal. Already before the introduction of hybrid scanners, that combined computed tomography (CT) and positron emission tomography (PET), the advent of PET with F-18-fluoro-deoxy-glucose (FDG) significantly improved the diagnostic accuracy of imaging. FDG-PET/CT has made a significant impact on both the guidance of invasive diagnostic procedures as well as on the selection of treatment options. Nowadays, FDG-PET/CT with contrast-enhanced CT has become a standard modality in the work-up of NSCLC (2). In this short review, we will focus on the most recent and pertinent progress in the application of PET/CT in non-disseminated NSCLC. We will summarise the indications of FDG-PET/CT for early diagnosis, the evaluation of pulmonary lesions and staging, and we will review the emerging evidence of FDG-PET/CT in (early) response monitoring and in radiation treatment planning. We end with the potential role of PET/CT in targeted therapy and follow-up.

Evaluation of lung lesions with FDG-PET/CT

Currently, we are frequently confronted with incidental findings of solitary pulmonary nodules (SPN), which can be partly explained by the increasing use of CT for indications other than cancer, e.g. cardiac CT for assessment of coronary artery disease or CT angiography for diagnosis of pulmonary embolism. Due to the relatively low specificity of CT, various risk assessments are available to predict the chance of malignancy of the nodules (3, 4). When the pretest chance of malignancy is 5-60% and the nodule is at least 8-10 mm, the evidence-based recommendation from Gould *et al.* (5) states that FDG-PET/CT is recommended to characterise the nodule. In nodules measuring <8-10 mm PET is less sensitive in detecting malignancy (e.g. with decreasing size of the nodule the false-negative rate rises). A recent meta-analysis by Deppen *et al.* 70 FDG-PET and FDG-PET/CT (6) studies were included showing a pooled sensitivity of 89% (95%-CI 86%-91%) and a specificity of 75% (95%-CI 71%-79%) for the detection of malignancy of the SPN. Ten studies, reporting a high prevalence of inflammatory pulmonary disease, showed an adjusted pooled specificity of 61% (95%-CI 49%-72%). It is important to realise that in populations with endemic lung disease FDG-PET/CT suffers from lower specificity. Overall, the results of this meta-analysis support the role of PET in the detection of pulmonary malignancy in SPN and showing a similar performance compared to a previous

meta-analysis by Gould *et al.* (7) who reported in 2003 a sensitivity and specificity of 96.8% and 77.8%. Nevertheless, evolving technology (e.g. the introduction of PET/CT, improving spatial and contrast resolution of PET) has resulted in a significantly better performance of modern FDG-PET/CT compared to stand-alone FDG-PET as when it was introduced in the clinic 15 years ago. Combining information from FDG-PET/CT and CT may lead to further improvement as shown by Asharf *et al.* (8). They reported that the combination of a volume doubling time (VDT) of the tumour in less than one year and FDG-uptake higher than the mediastinal blood pool was highly predictive of a malignant SPN. All ten nodules with high FDG uptake and VDT of less than one year were malignant, while only 2 of 30 nodules (7%) with low FDG uptake and long VDT were malignant. The combination of FDG-PET/CT and VDT resulted in a sensitivity of 90% and a specificity of 82%. In a multivariate analysis, both FDG uptake and VDT were independently associated with malignancy. In the evaluation of SPN, the inclusion of FDG-PET/CT has proven to be a cost-effective imaging modality (9-14).

Staging of NSCLC using FDG-PET/CT

Accurate staging of NSCLC is crucial for the management in NSCLC. The principal advantage of staging with FDG-PET/CT, over CT alone, is the superior performance in terms of mediastinal staging and the detection of distant metastases. Consequently, implementation of FDG-PET/CT resulted in a lower rate of futile thoracotomies (15). Nowadays, FDG-PET/CT has become a routine investigation in preoperative staging. The introduction of FDG-PET/CT improved the detection of distant metastasis, leading to a stage migration resulting in an increase of 8.4% stage IV disease in NSCLC (16).

Numerous studies investigated the role of FDG-PET/CT in the detection of metastatic lymph nodes (17-24). In a recent meta-analysis by Lv *et al.* (25), including fourteen studies with a total of 2550 patients, the pooled weighted sensitivity was 76% (95%-CI 65%-84%) and specificity was 88% (95%-CI 82%-92%). In mediastinal staging, a meta-analysis by Schmidt-Hansen (26) including 45 studies on integrated FDG-PET/CT for mediastinal staging reported a sensitivity and specificity of 77.4% (95%-CI 65.3%-86.1%) and 90.1% (95% CI 85.3%-93.5%), respectively. Fisher *et al.* (27) randomised 189 patients between workup without and with FDG-PET/CT, showing that FDG-PET/CT is false negative in 4% of the cases where nodes are not significantly enlarged on CT. Several studies showed that FDG-PET/CT is sensitive for the detection of metastasis in adrenal glands (28) and bone (29-32).

A new development is the arrival of integrated PET and magnetic resonance imaging (PET/MR), currently introduced in just a few institutions worldwide. However, PET/MR scanners did not change the pivotal role of FDG-PET/CT as the standard of care in

staging. Heusch *et al.* (33) reported no advantage of PET/MR over PET/CT in thoracic staging. No differences were found for the detection of metastatic lymph nodes or T-stage of the primary tumour. While only a few studies are published on this subject, these studies do not show a clear benefit of FDG-PET/MR over FDG-PET/CT yet.

Concluding, FDG-PET/CT is considered standard of care for non-invasive mediastinal staging and detection of distant metastasis in NSCLC. For the detection of brain metastasis, FDG-PET/CT has limited value as the high physiologic uptake of FDG in the cerebral cortex may obscure pathological uptake.

FDG-PET/CT in Radiotherapy

Radiotherapy plays an important role in the treatment of lung cancer (34). For defining the treatment target (e.g. the gross tumour volume or GTV), CT is the standard imaging modality required to determine electron density for dose calculation. A robust definition of the tumour volume to be irradiated is a prerequisite for successful radiotherapy, which can be quite challenging with CT, e.g. in centrally located tumours or in case of concomitant atelectasis. Therefore, FDG-PET/CT was explored to provide better data for tumour delineation and to improved local treatment. Selective irradiation of FDG-positive nodes is proposed, based on the high sensitivity for staging of mediastinal lymph nodes. De Ruysscher *et al.* (35) showed in a prospective study that selective nodal irradiation resulted in only low isolated nodal failure. The same group showed that this would allow an increase of dose delivery to the tumour (36).

For defining the primary tumour, incorporation of FDG-PET data in target volume delineation leads to significant changes in the shape and the volume of the target and allows shaping of the radiotherapy dose distribution accordingly (37). FDG-PET/CT can provide useful information on the extent of the tumour involvement and hypermetabolic regional lymph nodes. It prevents the inclusion of normal tissue, for example atelectasis. In those cases, FDG-PET/CT allows a reduction of the target volume by separating atelectasis from viable metabolic active tumour tissue (38). An example of FDG-PET/CT radiotherapy planning is shown in *Figure 1*.

FIGURE 1. FDG-PET/CT radiotherapy planning. Stage cT1bN3M0 NSCLC treated by concurrent chemo radiotherapy to a total irradiation dose of 66 Gy at 2 Gy per fraction. Left transversal, coronal and sagittal images of fused FDG-PET/CT images those were used for delineation of the gross tumour volume. Right same sections with radiation dose distribution (red line is PTV).

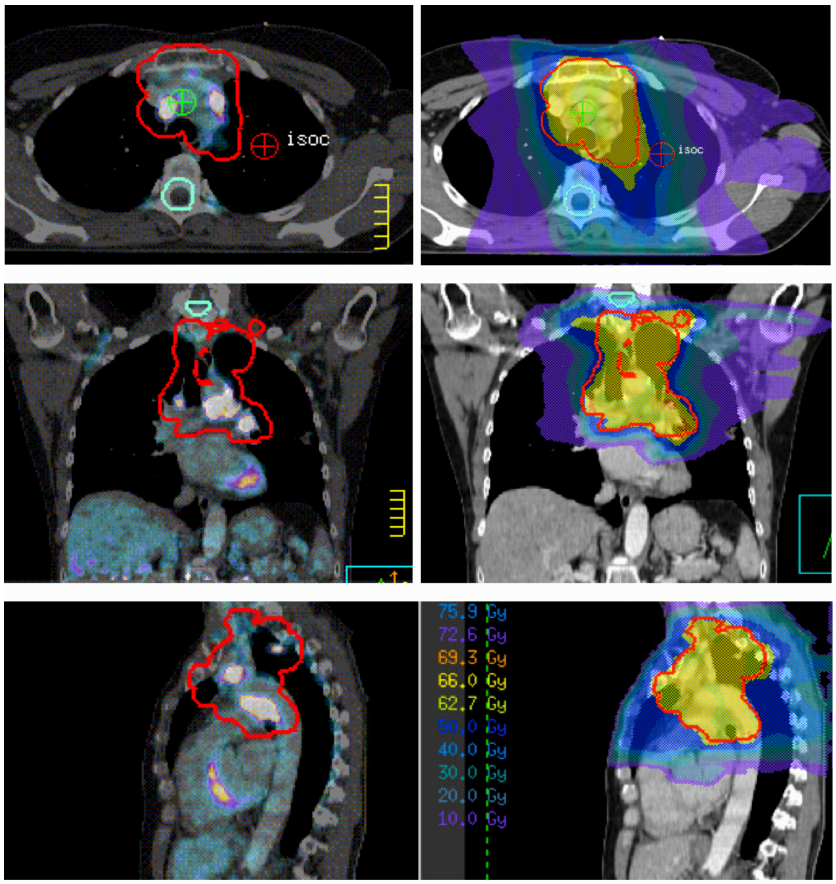

A number of issues may arise upon introduction of FDG-PET/CT data in radiation treatment planning. The spatial resolution of FDG-PET/CT is lower as compared to CT. However, with modern PET/CT scanners, this drawback has mostly been overcome. When tumour delineation is performed manually, it is subjective by definition and dependent on the experience of the radiation oncologist. FDG-PET/CT, however, significantly reduced inter-observer variations in tumour delineation (39, 40). Different approaches for (semi-) automatic delineation methods are proposed, based on the standardised uptake value (SUV), such as absolute threshold- (SUV $\geq$ 2.5) and relative threshold based methods (e.g. 40% - 50% of maximum SUV, signal to background (41). All methods are dependent on sufficiently high signal-to-background ratios and the

heterogeneity of the FDG-uptake in tumours (42-44). Therefore, other techniques, such as Watershed and Clustering algorithms (45) are proposed to overcome these issues. One important uncertainty in tumour volume delineation is caused by respiratory motion. FDG-PET/CT of the chest cannot be performed during a single breath hold but has to be acquired during shallow free breathing. Therefore, FDG-PET/CT is prone to respiratory motion-induced mismatches between PET and CT (46). The result can cause inaccuracies in the quantification of FDG-PET/CT. Several methods for respiratory-gated FDG-PET/CT have been developed (47, 48). Further clinical studies are needed to evaluate the added value in routine clinical practice.

Prognostic value of FDG-PET/CT

To quantify a lesion on PET, the most commonly used parameter is SUV. This semi-quantitative parameter reflects the radioactivity concentration in a tumour, normalised to injected dose and body weight. SUV_{max} reflects the voxel with the highest radioactivity concentration. The SUV parameter has been recognised as an important prognostic factor in NSCLC (49-53). Recently, a large prospective multicentre study by Machtay *et al.* (54) showed in 250 stage III NSCLC patients, that pre-treatment SUV_{max} was not associated with survival. Only the post-treatment SUV was predictive of overall survival in a multivariate Cox proportional hazards analysis (HR 1.125, 95% CI 1.049-1.206). As SUV_{max} only reflects the uptake in one voxel, volumetric parameters (representing the total tumour metabolism) have been considered as a prognostic biomarker. Metabolic tumour volume (MTV) is defined as the volume of the delineated tumour on PET. To delineate the tumour several methods exists, such as specific threshold, gradient (45) or adaptive threshold methods (41). Total lesion glycolysis (TLG) is calculated as the product of MTV and the mean SUV of all voxels. An increasing body of evidence underlines the prognostic value of TLG (55-58) and MTV (59-62). A recent meta-analysis by Im *et al.* (63) showed for MTV a pooled hazard ratio for overall survival (OS) of 2.31 (95%-CI 1.54–3.47). It is indicating that a high MTV is associated with worse survival rates compared to a low MTV. Also, patients with a high TLG show worse survival (pooled HR for OS of 2.94 (95%-CI 1.94–3.18). In multivariate analysis for OS, MTV (64) and TLG (65) showed to be independent prognostic markers regardless of tumour size and disease stage.

Response Assessment with FDG-PET/CT

The role of FDG-PET/CT in response assessment in NSCLC has been extensively studied in the past years. Traditionally response assessment is done by size criteria, for which CT is the method of choice in NSCLC. However, several limitations can be identified when using the tumour diameter as a measure for response. Morphological changes tend to occur relatively late during treatment and may suffer for limitations to differentiate residual viable tumour from fibrosis or necrosis. Molecular imaging using FDG can depict metabolic changes in the tumour at an early stage during treatment (*Figure 2*). Ultimately, an in-treatment assessment with PET can offer the opportunity for treatment adaptation in the individual patient. In this personalised medicine approach, patients, who may not benefit from therapy, might be spared unnecessary toxicity of ineffective treatment. Switching to another treatment can be considered. This can lead to improved tumour control and avoid futile costs of ineffective treatment.

In early response monitoring, metabolic change is evaluated during treatment with the objective to predict clinical outcome. In patients with locally advanced NSCLC treated with concomitant chemoradiotherapy, the evolution of TLG is predictive of progression-free survival (PFS) (66) and OS (67). Yossi *et al.* (67) showed that a decrease of >15% TLG after 30 Gy (up to a total dose of 66–70 Gy in 2 Gy fractions) was associated with a better OS (P = 0.007 HR 7.439; 95%-CI 1.168–28.897) and PFS (P = 0.010; HR 5.695; 95%-CI 1.506–21.537). Huang *et al.* (68) showed in locally advanced NSCLC that decrease of MTV after 40 Gy (was predictive for local recurrence-free survival (LRFS). 40 Gy was given conventionally at 2 Gy fractions and late-course accelerated hyper-fractionated with 1.4 Gy twice daily up to a total dose of 62.4 to 76.4 Gy. A decrease in MTV of more than 29.7% (optimal cut-off) was associated with a median LRFS of 35 months, compared to a decrease in MTV of less than 29.7% with a median LRFS of 13 months (P < 0.001).

Several studies investigated FDG-PET/CT to address metabolic response (69-71) in NSCLC patients treated with epidermal growth factor receptor tyrosine kinase inhibitors (EGFR-TKI). Takahashi *et al.* (69) showed that in 19 patients (stage IIIA, IIIB, IV) after two days of treatment a ≥20% decrease in maximum SUV (optimal cut-off) was associated with a significantly longer PFS. Another study by O'Brien *et al.* (70) showed in 38 patients (stage IIIB – IV) that a decrease in SUV ≥ 25% after six weeks showing significantly longer survival in patients treated with EGFR-TKI. A study by Bengtsson *et al.* (71) showed that

FIGURE 2. Early FDG-PET/CT response during concomitant chemo radiotherapy. Patient with a tumour in the right upper lobe, affected lymph nodes hilar right and contralateral mediastinal lymph node (N3 node not shown), staged cT2N3M0. Patient was treated with concomitant chemo radiotherapy with a total irradiation dose of 66 Gy at 2 Gy fractions. Pre-treatment scan is shown in the left column while the in-treatment scan 20 Gy into concomitant chemo-radiotherapy is shown on the right. The in-treatment scan showed significant reduction in FDG-uptake of the tumour, while no size reduction was seen on CT.

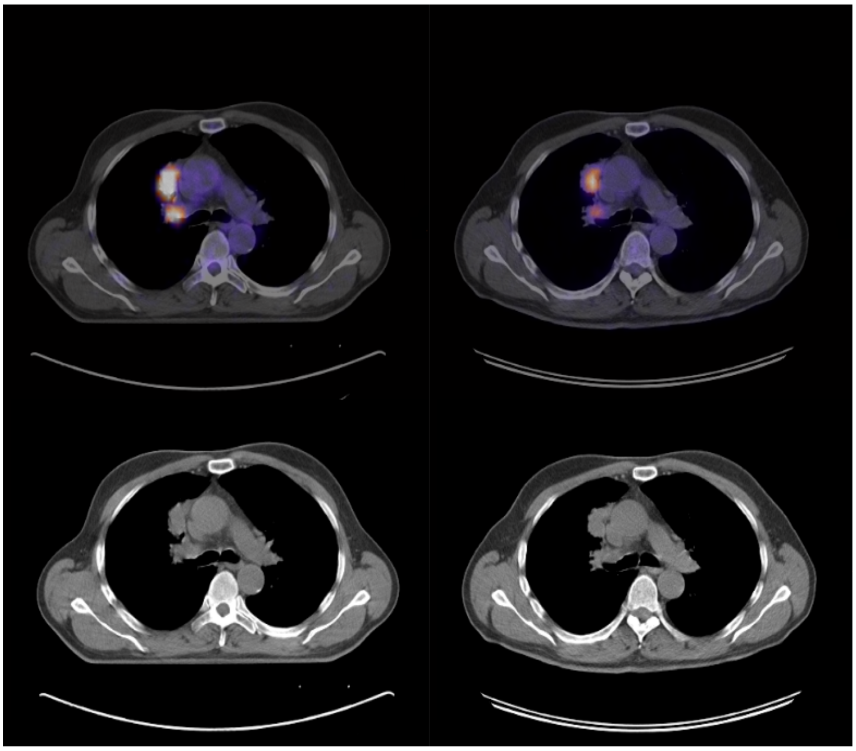

after two weeks of EGFR-TKI treatment, new lesions on PET were independent and significant predictors of overall survival. While FDG is a widely used radiotracer, other tracers for early response prediction for EGFR-TKI's are promising, such as F-18-fluoro-thymidine (FLT), which reflects cellular proliferation. In patients with advanced NSCLC, a marked decrease in FLT uptake under erlotinib treatment was a strong predictive factor for PFS (72).

The mentioned studies show the predictive implications of (early) in-treatment FDG-PET/CT in NSCLC. However, implementation of these FDG-PET/CT data in clinical practice is not straightforward. First of all, variations in measurements of response and response criteria exist (73, 74). The proposed PET Response Criteria in Solid Tumours (PERCIST) (75) could serve as structured criteria in PET response studies. Also, the lack

of consensus on measurement method and PET parameters is hampering clinical implementation. Furthermore, harmonisation of optimal in-treatment timing of FDG-PET/CT is important to compare studies (76). Consequently, adequately powered, prospective interventional trials, in which the PET-data are used to modify treatment, prove to be very difficult to organise.

FDG-PET/CT in follow-up

Currently, routine surveillance FDG-PET/CT after definite therapy is not included as a part of follow-up. When recurrent disease on conventional imaging is suspected, FDG-PET/CT is useful for the detection of recurrence. In a meta-analysis including 13 articles, FDG-PET/CT was a superior modality compared to conventional imaging for the detection of recurrent lung cancer (77). A recent retrospective study of surveillance FDG-PET/CT during follow-up more than six months after treatment showed that FDG-PET is a prognostic marker of OS (78). Patients with a negative FDG-PET/CT for recurrence had a median survival time of 81.6 months versus 32.9 months in patients with an FDG-PET/CT suspected of recurrence ($P < 0.0001$).

CONCLUSION

In this review we discussed recent and clinically most relevant progress in the use of FDG-PET/CT in NSCLC. FDG-PET plays an important role in the staging and restaging of NSCLC, providing complementary information to conventional morphological imaging modalities. Furthermore, FDG-PET/CT is useful for characterisation of solitary pulmonary nodules. FDG-PET/CT can aid the radiation oncologist in treatment planning for optimal dose delivery to the tumour, while sparing healthy tissues. Evidence is accumulating for the prognostic and predictive implications of FDG-PET/CT. FDG-PET/CT is promising as a useful biomarker for response assessment. However, validation with adequately powered prospective studies is still needed. FDG-PET/CT after primary therapy is recommended when recurrent disease on conventional imaging is suspected.

Key Points

- FDG-PET/CT is recommended to characterise the solitary pulmonary nodule.
- FDG-PET/CT is a standard staging instrument for mediastinal staging and detection of distant metastasis in non-small cell lung cancer.
- The use of FDG-PET/CT in radiotherapy planning leads to significant changes in the GTV of the primary tumour and involved lymph nodes, providing valuable data for improved tumour delineation.

References

1. DeSantis CE, Lin CC, Mariotto AB, et al. Cancer treatment and survivorship statistics, 2014. CA Cancer J Clin 2014;64: 252-271.
2. Brocken P, van der Heijden HF, Dekhuijzen PN, et al. High performance of F-fluorodeoxyglucose positron emission tomography and contrast-enhanced CT in a rapid outpatient diagnostic program for patients with suspected lung cancer. Respiration 2014;87: 32-37.
3. Swensen SJ, Silverstein MD, Ilstrup DM, et al. The probability of malignancy in solitary pulmonary nodules. Application to small radiologically indeterminate nodules. Arch Intern Med 1997;157: 849-855.
4. Gould MK, Ananth L, Barnett PG. A clinical model to estimate the pretest probability of lung cancer in patients with solitary pulmonary nodules. Chest 2007;131: 383-388.
5. Gould MK, Fletcher J, Iannettoni MD, et al. Evaluation of patients with pulmonary nodules: when is it lung cancer?: ACCP evidence-based clinical practice guidelines (2nd edition). Chest 2007;132: 108S-130S.
6. Deppen SA, Blume JD, Kensinger CD, et al. Accuracy of FDG-PET to diagnose lung cancer in areas with infectious lung disease: a meta-analysis. JAMA 2014;312: 1227-1236.
7. Gould MK, Maclean CC, Kuschner WG, et al. Accuracy of positron emission tomography for diagnosis of pulmonary nodules and mass lesions: a meta-analysis. JAMA 2001;285: 914-924.
8. Ashraf H, Dirksen A, Loft A, et al. Combined use of positron emission tomography and volume doubling time in lung cancer screening with low-dose CT scanning. Thorax 2011;66: 315-319.
9. Dietlein M, Weber K, Gandjour A, et al. Cost-effectiveness of FDG-PET for the management of solitary pulmonary nodules: a decision analysis based on cost reimbursement in Germany. Eur J Nucl Med 2000;27: 1441-1456.
10. Keith CJ, Miles KA, Griffiths MR, et al. Solitary pulmonary nodules: accuracy and cost-effectiveness of sodium iodide FDG-PET using Australian data. Eur J Nucl Med Mol Imaging 2002;29: 1016-1023.
11. Kosuda S, Ichihara K, Watanabe M, et al. Decision-tree sensitivity analysis for cost-effectiveness of chest 2-fluoro-2-D-[(18)F]fluorodeoxyglucose positron emission tomography in patients with pulmonary nodules (non-small cell lung carcinoma) in Japan. Chest 2000;117: 346-353.
12. Barnett PG, Ananth L, Gould MK. Cost and outcomes of patients with solitary pulmonary nodules managed with PET scans. Chest 2010;137: 53-59.

13. Lejeune C, Bismuth MJ, Conroy T, et al. Use of a decision analysis model to assess the cost-effectiveness of 18F-FDG PET in the management of metachronous liver metastases of colorectal cancer. J Nucl Med 2005;46: 2020-2028.
14. Gould MK, Sanders GD, Barnett PG, et al. Cost-effectiveness of alternative management strategies for patients with solitary pulmonary nodules. Ann Intern Med 2003;138: 724-735.
15. van Tinteren H, Hoekstra OS, Smit EF, et al. Effectiveness of positron emission tomography in the preoperative assessment of patients with suspected non-small-cell lung cancer: the PLUS multicentre randomised trial. Lancet 2002;359: 1388-1393.
16. Chee KG, Nguyen DV, Brown M, et al. Positron emission tomography and improved survival in patients with lung cancer: the Will Rogers phenomenon revisited. Arch Intern Med 2008;168: 1541-1549.
17. Birim O, Kappetein AP, Stijnen T, Bogers AJ. Meta-analysis of positron emission tomographic and computed tomographic imaging in detecting mediastinal lymph node metastases in nonsmall cell lung cancer. Ann Thorac Surg 2005;79: 375-382.
18. Toloza EM, Harpole L, McCrory DC. Noninvasive staging of non-small cell lung cancer: a review of the current evidence. Chest 2003;123: 137S-146S.
19. Gould MK, Kuschner WG, Rydzak CE, et al. Test performance of positron emission tomography and computed tomography for mediastinal staging in patients with non-small-cell lung cancer: a meta-analysis. Ann Intern Med 2003;139: 879-892.
20. Yang W, Fu Z, Yu J, et al. Value of PET/CT versus enhanced CT for locoregional lymph nodes in non-small cell lung cancer. Lung Cancer 2008;61: 35-43.
21. Kubota K, Murakami K, Inoue T, et al. Additional value of FDG-PET to contrast enhanced-computed tomography (CT) for the diagnosis of mediastinal lymph node metastasis in non-small cell lung cancer: a Japanese multicenter clinical study. Ann Nucl Med 2011;25: 777-786.
22. Fischer B, Lassen U, Mortensen J, et al. Preoperative staging of lung cancer with combined PET-CT. N Engl J Med 2009;361: 32-39.
23. Gomez-Caro A, Boada M, Cabanas M, et al. False-negative rate after positron emission tomography/computer tomography scan for mediastinal staging in cI stage non-small-cell lung cancer. Eur J Cardiothorac Surg 2012;42: 93-100; discussion 100.
24. Wang J, Welch K, Wang L, Kong FM. Negative predictive value of positron emission tomography and computed tomography for stage T1-2N0 non-small-cell lung cancer: a meta-analysis. Clin Lung Cancer 2012;13: 81-89.
25. Lv YL, Yuan DM, Wang K, et al. Diagnostic performance of integrated positron emission tomography/computed tomography for mediastinal lymph node staging in non-small cell lung cancer: a bivariate systematic review and meta-analysis. J Thorac Oncol 2011;6: 1350-1358.

26. Schmidt-Hansen M, Baldwin DR, Hasler E, et al. PET-CT for assessing mediastinal lymph node involvement in patients with suspected resectable non-small cell lung cancer. Cochrane Database Syst Rev 2014;11: CD009519.
27. Fischer BM, Mortensen J, Hansen H, et al. Multimodality approach to mediastinal staging in non-small cell lung cancer. Faults and benefits of PET-CT: a randomised trial. Thorax 2011;66: 294-300.
28. Schuurbiers OC, Tournoy KG, Schoppers HJ, et al. EUS-FNA for the detection of left adrenal metastasis in patients with lung cancer. Lung Cancer 2011;73: 310-315.
29. Gayed I, Vu T, Johnson M, et al. Comparison of bone and 2-deoxy-2-[18F]fluoro-D-glucose positron emission tomography in the evaluation of bony metastases in lung cancer. Mol Imaging Biol 2003;5: 26-31.
30. Qu X, Huang X, Yan W, et al. A meta-analysis of (1)(8)FDG-PET-CT, (1)(8)FDG-PET, MRI and bone scintigraphy for diagnosis of bone metastases in patients with lung cancer. Eur J Radiol 2012;81: 1007-1015.
31. Bury T, Barreto A, Daenen F, et al. Fluorine-18 deoxyglucose positron emission tomography for the detection of bone metastases in patients with non-small cell lung cancer. Eur J Nucl Med 1998;25: 1244-1247.
32. Liu N, Ma L, Zhou W, et al. Bone metastasis in patients with non-small cell lung cancer: the diagnostic role of F-18 FDG PET/CT. Eur J Radiol 2010;74: 231-235.
33. Heusch P, Buchbender C, Kohler J, et al. Thoracic staging in lung cancer: prospective comparison of 18F-FDG PET/MR imaging and 18F-FDG PET/CT. J Nucl Med 2014;55: 373-378.
34. Bussink J, Kaanders JH, van der Graaf WT, Oyen WJ. PET-CT for radiotherapy treatment planning and response monitoring in solid tumors. Nat Rev Clin Oncol 2011;8: 233-242.
35. De Ruysscher D, Wanders S, van Haren E, et al. Selective mediastinal node irradiation based on FDG-PET scan data in patients with non-small-cell lung cancer: a prospective clinical study. Int J Radiat Oncol Biol Phys 2005;62: 988-994.
36. De Ruysscher D, Wanders S, Minken A, et al. Effects of radiotherapy planning with a dedicated combined PET-CT-simulator of patients with non-small cell lung cancer on dose limiting normal tissues and radiation dose-escalation: a planning study. Radiother Oncol 2005;77: 5-10.
37. Hoffmann AL, Troost EG, Huizenga H, et al. Individualized dose prescription for hypofractionation in advanced non-small-cell lung cancer radiotherapy: an in silico trial. Int J Radiat Oncol Biol Phys 2012;83: 1596-1602.
38. Bradley J, Thorstad WL, Mutic S, et al. Impact of FDG-PET on radiation therapy volume delineation in non-small-cell lung cancer. Int J Radiat Oncol Biol Phys 2004;59: 78-86.

39. Steenbakkers RJ, Duppen JC, Fitton I, et al. Reduction of observer variation using matched CT-PET for lung cancer delineation: a three-dimensional analysis. Int J Radiat Oncol Biol Phys 2006;64: 435-448.
40. Werner-Wasik M, Nelson AD, Choi W, et al. What is the best way to contour lung tumors on PET scans? Multiobserver validation of a gradient-based method using a NSCLC digital PET phantom. Int J Radiat Oncol Biol Phys 2012;82: 1164-1171.
41. van Dalen JA, Hoffmann AL, Dicken V, et al. A novel iterative method for lesion delineation and volumetric quantification with FDG PET. Nucl Med Commun 2007;28: 485-493.
42. Schuurbiers OC, Meijer TW, Kaanders JH, et al. Glucose metabolism in NSCLC is histology-specific and diverges the prognostic potential of 18FDG-PET for adenocarcinoma and squamous cell carcinoma. J Thorac Oncol 2014;9: 1485-1493.
43. Meijer TW, Schuurbiers OC, Kaanders JH, et al. Differences in metabolism between adeno- and squamous cell non-small cell lung carcinomas: Spatial distribution and prognostic value of GLUT1 and MCT4. Lung Cancer 2012;76: 316-323.
44. Vriens D, Disselhorst JA, Oyen WJ, et al. Quantitative assessment of heterogeneity in tumor metabolism using FDG-PET. Int J Radiat Oncol Biol Phys 2012;82: e725-731.
45. Geets X, Lee JA, Bol A, et al. A gradient-based method for segmenting FDG-PET images: methodology and validation. Eur J Nucl Med Mol Imaging 2007;34: 1427-1438.
46. van der Vos CS, Grootjans W, Meeuwis AP, et al. Comparison of a free-breathing CT and an expiratory breath-hold CT with regard to spatial alignment of amplitude-based respiratory-gated PET and CT images. J Nucl Med Technol 2014;42: 269-273.
47. Chi A, Nguyen NP. 4D PET/CT as a Strategy to Reduce Respiratory Motion Artifacts in FDG-PET/CT. Front Oncol 2014;4: 205.
48. Grootjans W, de Geus-Oei LF, Meeuwis AP, et al. Amplitude-based optimal respiratory gating in positron emission tomography in patients with primary lung cancer. Eur Radiol 2014;24: 3242-3250.
49. Tong AN, Han SR, Yan P, et al. Prognostic value of FDG uptake in primary inoperable non-small cell lung cancer. Med Oncol 2014;31: 780.
50. Clarke K, Taremi M, Dahele M, et al. Stereotactic body radiotherapy (SBRT) for non-small cell lung cancer (NSCLC): is FDG-PET a predictor of outcome? Radiother Oncol 2012;104: 62-66.
51. Takeda A, Yokosuka N, Ohashi T, et al. The maximum standardized uptake value (SUVmax) on FDG-PET is a strong predictor of local recurrence for localized non-small-cell lung cancer after stereotactic body radiotherapy (SBRT). Radiother Oncol 2011;101: 291-297.

52. Aerts HJ, Bussink J, Oyen WJ, et al. Identification of residual metabolic-active areas within NSCLC tumours using a pre-radiotherapy FDG-PET-CT scan: a prospective validation. Lung Cancer 2012;75: 73-76.
53. de Geus-Oei LF, van der Heijden HF, Corstens FH, Oyen WJ. Predictive and prognostic value of FDG-PET in nonsmall-cell lung cancer: a systematic review. Cancer 2007;110: 1654-1664.
54. Machtay M, Duan F, Siegel BA, et al. Prediction of survival by [18F]fluorodeoxyglucose positron emission tomography in patients with locally advanced non-small-cell lung cancer undergoing definitive chemoradiation therapy: results of the ACRIN 6668/RTOG 0235 trial. J Clin Oncol 2013;31: 3823-3830
55. Mehta G, Chander A, Huang C, et al. Feasibility study of FDG PET/CT-derived primary tumour glycolysis as a prognostic indicator of survival in patients with non-small-cell lung cancer. Clin Radiol 2014;69: 268-274.
56. Chen HH, Chiu NT, Su WC, et al. Prognostic Value of Whole-Body Total Lesion Glycolysis at Pretreatment FDG PET/CT in Non-Small Cell Lung Cancer. Radiology 2012; 264 (2):559-66
57. Park SY, Cho A, Yu WS, et al. Prognostic Value of Total Lesion Glycolysis by 18F-FDG PET/CT in Surgically Resected Stage IA Non-Small Cell Lung Cancer. J Nucl Med 2015;56: 45-49.
58. Davison J, Mercier G, Russo G, Subramaniam RM. PET-based primary tumor volumetric parameters and survival of patients with non-small cell lung carcinoma. AJR Am J Roentgenol 2013;200: 635-640.
59. Zhang H, Wroblewski K, Liao S, et al. Prognostic value of metabolic tumor burden from (18)F-FDG PET in surgical patients with non-small-cell lung cancer. Acad Radiol 2013;20: 32-40.
60. Kim DH, Son SH, Kim CY, et al. Prediction for recurrence using F-18 FDG PET/CT in pathologic N0 lung adenocarcinoma after curative surgery. Ann Surg Oncol 2014;21: 589-596.
61. Melloni G, Gajate AM, Sestini S, et al. New positron emission tomography derived parameters as predictive factors for recurrence in resected stage I non-small cell lung cancer. Eur J Surg Oncol 2013;39: 1254-1261.
62. Hyun SH, Choi JY, Kim K, et al. Volume-based parameters of (18)F-fluorodeoxyglucose positron emission tomography/computed tomography improve outcome prediction in early-stage non-small cell lung cancer after surgical resection. Ann Surg 2013;257: 364-370.
63. Im HJ, Pak K, Cheon GJ, et al. Prognostic value of volumetric parameters of F-FDG PET in non-small-cell lung cancer: a meta-analysis. Eur J Nucl Med Mol Imaging 2015;42(2): 241-51.

64. Hyun SH, Ahn HK, Kim H, et al. Volume-based assessment by (18)F-FDG PET/CT predicts survival in patients with stage III non-small-cell lung cancer. Eur J Nucl Med Mol Imaging 2014;41: 50-58.
65. Zaizen Y, Azuma K, Kurata S, et al. Prognostic significance of total lesion glycolysis in patients with advanced non-small cell lung cancer receiving chemotherapy. Eur J Radiol 2012;81: 4179-4184.
66. Usmanij EA, Geus-Oei LF, Troost EG, et al. 18F-FDG PET Early Response Evaluation of Locally Advanced Non-Small Cell Lung Cancer Treated with Concomitant Chemoradiotherapy. J Nucl Med 2013;54: 1528-1534.
67. Yossi S, Krhili S, Muratet JP, et al. Early Assessment of Metabolic Response by 18F-FDG PET During Concomitant Radiochemotherapy of Non-Small Cell Lung Carcinoma Is Associated With Survival: A Retrospective Single-Center Study. Clin Nucl Med 2015; 40:e215-e221.
68. Huang W, Liu B, Fan M, et al. The early predictive value of a decrease of metabolic tumor volume in repeated F-FDG PET/CT for recurrence of locally advanced non-small cell lung cancer with concurrent radiochemotherapy. Eur J Radiol 2014; 84(3): 482-8
69. Takahashi R, Hirata H, Tachibana I, et al. Early [18F]fluorodeoxyglucose positron emission tomography at two days of gefitinib treatment predicts clinical outcome in patients with adenocarcinoma of the lung. Clin Cancer Res 2012;18: 220-228.
70. O'Brien ME, Myerson JS, Coward JI, et al. A phase II study of (1)(8)F-fluorodeoxyglucose PET-CT in non-small cell lung cancer patients receiving erlotinib (Tarceva); objective and symptomatic responses at 6 and 12 weeks. Eur J Cancer 2012;48: 68-74.
71. Bengtsson T, Hicks RJ, Peterson A, Port RE. 18F-FDG PET as a surrogate biomarker in non-small cell lung cancer treated with erlotinib: newly identified lesions are more informative than standardized uptake value. J Nucl Med 2012;53: 530-537.
72. Kahraman D, Holstein A, Scheffler M, et al. Tumor lesion glycolysis and tumor lesion proliferation for response prediction and prognostic differentiation in patients with advanced non-small cell lung cancer treated with erlotinib. Clin Nucl Med 2012;37: 1058-1064.
73. Vriens D, De Geus-Oei LF, Van Laarhoven HW, et al. Comparison of two region of interest definition methods for metabolic response evaluation with [(1)(8)F]FDG-PET. Q J Nucl Med Mol Imaging 2010;54: 677-688.
74. Vriens D, de Geus-Oei LF, van Laarhoven HW, et al. Evaluation of different normalization procedures for the calculation of the standardized uptake value in therapy response monitoring studies. Nucl Med Commun 2009;30: 550-557.

75. Wahl RL, Jacene H, Kasamon Y, Lodge MA. From RECIST to PERCIST: Evolving Considerations for PET response criteria in solid tumors. J Nucl Med 2009;50 Suppl 1: 122S-150S.
76. Boellaard R, Delgado-Bolton R, Oyen WJ, et al. FDG PET/CT: EANM procedure guidelines for tumour imaging: version 2.0. Eur J Nucl Med Mol Imaging 2015;42: 328-354.
77. He YQ, Gong HL, Deng YF, Li WM. Diagnostic efficacy of PET and PET/CT for recurrent lung cancer: a meta-analysis. Acta Radiol 2014;55: 309-317.
78. Antoniou AJ, Marcus C, Tahari AK, et al. Follow-up or Surveillance 18F-FDG PET/CT and Survival Outcome in Lung Cancer Patients. J Nucl Med 2014;55: 1062-1068.


Read online

CHAPTER III

^{18}F-FDG-PET Early Response Evaluation of Locally Advanced Non-Small Cell Lung Cancer treated with Concomitant Chemo-Radiotherapy

Edwin A. Usmanij, Lioe-Fee de Geus-Oei, Esther G.C. Troost,
Liesbeth Peters-Bax, Erik H.F.M. van der Heijden,
Johannes H.A.M. Kaanders, Wim J.G. Oyen,
Olga C.J. Schuurbiers, Johan Bussink

Adapted from: Journal of Nuclear Medicine 2013; 54(9):1528-34

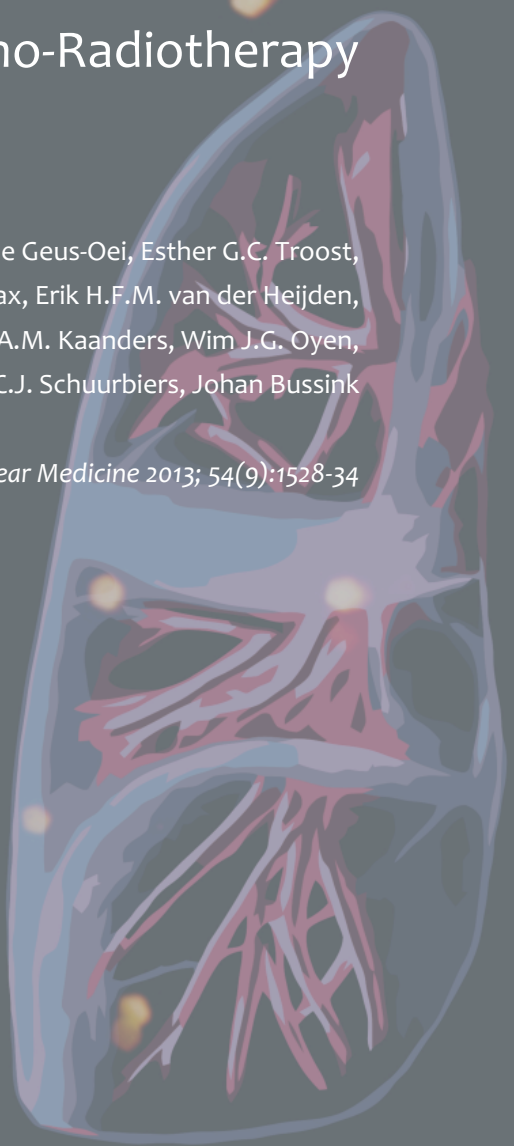

3

ABSTRACT

Objectives

The potential of ^{18}F-fluorodeoxyglucose-positron-emission-tomography (^{18}F-FDG PET) changes was evaluated for prediction of response to concomitant chemoradiotherapy in patients with locally advanced non-small cell lung cancer (NSCLC).

Methods

For 28 patients, ^{18}F-FDG PET was performed before treatment, at the end of the second week of treatment, and after the completion of treatment (after two weeks and three months). Standardised uptake value (SUV), maximum SUV (SUV_{max}), metabolic tumour volume (MTV), and total lesion glycolysis (TLG) were obtained. Early metabolic changes were defined as fractional change (ΔTLG) when ^{18}F-FDG PET at the end of the second week was compared with pretreatment ^{18}F-FDG PET. In-treatment metabolic changes, as measured by serial ^{18}F-FDG PET, were correlated with standard criteria of response evaluation of solid tumours by means of CT imaging (Response Evaluation Criteria In Solid Tumours 1.1). Parameters were analysed for stratification in progression-free survival (PFS).

Results

When compared with early metabolic non- responders, a ΔTLG decrease of 38% or more was associated with a significantly longer PFS (1-year PFS 80% vs 36%, P = 0.02). Pre-treatment TLG was found to be a prognostic factor for PFS.

Conclusion

The degree of change in TLG was predictive for response to concomitant chemoradiotherapy as early as the end of the second week into treatment for patients with locally advanced NSCLC. Pre-treatment TLG was prognostic for PFS.

Key Words

early response prediction, non-small cell lung cancer; concomitant radiotherapy chemotherapy; ^{18}F-FDG PET, standardised uptake value; total lesion glycolysis

INTRODUCTION

Management of patients with locally advanced non-small cell lung cancer (NSCLC) has changed significantly in the past few years (1, 2). Concomitant chemo-radiotherapy (CRT) is the standard of care in fit patients (ECOG performance status grade 0 – 1) (3). However, intensification of treatment significantly increases morbidity while yielding modest improvements in terms of overall survival (3). If a good response is obtained after CRT, surgery with curative intent can be beneficial (4), but only if a complete eradication of vital tumour cells in involved lymph nodes is achieved. On the other end, there are some patients that do not respond to CRT while they do experience the side effects (3). With recent developments in dose escalation in NSCLC, a further increase in toxicity is reported (5, 6). Therefore, a need arises to predict therapy response at an early phase on an individual patient basis. This could lead to improved tumour control, reduction in side effects and eventually avoid futile costs of ineffective treatment (7).

Imaging of treatment response is mainly static, based on the assessment of tumour size on CT and classification of metric changes using international Response Evaluation Criteria In Solid Tumours (RECIST) (8). However, these morphologic methods are of limited value for the detection of early therapy response. Anatomic imaging cannot distinguish atelectasis or fibrotic tissue from residual tumour (9,10). Consequently, a radiographic response does not show correlation with histopathologic regression after neoadjuvant chemoradiotherapy in NSCLC (11). Thus, response assessment by standard radiologic imaging is only meaningful after the end of therapy, when the opportunity to modify possible ineffective treatment has passed. Functional imaging using ^{18}F-FDG PET/CT has gained widespread acceptance for diagnosis and staging in oncology and has proven prognostic value for NSCLC (12). The application of ^{18}F-FDG PET/CT for the prediction of therapy response and treatment outcome has been shown in advanced stage NSCLC during induction chemotherapy (13–16), during radiotherapy (17), and after neoadjuvant chemotherapy (18). Data for response prediction of ^{18}F-FDG PET/CT in locally advanced NSCLC treated with concomitant therapy are limited. The aim of this study was to assess the predictive value of ^{18}F-FDG PET/CT in locally advanced NSCLC, performed after two weeks of concomitant chemoradiotherapy. We hypothesised that early treatment-induced glucose metabolic changes, measured by ^{18}F-FDG PET/CT scans, can predict clinical outcome.

MATERIALS AND METHODS

Patients

From January 2008 to January 2012, patients with newly diagnosed locally advanced NSCLC eligible for concomitant chemoradiotherapy were enrolled in this study. Inclusion criteria were cytologically or histologically proven NSCLC stage IIIA (TNM sixth edition, Union for International Cancer Control [UICC], T3 or N2) or stage IIIB (TNM sixth edition, UICC, T4 or N3); age, 18–80 y; and ECOG performance status grade, 0–1. The exclusion criterion was previous thoracic radiotherapy. The study was approved by the Institutional Review Board of the Radboud University Nijmegen Medical Centre. All patients gave written informed consent.

Treatment

Patients were treated with chemoradiotherapy in a concomitant scheme. An intensity-modulated radiotherapy technique (IMRT) was delivered to a total dose of 66 Gy in 33 fractions of 2 Gy, five fractions per week, using 10-MV photons. The gross tumour volume consisted of the primary tumour and involved hilar or mediastinal lymph nodes (i.e., PET-positive or cytologically proven lymph nodes). The clinical target volume contained gross tumour volume plus a 1.0-cm margin for the primary tumour and 0.5-cm margin for the lymph nodes. The planning target volume consisted of the clinical target volume plus a 0.5-cm margin. The chemotherapy regimen consisted of two cycles of cisplatin (50 mg/m^2 of body surface area [days 1 and 8 of the first cycle and days 22 and 29 of the second cycle]) and etoposide (100 mg/m^2 of body surface area intravenously [days 1–3 of the first cycle and days 22–24 of the second cycle]), starting on the first day of radiotherapy. The planned overall treatment period was 45 days.

Staging and Follow-up

All patients underwent diagnostic work-up, including contrast-enhanced CT of the thorax and upper abdomen; whole-body ^{18}F-FDG PET/CT; MR imaging of the brain; bronchoscopy with transbronchial needle aspiration (TBNA), esophageal ultrasound fine-needle aspiration (EUS-FNA), or endobronchial ultrasound with TBNA (EBUS-TBNA); and mediastinoscopy in the case of PET-positive, cytologically negative mediastinal lymph nodes. After work-up, all patients were discussed in a thoracic oncology multidisciplinary board. Before chemoradiotherapy, ^{18}F-FDG PET/CT of the thorax was performed in radiotherapy position for radiotherapy planning (median interval, 11 d; range, 1–27 d).

Early response measurement, using ^{18}F-FDG-PET/CT, was performed at the beginning of week three (after a median dose of 20 Gy, range 20-24 Gy), always prior to the second chemotherapy cycle. All attending physicians were blinded to the results of this ^{18}F-FDG-PET/CT, which was part of the study protocol. Therefore, the study data did not affect treatment decisions. The study design is shown in *Figure 1*.

Two to three weeks after the end of therapy (median 19 days, range 14 – 21 d), patients were re-staged with a whole body ^{18}F-FDG-PET/CT and a contrast-enhanced CT of the chest/upper abdomen. All tumour response assessment was done according to RECIST 1.1 criteria (8). If findings indicated an objective response to therapy and the primary tumour was considered resectable by lobectomy and if patients were considered operable, a restaging of mediastinal nodes by EUS or EBUS was performed, followed by mediastinoscopy in the case of negative cytology (normal cytologic lymph node punctate or non-representative punctures). Patients underwent lobectomy in the case of complete mediastinal histopathologic response (i.e., cytologically or histologically no vital tumour cells in previously affected nodes). In the case of persistent N2 disease or if patients were not eligible for surgery (tumour unresectability or inoperable patients), follow-up was performed.

Final treatment response after chemoradiotherapy was assessed using ^{18}F-FDG PET 3 months after treatment (range, 2–5 months) in the nonsurgical group. Follow-up during and after treatment for all patients consisted of standard follow-up according to the following international guidelines: clinical examination at regular intervals (every three months in the first year), chest X-rays, and chest CT scans if clinically indicated.

^{18}F-FDG-PET/CT scan

All PET investigations were performed with a hybrid PET/CT scanner (Biograph Duo Siemens Medical Solutions USA, Inc.) according to guidelines of the European Association of Nuclear Medicine (19). Patients fasted for at least six hours. Blood glucose levels were lower than 8.2 mmol/L in all patients (mean, 6.0 mmol/L). According to protocol, 60 min (mean ± SD, 77.94 ± 9.1 min) after intravenous injection of ^{18}F-FDG (3.45 MBq/kg; Covidien) and furosemide (10 mg), static emission scans in 3-dimensional mode were obtained, covering the neck, thorax, abdomen, and pelvis.

FIGURE 1. Study design. CRT = chemoradiotherapy.

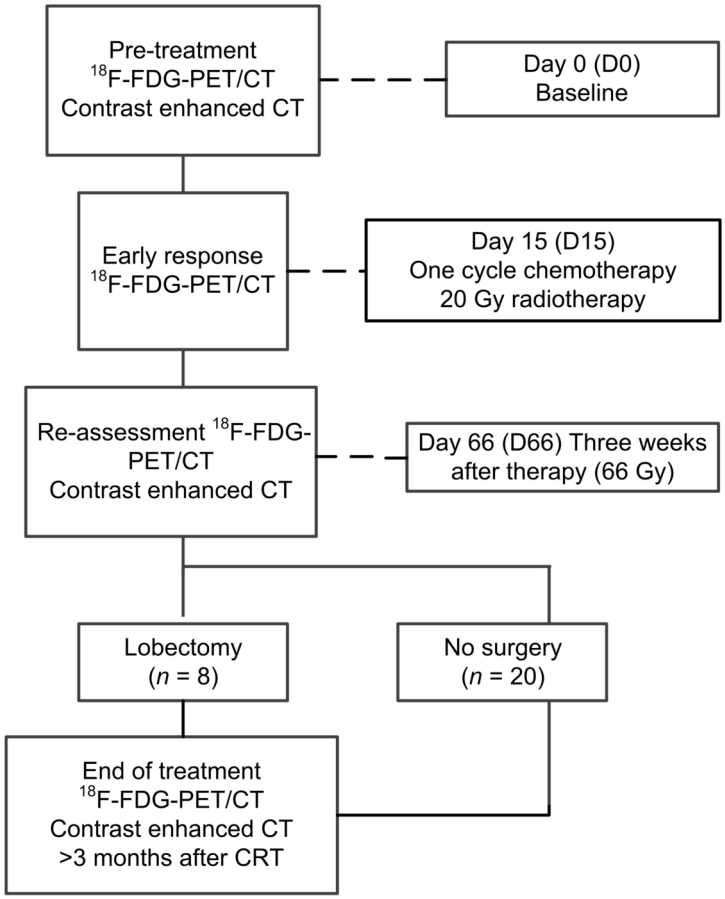

The PET acquisition time was 4 min per bed position. The second and third ^{18}F-FDG PET/CT scans were obtained covering the thorax only. PET scans were processed using iterative reconstruction with the ordered-subsets expectation maximisation algorithm (image matrix size, 128 · 128; 4 iterations, 16 subsets; and a 5-mm 3-dimensional Gaussian filter). The reconstructed images were corrected for injected dose, the decay of ^{18}F-FDG, patient body weight, and attenuation using a low-dose CT scan.

Standardised Uptake Value (SUV) and Total Lesion Glycolysis (TLG)

PET and CT scans were imported into Pinnacle^3 (version 8.0d; Philips Radiation Oncology Systems). All SUVs were derived from the ^{18}F-FDG PET/CT scans using semiautomatic delineation techniques. ^{18}F -FDG uptake was calculated as maximum SUV (SUV_{max}) within the metabolic active tumour volume (MTV) of the primary tumour and mean SUV. MTVs were delineated using 50% isocontour thresholds based on a fixed percentage of the maximum activity within the lesion, without background correction. Metastatic lymph nodes were analysed separately using a 50% method. Volume-weighted mean values of SUV in all ^{18}F-FDG–avid lesions per PET scan were derived to provide one value for each study. TLG was calculated using a summation of SUV · MTV (cm^3), including both the primary tumour and all metastatic lymph nodes.

Clinical Follow-up

The patient outcome data for time to progression was defined as the interval between the start of treatment and the date of documented disease progression as confirmed by imaging or biopsy. If a patient was progression-free at the closeout date (May 29, 2012), time to progression was censored to that date. Overall survival was measured from the date of treatment start to death. Patients still alive at the closeout date were censored for survival at that date.

Data and Statistical Analysis

All CT images were read by one experienced radiologist, who was masked for the early response PET data. The PET scans were read by consensus of 2 experienced nuclear medicine physicians. Regions of interest were defined using semiautomatic scripts, after input of target region of interest. The radiologists and nuclear physicians were masked to clinical outcome. Variation in parameters in sequential scans was normalised to baseline:
Δ = (pre-treatment – in treatment)/pre-treatment x 100%

Univariate analysis for progression-free survival (PFS) was performed on TLG, SUV, and TNM parameters. All SUV and TLG parameters were analysed as continuous variables. Variable selection for multivariate analysis was performed by both forward and backward stepwise covariate selection. The hazard ratio (HR) per unit parameter change and its 95% confidence interval were reported unless indicated otherwise. Survival curves were generated using the Kaplan–Meier method. Log-rank statistics were performed at different dichotomisation levels. All statistical analyses were performed using SPSS 18.0

(SPSS Inc.) for Windows (IBM). The level of statistical significance was defined as a P-value of less than 0.05 based on 2-sided tests.

RESULTS

Patients Characteristics and Follow-up

Thirty patients were included. Two patients were excluded because they did not receive an appropriate early in-treatment ^{18}F- FDG PET scan. Patient characteristics are summarised in *Table 1*. All patients received 60–66 Gy of radiotherapy and 2 cycles of chemotherapy. Total median treatment time was 45 days (range, 43–49 d). The end-of-treatment reassessment according to RECIST 1.1 revealed 16 patients as responders (complete responders, 0; partial responders, 16) and 12 patients as non-responders (stable disease, 11; progressive disease, 1). Seven patients, successfully pathologically downstaged and considered resectable, received a lobectomy. Protocol violation took place in 1 patient with persistent N2 disease (1 level). Thus, a total of 8 patients underwent lobectomy, with complete tumour resection (R0) in 7 of 8 patients. Pathologic assessment showed ypT0N0M0 status in 4 of 8 patients. Four patients showed residual viable tumour cells in the resected lobe, including the patient with persistent N2 disease.

Median follow-up was 16 months (range, 4–34 months), for the surviving patients 17 months (range, 4–34 months), and for deceased patients ten months (range, 4–23 months). During follow-up, nine patients died, all related to cancer progression. Overall survival at one and two years was 76% and 28%, respectively. Sixteen patients developed recurrent disease, three with progression of local disease, whereas distant metastases were detected in 13 patients (cerebral, n = 9; liver, n = 1; adrenal gland, n = 1; skin, n = 1; and bone, n = 1). Median time to progression was 12 months. PFS after treatment start was 62% after one year and 19% after two years.

TLG and Progression Free Survival

Pre-treatment TLG was 250.48 (±274.54) for the whole study group, whereas in-treatment TLG was 158.96 (±224.33). In stage IIIA patients, mean pre-treatment and in-treatment TLG were 176.51 (±171.59) and 108.66 (±147.26), respectively, whereas stage IIIB patients

TABLE 1. Patient Characteristics

Characteristic	Value
Age (y)	
Mean	59
Range	41–77
Age < 65	15 (54%)
Age ≥ 65	13 (46%)
Sex	
Male	18 (64%)
Female	10 (36%)
Histology	
Squamous cell carcinoma	11 (39%)
Adenocarcinoma	14 (50%)
Non–small cell not otherwise specified	3 (11%)
TNM stage (sixth edition)	
IIIA	17 (61%)
T0N2	1 (4%)
T1N2	3 (11%)
T2N2	8 (29%)
T3N2	5 (18%)
IIIB	11 (39%)
T1N3	3 (11%)
T2N3	1 (4%)
T4N0	3 (11%)
T4N2	2 (7%)
T4N3	2 (7%)
Performance score (ECOG)	
0	20 (71%)
1	8 (29%)
Smoking status	
Current smoker	12 (43%)
Former smoker	16 (57%)
Previous malignancy	
No	24 (86%)
Yes	4 (14%)
Adjuvant surgery	
No surgery	20 (71%)
Lobectomy	8 (29%)

had a mean TLG of 364.81 (±364.30) and 236.70 (±300.38). An overview of baseline TLG, in-treatment TLG, and ΔTLG for all patients is shown in *Table 2*. Univariate Cox regression analysis for PFS was used to analyse the relationships between covariates of interest (*Table 3*). Significant parameters for PFS were pre-treatment TLG, in-treatment TLG, MTV and ΔTLG. When ΔTLG for pre-treatment TLG was corrected, both factors remained significant for PFS (*Table 4*). A 10% less decrease in ΔTLG was associated with HR 1.169 (P = 0.033) for PFS. Every 10-unit increase from baseline TLG index was associated with HR 1.047 (P = 0.009).

To avoid data-driven significance for cut-off, ΔTLG was stratified at the median level. At a median level of 45% cut-off, patients with less than 45% decrease in ΔTLG (n = 14) had median PFS of 9.8 months, while patients with ≥ 45% decrease in ΔTLG (n = 14) had median PFS of 15.9 months (P = 0.032, log-rank test). PFS beyond 2 years occurred only in patients with ≥45% decrease in ΔTLG. Survival data and Kaplan-Meier curve for PFS at a median cut-off ΔTLG is shown in *Figure 2*, and PFS data at various cut-off points are shown in *Table 5*.

The following three risk groups were stratified: Favourable (baseline TLG < 500 and ≥ 38 % decrease in ΔTLG), intermediate (baseline TLG < 500 or ≥ 38 % decrease in ΔTLG) and unfavourable risk (baseline TLG ≥ 500 and < 38 % decrease in ΔTLG). A Kaplan-Meier of stratified risk groups is shown in *Figure 3*. Median survival in the favourable group was 17 months (range, 45.9–34.0 months), whereas in the intermediate group median survival was 11.8 months (range, 3.3–31.7 months). The unfavourable group had a median survival of 2.3 months (range, 2.1–4.5 months).

Figure 4 shows an example of two patients with sequential scans. Because ΔSUV showed a similar decrease, the difference in ΔTLG was apparent.

TABLE 2. TLG Evolution Sorted by TNM Subgroups

TNM stage (sixth edition)	n	Pre-treatment TLG	In-treatment TLG	ΔTLG (%)
IIIA (*n* = 17)				
T0N2	1 (4)	83.60	26.93	−67.79
T1N2	3 (11)	27.35	15.34	+ 43.91
		127.97	108.18	−15.46
		6.33	3.27	−48.31
T2N2	8 (29)	156.81	59.93	−61.78
		323.93	278.08	−14.16
		199.1	48.63	−75.57
		31.83	30.05	−5.59
		60.21	76.13	+26.45
		92.89	51.88	−44.15
		72.18	45.47	−37.00
		243.41	92.01	−62.20
T3N2	5 (18)	188.80	145.7	−22.83
		339.14	68.61	−79.77
		95.80	64.47	−32.70
		233.48	108.07	−53.71
		717.87	624.52	−13.00
IIIB (*n* = 11)				
T1N3	3 (11)	263.68	398.50	+51.13
		49.79	20.44	−58.94
		163.20	74.16	−54.56
T2N3	1 (4)	224.42	84.67	−62.27
T4N0	3 (11)	77.19	36.98	−52.10
		199.84	26.00	−86.99
		676.20	416.06	−38.47
T4N2	2 (7)	489.18	174.15	−64.40
		1319.04	1042.25	−20.98
T4N3	2 (7)	339.64	177.56	−47.72
		210.71	152.9	−27.43

Data in parentheses are percentages.

TABLE 3. Univariate Analysis Covariates and Effect on PFS (per Unit Change)

PET parameter	HR	95% confidence interval	p
Pre-treatment TLG	1.005	1.002–1.007	0.004
In-treatment TLG	1.005	1.003–1.008	0.001
ΔTLG	1.016	1.002–1.030	0.025
Pre-treatment SUV	Not significant	0.999–1.002	0.575
In-treatment SUV	Not significant	0.999–1.003	0.327
ΔSUV	Not significant	0.995–1.022	0.231
Pre-treatment SUVmax	Not significant	0.999–1.000	0.447
In-treatment SUVmax	Not significant	0.999–1.002	0.579
ΔSUVmax	Not significant	0.998–1.027	0.087
TNM (IIIA–IIIB)	Not significant	0.299–2.136	0.655

TABLE 4. Analysis of PFS, with ΔTLG Corrected for Pre-treatment TLG (per 10 Unit Change)

PET parameter	HR	95% confidence interval	P
ΔTLG	1.169	1.013–1.350	0.033
Pre-treatment TLG	1.047	1.020–1.076	0.009

TABLE 5. PFS at Various Cut-off Points in ΔTLG

	Median PFS (mo)	1-y PFS (%)	2-y PFS (%)	P
All patients	15.7	76	28	
ΔTLG decrease < 38% (n = 12)	6.3	36	0	0.020
ΔTLG decrease ≥ 38% (n = 16)	15.9	80	33	
ΔTLG decrease < 45% (n = 14)	9.8	46	0	0.032
ΔTLG decrease ≥ 45% (n = 14)	15.9	73	40	
ΔTLG decrease < 52% (n = 16)	9.8	47	0	0.035
ΔTLG decrease ≥ 52% (n = 12)	17.1	82	44	

FIGURE 2. Kaplan–Meier analysis of PFS at median cutoff in ΔTLG. Median, 1-y, and 2-y PFS was 15.9 mo, 73%, and 40%, respectively, for ΔTLG decrease ≥ 45% vs. 9.8 mo, 46%, and 0%, respectively, for ΔTLG decrease < 45% (log-rank test, P = 0.032).

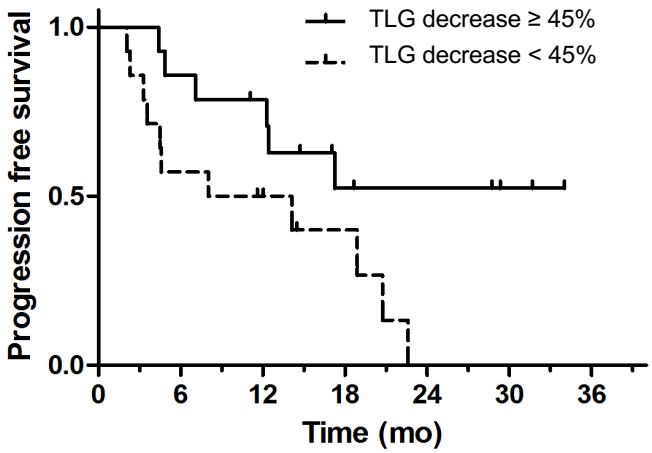

FIGURE 3. Kaplan–Meier analysis of favourable, intermediate, and unfavourable risk groups (log-rank test, P < 0.02).

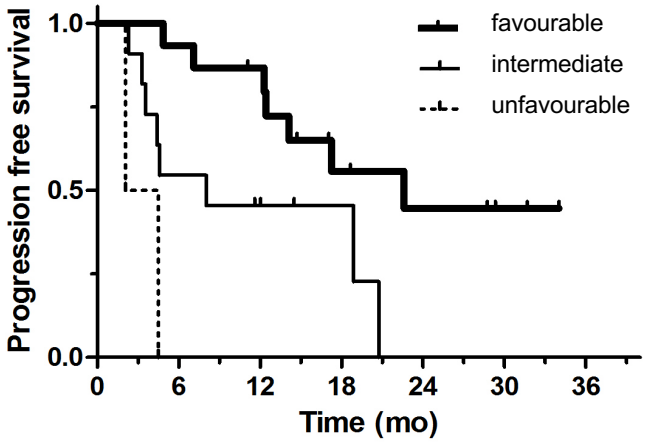

FIGURE 4. Typical example of 2 patients with stage III NSCLC and their sequential ^{18}F-FDG PET/CT scans: pre-treatment (D0), in-treatment (D15), and end of treatment (D66). Two weeks into concomitant chemoradiotherapy, patient A showed 14% decrease in in-treatment SUV, and 54% decrease in TLG, censored for both overall survival and PFS at 19 mo. Patient B showed 14% decrease in in-treatment SUV and TLG, PFS of 12 mo, and overall survival of 16 mo. All series are shown using equal window scaling.

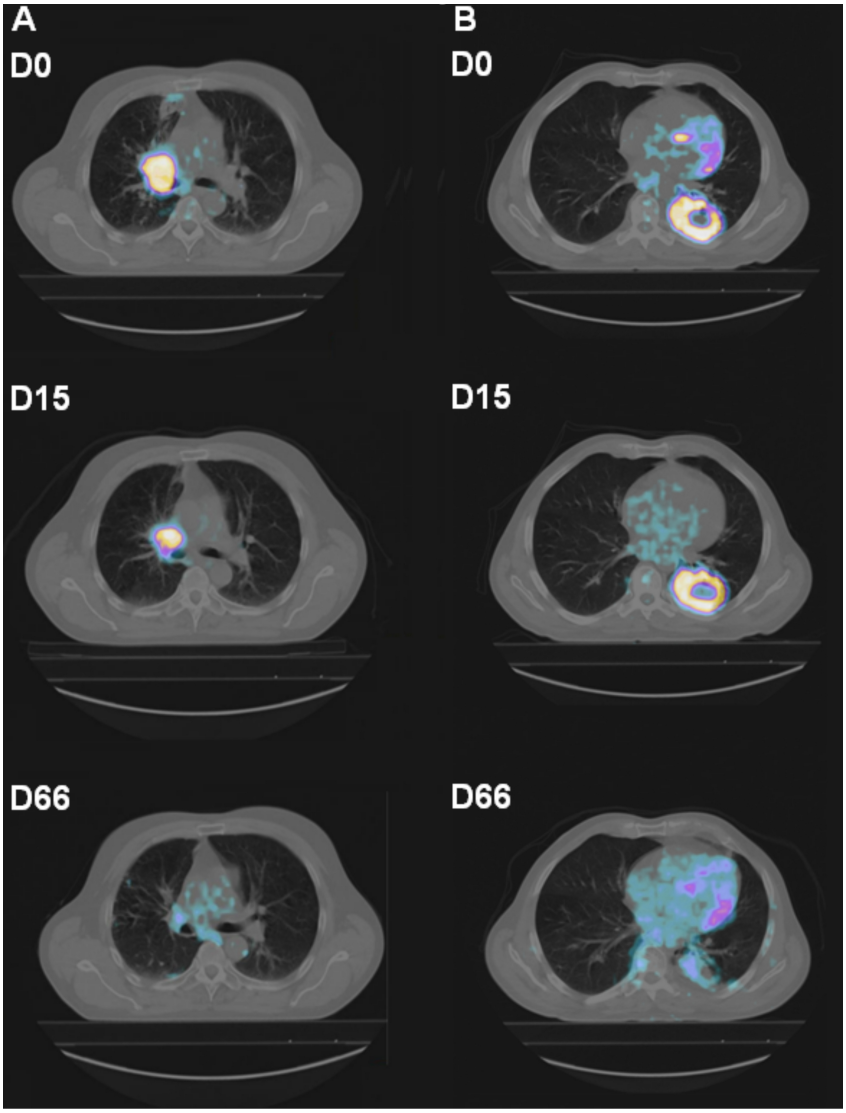

DISCUSSION

In the present prospective study, we investigated the predictive value of metabolic change assessed by ^{18}F-FDG PET/CT in locally advanced NSCLC treated with concomitant chemoradiotherapy. Pre-treatment and early in-treatment ^{18}F -FDG PET scans were compared with clinical outcome. Proportional hazards analysis revealed that a smaller decrease in ΔTLG was associated with earlier disease progression. Despite our relatively small study group of 28 patients, ΔTLG showed significant association with PFS. For a broad range of cut-off points in ΔTLG, with a corresponding range of 38%–52% decrease in ΔTLG, a significantly different log-rank probability between strata for PFS was repeatedly found ($P < 0.05$). However, an early metabolic response did not show a significant association with overall survival ($P = 0.10$). The absence of a significant correlation can at least partly be explained by the relatively short follow-up in this study.

Another finding was that pre-treatment TLG was prognostic for PFS. Only recently has the prognostic value of TLG in NSCLC been elucidated (20–22). Chen *et al.* (20) demonstrated that a whole-body TLG is a potentially useful indicator for PFS in NSCLC, because a high whole-body TLG (>655) is associated with poor prognosis. Concerning our study, one might reasonably question whether pre-treatment TLG was correlated with ΔTLG, arguing that a high-baseline TLG tends to show more decrease during treatment than lesions with low TLG. However, expression as a fractional change overcomes this issue by expressing ΔTLG as a fractional change from baseline. Furthermore, we showed in Cox regression that both ΔTLG and pre-treatment TLG remained significant for PFS. This significance indicates that both factors are independently associated with PFS, pre-treatment TLG being prognostic for survival before treatment, whereas ΔTLG is predictive of treatment response.

We can only hypothesise about the different trends in ΔTLG between patients. As treatment starts, the time course in ^{18}F-FDG uptake is dependent on many factors. First, a decrease in ^{18}F-FDG tumour uptake is expected from both tumour cell kill and a reversible metabolic effect (caused by quiescence of tumour cells) while the cells remain viable (23). Second, an increase in metabolic activity is expected from increased tumour cell repopulation, inflammation, and tumour-resistance mechanisms. Because radiation requires oxygen for its cytotoxic effects, cellular metabolism is changed under hypoxic conditions. Via upregulation of hypoxia-inducible factor -1α, change in cellular metabolism under hypoxic conditions leads to increased glycolysis, with a subsequent increased demand of glucose leading to upregulation of glucose transporters and eventually increased ^{18}F-FDG uptake (24–26). Because a high hypoxia-inducible factor-1α expression in NSCLC is associated with an earlier disease progression (27), we suspect resistance mechanisms to be correlated with less decrease in ΔTLG.

Unreliable outcome prediction of the end-of-treatment ^{18}F-FDG PET scans was most likely caused by postradiotherapy changes (28): ^{18}F-FDG uptake is not limited to accumulation in tumour tissue, but it also accumulates in macrophages, neutrophils, fibroblast, and granulation tissue (29). Multiple biologic processes such as proliferation, cell repair, and inflammation may conceal vital tumour residue. Serial follow-up PET/CT 3 and 6 months after treatment was performed to evaluate the evolution of ^{18}F-FDG uptake and post-irradiation inflammation. Using an in-treatment scan as early as 2-weeks of therapy possibly avoids confounding effects of multiple biologic processes. We suggest that in the second week, a metabolic tumour effect is at play, whereas other non–tumour-related biologic processes have a less significant role in the second week. A substantial decrease in ^{18}F-FDG uptake and volume might suggest tumour response to therapy.

The number of studies addressing response prediction using early in-treatment ^{18}F-FDG PET in locally advanced (stage III) NSCLC treated with concomitant therapy is limited. A previous study by Huang *et al.* (30) in stage III and IV NSCLC found that ^{18}F-FDG PET after three weeks (and 40 Gy) of concomitant chemoradiotherapy had preceded morphologic response. However, no effect on PFS and overall survival was presented. Macchessi *et al.* (31) showed in unresectable stage II and III NSCLC no correlation for metabolic change on in-treatment ^{18}F-FDG PET and clinical outcome. The relatively wide range (10–25 days relative to 10–12 days in our study) of the second scan may have hampered the study. By applying TLG, both volumetric (MTV) and metabolic information (SUV) are incorporated, resulting in a more sensitive method for detection of treatment response relative to SUV alone. The general concept of using TLG and ΔTLG for tumour treatment response was first introduced by Larson *et al.* (32), who calculated ΔTLG as a response index, also called the Larson–Ginsberg index. To our knowledge, the present study is the first study to show the predictive value of ΔTLG for early response monitoring in locally advanced NSCLC treated with concomitant chemoradiotherapy. Despite the promising results, the small number of patients and large heterogeneity in metabolic tumour activity are limiting factors. We could not investigate the reliability of response monitoring in small tumours (i.e., <1 cm) or tumours with low metabolic uptake, in which a variety of technical factors may hamper adequate and reproducible calculation of the fractional change in tumour lesion glycolysis. However, by implementing standard methods of data analysis, the use of ^{18}F-FDG PET early during treatment seems clinically feasible. One major restriction of the current study was the relatively small number of patients included. Even though TLG displayed prognostic and predictive potential in univariate analysis, a robust multivariate analysis, correcting for known prognostic factors (i.e., age, histology, disease stage, performance status), remained unexplained. Therefore, other confounding factors cannot be fully excluded in this study.

Consequently, confirmation of our findings is needed in larger study populations. Also, research is needed to further individualise treatment in stage III non–small cell lung cancer. Patients showing early metabolic nonresponse could prove to be candidates for dose escalation regimes, possibly improving clinical outcome (33). These kinds of studies set the basis for PET-based response–adapted treatment algorithms, which are the promise of the near future; the choice of therapy, its intensity, and its duration will become better adjusted to the biology of the individual patient.

CONCLUSION

The current study in locally advanced NSCLC patients treated with concomitant chemoradiotherapy indicates that early in-treatment ^{18}F-FDG PET can be used to predict outcome. The effect of combined treatment does not preclude its predictive capabilities, because we found ΔTLG was predictive of PFS. Both pre-treatment TLG and the degree of change in TLG may be useful tools for individualising treatment in locally advanced NSCLC.

References

1. El-Sharouni SY, Kal HB, Battermann JJ, Schramel FM. Sequential versus concurrent chemo-radiotherapy in inoperable stage III non-small cell lung cancer. Anticancer Res. 2006;26:495–505.
2. Govindan R, Bogart J, Vokes EE. Locally advanced non-small cell lung cancer: the past, present, and future. J Thorac Oncol. 2008;3:917–928.
3. Aupérin A, Le Pechoux C, Rolland E, et al. Meta-analysis of concomitant versus sequential radiochemotherapy in locally advanced non-small-cell lung cancer. J Clin Oncol. 2010;28:2181–2190.
4. Albain KS, Swann RS, Rusch VW, et al. Radiotherapy plus chemotherapy with or without surgical resection for stage III non-small-cell lung cancer: a phase III randomised controlled trial. Lancet. 2009;374:379–386.
5. van Baardwijk A, Reymen B, Wanders S, et al. Mature results of a phase II trial on individualised accelerated radiotherapy based on normal tissue constraints in concurrent chemo-radiation for stage III non-small cell lung cancer. Eur J Cancer. 2012;48:2339–2346.
6. Machtay M, Bae K, Movsas B, et al. Higher biologically effective dose of radiotherapy is associated with improved outcomes for locally advanced nonsmall cell lung carcinoma treated with chemoradiation: an analysis of the Radiation Therapy Oncology Group. Int J Radiat Oncol Biol Phys. 2012;82:425–434.
7. Bussink J, Kaanders JH, van der Graaf WT, Oyen WJ. PET-CT for radiotherapy treatment planning and response monitoring in solid tumors. Nat Rev Clin Oncol. 2011;8:233–242.
8. Eisenhauer EA, Therasse P, Bogaerts J, et al. New response evaluation criteria in solid tumours: revised RECIST guideline (version 1.1). Eur J Cancer. 2009;45:228–247.
9. Wahl RL, Jacene H, Kasamon Y, Lodge MA. From RECIST to PERCIST: evolving considerations for PET response criteria in solid tumors. J Nucl Med. 2009; 50:122S–150S.
10. Mac Manus MP, Hicks RJ, Matthews JP, et al. Positron emission tomography is superior to computed tomography scanning for response-assessment after radical radiotherapy or chemoradiotherapy in patients with non-small-cell lung cancer. J Clin Oncol. 2003;21:1285–1292.
11. Liu-Jarin X, Stoopler MB, Raftopoulos H, Ginsburg M, Gorenstein L, Borczuk AC. Histologic assessment of non-small cell lung carcinoma after neoadjuvant therapy. Mod Pathol. 2003;16:1102–1108.

12. de Geus-Oei LF, van der Heijden HF, Corstens FH, Oyen WJ. Predictive and prognostic value of FDG-PET in nonsmall-cell lung cancer: a systematic review. Cancer. 2007;110:1654–1664.
13. Lee DH, Kim SK, Lee HY, et al. Early prediction of response to first-line therapy using integrated 18F-FDG PET/CT for patients with advanced/metastatic nonsmall cell lung cancer. J Thorac Oncol. 2009;4:816–821.
14. Vansteenkiste JF, Stroobants SG, De Leyn PR, Dupont PJ, Verbeken EK. Potential use of FDG-PET scan after induction chemotherapy in surgically staged IIIa-N2 non-small-cell lung cancer: a prospective pilot study. The Leuven Lung Cancer Group. Ann Oncol. 1998;9:1193–1198.
15. Nahmias C, Hanna WT, Wahl LM, Long MJ, Hubner KF, Townsend DW. Time course of early response to chemotherapy in non-small cell lung cancer patients with 18F-FDG PET/CT. J Nucl Med. 2007;48:744–751.
16. Weber WA, Petersen V, Schmidt B, et al. Positron emission tomography in non small-cell lung cancer: prediction of response to chemotherapy by quantitative assessment of glucose use. J Clin Oncol. 2003;21:2651–2657.
17. van Baardwijk A, Bosmans G, Dekker A, et al. Time trends in the maximal uptake of FDG on PET scan during thoracic radiotherapy: a prospective study in locally advanced non-small cell lung cancer (NSCLC) patients. Radiother Oncol. 2007;82:145–152.
18. de Geus-Oei LF, van der Heijden HF, Visser EP, et al. Chemotherapy response evaluation with 18F-FDG PET in patients with non-small cell lung cancer. J Nucl Med. 2007;48:1592–1598.19. Boellaard R, O'Doherty MJ, Weber WA, et al. FDG PET and PET/CT: EANMprocedure guidelines for tumour PET imaging—version 1.0. Eur J Nucl Med Mol Imaging. 2010;37:181–200.
19. Chen HH, Chiu NT, Su WC, Guo HR, Lee BF. Prognostic value of whole-body total lesion glycolysis at pretreatment FDG PET/CT in non-small cell lung Cancer. Radiology. 012;264:559–566.
20. Zhang H, Wroblewski K, Liao S, et al. Prognostic value of metabolic tumor burden from 18F-FDG PET in surgical patients with non-small-cell lung cancer. Acad Radiol. 2013;20:32–40.
21. Liao S, Penney BC, Wroblewski K, et al. Prognostic value of metabolic tumor burden on 18F-FDG PET in nonsurgical patients with non-small cell lung cancer. Eur J Nucl Med Mol Imaging. 2012;39:27–38.
22. Patz EF Jr, Connolly J, Herndon J. Prognostic value of thoracic FDG PET imaging after treatment for non-small cell lung cancer. AJR. 2000;174:769–774.

23. Moeller BJ, Cao Y, Li CY, Dewhirst MW. Radiation activates HIF-1 to regulate vascular radiosensitivity in tumors: role of reoxygenation, free radicals, and stress granules. Cancer Cell. 2004;5:429–441.
24. Meijer TW, Kaanders JH, Span PN, Bussink J. Targeting hypoxia, HIF-1, and tumor glucose metabolism to improve radiotherapy efficacy. Clin Cancer Res.2012;18:5585–5594.
25. Meijer TW, Schuurbiers OC, Kaanders JH, et al. Differences in metabolism between adeno- and squamous cell non-small cell lung carcinomas: spatial distribution and prognostic value of GLUT1 and MCT4. Lung Cancer. 2012;76:316–323.
26. Yohena T, Yoshino I, Takenaka T, et al. Upregulation of hypoxia-inducible factor-1alpha mRNA and its clinical significance in non-small cell lung cancer. J Thorac Oncol. 2009;4:284–290.
27. Kong FM, Frey KA, Quint LE, et al. A pilot study of [18F]fluorodeoxyglucose positron emission tomography scans during and after radiation-based therapy in patients with non small-cell lung cancer. J Clin Oncol. 2007;25:3116–3123.
28. Kubota R, Yamada S, Kubota K, Ishiwata K, Tamahashi N, Ido T. Intratumoral distribution of fluorine-18-fluorodeoxyglucose in vivo: high accumulation in macrophages and granulation tissues studied by microautoradiography. J Nucl Med. 1992;33:1972–1980.
29. Huang W, Zhou T, Ma L, et al. Standard uptake value and metabolic tumor volume of 18F-FDG PET/CT predict short-term outcome early in the course of chemoradiotherapy in advanced non-small cell lung cancer. Eur J Nucl Med Mol Imaging. 2011;38:1628–1635.
30. Massaccesi M, Calcagni ML, Spitilli MG, et al. 18 F-FDG PET-CT during chemoradiotherapy in patients with non-small cell lung cancer: the early metabolic response correlates with the delivered radiation dose. Radiat Oncol. 2012;7:106.
31. Larson SM, Erdi Y, Akhurst T, et al. Tumor treatment response based on visual and quantitative changes in global tumor glycolysis using PET-FDG imaging: the visual response score and the change in total lesion glycolysis. Clin Positron Imaging. 1999;2:159–171.
32. De Ruysscher D, van Baardwijk A, Steevens J, et al. Individualised isotoxic accelerated radiotherapy and chemotherapy are associated with improved longterm survival of patients with stage III NSCLC: a prospective population-based study. Radiother Oncol. 2012;102:228–233


Read online

CHAPTER IV

Lung cancer - Metabolic activity measured by FDG PET predicts pathological response in locally advanced superior sulcus NSCLC

Edwin A. Usmanij, Johan Bussink, Lioe-Fee de Geus-Oei

Adapted from: Lung Cancer 2014; 86(3):374

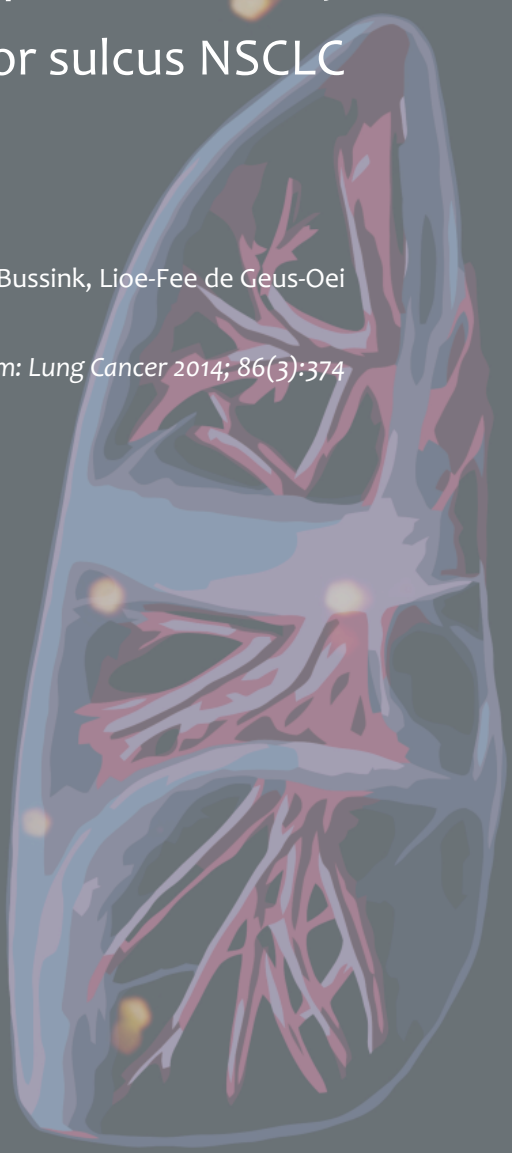

4

Lung cancer - Metabolic activity measured by FDG PET predicts pathological response in locally advanced superior sulcus NSCLC

To the Editor,

We commended Bahce *et al.* for their excellent paper entitled "Metabolic activity measured by FDG PET predicts pathological response in locally advanced superior sulcus NSCLC" (1). This study shows the prognostic and predictive performance of FDG PET in non-small cell lung cancer (NSCLC) in correlation with the post-induction pathological response. Metabolic activity after chemoradiotherapy correlated with the amount of residual tumour cells. In this letter, we will discuss the moment of reassessment of response using FDG-PET/CT.

Many studies support the importance of reassessment using FDG-PET/CT for neo-adjuvant therapy before surgery, published in a review of Hicks (2). However, post-induction response assessment does not allow for early treatment adaptations. There is growing evidence of the usefulness of an early in-treatment measurement for response prediction: recent studies in locally advanced NSCLC show that in-treatment response measurement using functional information by means of FDG-PET is able to identify patients with long-term progression-free survival (3-6). In a series of 28 patients with locally advanced NSCLC, we showed that a change in FDG uptake, in terms of total lesion glycolysis, was associated with a significantly longer progression-free survival (1-y PFS 80% vs 36%, P = 0.02). We concluded that the degree of change in glycolysis at the end of the second week of chemoradiotherapy was predictive of response (6). Early in-treatment assessment may offer the opportunity to make response adapted-treatment decisions. An intensified scheme of induction radiotherapy can be offered to patients that are likely to fail locally, or adaptation of systemic treatment can be offered to patients who are at higher risk for distant relapse.

Therefore, we would like to underline the importance of early in-treatment response assessments, at a time point that treatment can still be adjusted. This might accelerate the adoption of personalised medicine in the field of advanced NSCLC. PET-guided treatment algorithms are the promise of the near future; the choice of the treatment regimen, its intensity, and its duration will become better adjusted to the biology of the individual patient. Today's primary challenge is to investigate the impact on patient outcome of personalised response-adapted treatment concepts.

References

1. Bahce I, Vos CG, Dickhoff C, Hartemink KJ, Dahele M, Smit EF, et al. Metabolicactivity measured by FDG PET predicts pathological response in locally advanced superior sulcus NSCLC. Lung Cancer 2014;85(2):205–12.
2. Hicks RJ. Role of 18F-FDG PET in assessment of response in non-small cell lung cancer. J Nucl Med 2009;5(Suppl. 1):31S–42S.
3. Novello S, Vavala T, Levra MG, Solitro F, Pelosi E, Veltri A, et al. Early response to chemotherapy in patients with non-small-cell lung cancer assessed by [18F]-fluoro-deoxy-d-glucose positron emission tomography and computedtomography. Clin Lung Cancer 2013;14(3):230–7.
4. van Elmpt W, Ollers M, Dingemans AM, Lambin P, De Ruysscher D. Response assessment using 18F-FDG PET early in the course of radiotherapy correlates with survival in advanced-stage non-small cell lung cancer. J Nucl Med 2012;53(October (10)):1514–20.
5. Everitt SJ, Ball DL, Hicks RJ, Callahan J, Plumridge N, Collins M, et al. Differential 18F-FDG and 18F-FLT uptake on serial PET/CT imaging before and during definitive chemoradiation for non-small cell lung cancer. J Nucl Med 2014;55(May(7)):1069–74.
6. Usmanij EA, de Geus-Oei LF, Troost EG, Peters-Bax L, van der Heijden EH, Kaanders JH, et al. 18F-FDG PET early response evaluation of locally advanced non-small cell lung cancer treated with concomitant chemoradiotherapy. J Nucl Med 2013;54(September (9)):1528–34.

4


Read online

CHAPTER V

Performance of automatic image segmentation algorithms for calculating total lesion glycolysis for early response monitoring in non-small cell lung cancer patients during concomitant chemoradiotherapy

Willem Grootjans*, Edwin A. Usmanij*, Wim J.G. Oyen,
Erik H.F.M. van der Heijden, Eric P. Visser, Dimitris Visvikis, Mathieu Hatt,
Johan Bussink, Lioe-Fee de Geus-Oei

*Willem Grootjans and Edwin A. Usmanij contributed equally to this work

Adapted from: Radiotherapy & Oncology. 2016 Jun;119(3):473-9

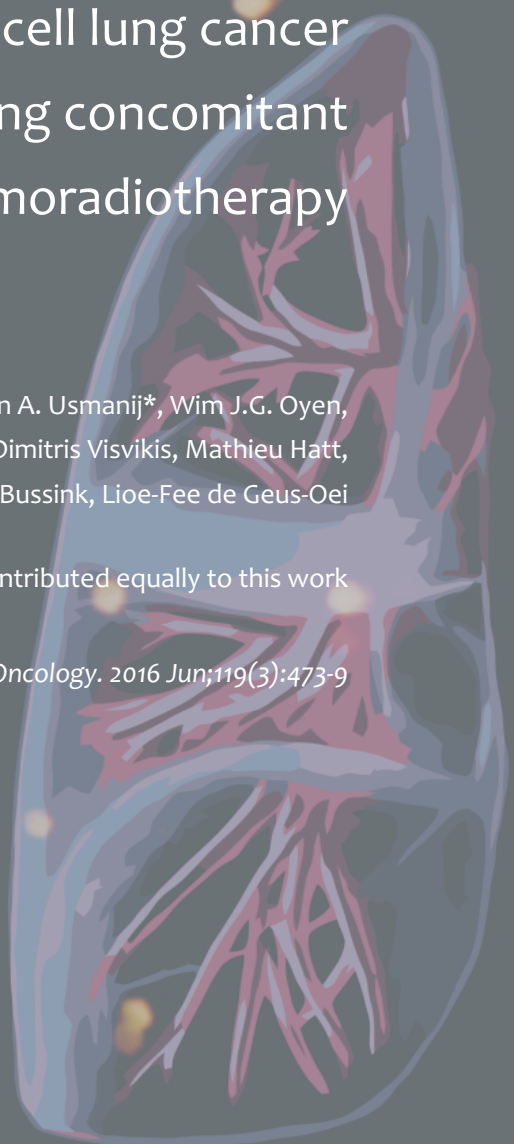

5

ABSTRACT

Objectives

This study evaluated the use of total lesion glycolysis (TLG) determined by different automatic segmentation algorithms, for early response monitoring in non-small cell lung cancer (NSCLC) patients during concomitant chemoradiotherapy.

Materials and methods

Twenty-seven patients with locally advanced NSCLC treated with concomitant chemoradiotherapy underwent ^{18}F-fluorodeoxyglucose (FDG) PET/CT imaging before and in the second week of treatment. Segmentation of the primary tumours and lymph nodes was performed using fixed threshold segmentation at (i) 40% SUVmax (T40), (ii) 50% SUVmax (T50), (iii) relative-threshold-level (RTL), (iv) signal-to-background ratio (SBR), and (v) fuzzy locally adaptive Bayesian (FLAB) segmentation. Association of primary tumour TLG (TLG_T), lymph node TLG (TLG_{LN}), summed TLG ($TLG_S = TLG_T + TLG_{LN}$), and relative TLG decrease (ΔTLG) with overall survival (OS) and progression-free survival (PFS) was determined using univariate Cox regression models.

Results

Pre-treatment TLG_T was predictive for PFS and OS, irrespective of the segmentation method used. The inclusion of TLG_{LN} improved disease and early response assessment, with pre-treatment TLG_S more strongly associated with PFS and OS than TLG_T for all segmentation algorithms. This was also the case for ΔTLG_S, which was significantly associated with PFS and OS, with the exception of RTL and T40.

Conclusion

ΔTLG_S was significantly associated with PFS and OS, except for RTL and T40. The inclusion of TLG_{LN} improves early treatment response monitoring during concomitant chemoradiotherapy with FDG-PET.

Keywords

Early response prediction, locally advanced non-small lung cancer, segmentation algorithms

INTRODUCTION

Non-small cell lung (NSCLC) cancer remains a disease with a generally poor prognosis (1). At the time of diagnosis, one-third of patients with NSCLC present with locally advanced non-metastatic disease (1). For these patients, radiotherapy in combination with chemotherapy is the accepted standard of care. With the aim of improving patient outcome, combined and intensified treatment approaches are increasingly being investigated. However, not all patients equally benefit from these treatment approaches and rational selection of available treatment options in a personalised medicine framework is required (2).

Positron emission tomography (PET) in combination with X-ray computed tomography (CT) with the glucose analogue ^{18}F-fluorodeoxyglucose (FDG) has proven to be a valuable tool to personalise treatment for this patient group (2). Firstly, the incorporation of FDG-PET images into the radiotherapy planning algorithm improves the definition of gross tumour volume (GTV) (3-5) and might facilitate the concept of selective nodal irradiation (6). Secondly, it has been shown that FDG-PET can identify areas that are at risk of local relapse (7, 8), permitting to use the concept of molecular imaging-based dose painting (9). Thirdly, several studies emphasise the ability of FDG-PET to monitor therapy response at an early treatment stage using quantitative PET indices (10-14). Early response monitoring during treatment can facilitate clinical decision-making and improve patient management through early treatment adaptation and thereby avoidance of unnecessary side effects and costs of ineffective treatment.

However, employing the concept of FDG-PET-guided treatment decisions requires robust and standardised methods to derive these quantitative indices from PET images. Particularly, the strong dependence of most image-derived response indices on quantification of lesion volume emphasises the need for standardised and consistent determination of these volumes in PET images. In this regard, there has been widespread interest in the development of automated segmentation algorithms for PET. Over the years, there has been a rapid growth of segmentation algorithms for PET reported in the literature (15), an event which is also referred to as "*yapetism*" ("yet another PET segmentation method") (16). Difficulties encountered by these algorithms for automatic lesion segmentation in PET images are local contrast variations due to heterogeneous FDG uptake in the lesion, adjacent FDG-avid anatomy and lymph nodes, and relatively high noise content of PET images, often rendering the task of automatic lesion delineation challenging (15). This becomes even more difficult when automatic segmentation has to be performed on low contrast interim and end-of-treatment PET images, where radiotracer uptake can be considerably reduced due to therapy effects. However, up until this day, there is no standardised method for automatically determining lesion volume on PET

images and many studies consider different segmentation algorithms for this purpose (17, 18). The purpose of this study was to evaluate this clinical applicability and performance of several established segmentation algorithms for generating plausible segmentation volumes that can be applied specifically to predict therapy response during treatment for patients with locally advanced stage IIIA or IIIB NSCLC treated with concomitant chemoradiotherapy. The predictive value of total lesion glycolysis (TLG), as determined by these different algorithms, for progression-free survival (PFS) and overall survival (OS) was evaluated.

MATERIALS AND METHODS

Patients

A total of 27 patients with newly diagnosed stage IIIA or stage IIIB NSCLC were prospectively included in this study, as described before (10). Patients were treated with concomitant radiotherapy and chemotherapy. This study was approved by the institutional review board (IRB) of the Radboud university medical centre. Written informed consent was obtained from every patient. Patient characteristics are summarised in *Table 1*.

Treatment and follow-up

Intensity-modulated radiotherapy (IMRT) was performed (10 MV photons), consisting of 33 fractions of 2 Gy (5 fractions a week for 6 weeks and 3 days) resulting in a total dose of 66 Gy on the primary tumour and affected lymph nodes (i.e. pathologically proven or FDG-avid lymph nodes). Chemotherapy consisted of two cycles of cisplatin 50 mg/m^2 intravenously (day 1, 8, 22, and 29) and etoposide 100 mg/m^2 intravenously (day 1–3, and day 22–24). Median overall treatment time was 45 days (range 43–48 days). Patients with progressive disease during follow-up received palliative treatment. Follow-up during and after treatment consisted of clinical examination at regular intervals. When residual or recurrent disease was suspected, chest X-ray and chest CT-scans were performed. For each patient, sequential FDG-PET/CT imaging was performed before and during treatment. The pre-treatment scan was obtained before treatment (median 11 days, range 1–28 days) whilst interim FDG-PET imaging was performed in the second week during concomitant treatment (median 14 days, range 13–16 days), always before the second cycle of chemotherapy after 20 Gy radiotherapy. According to the treatment protocol all patients started with radiotherapy on the first day of the first cycle of chemotherapy, i.e. no neo-adjuvant treatment was applied.

TABLE 1. Patients characteristics.

Characteristics of patient population	
Male (Female)	18 (9)
Median age (range) [y]	58 (42–77)
Histological type	
Non-small cell lung cancer (NSCLC)	
Squamous cell carcinoma	10
Adenocarcinoma	14
NSCLC not otherwise specified	3
Disease stage	
IIIA	20
IIIB	7
Performance-score (ECOG)	
0	20
1	7
Smoking status	
Current smoker	11
Former smoker	16
Lesion location	
Right upper lobe	10
Right middle lobe	4
Right lower lobe	2
Left upper lobe	7
Left lower lobe	2
Pre-treatment PET acquisition	
Number of bed positions	7–8
Administered FDG activity [MBq]	267 ± 48
Incubation time [min]	75 ± 7.5
Acquisition time per bed position [min]	4
Interim PET acquisition	
Number of bed positions	3–4
Administered FDG activity [MBq]	269 ± 49
Incubation time [min]	78 ± 8.0
Acquisition time per bed position [min]	4

Data are reported as mean ± standard deviation. PET = positron emission tomography, FDG = ^{18}F-fluorodeoxyglycose.

Patient preparation and FDG PET imaging

Imaging was performed using a hybrid Biograph Duo PET/CT scanner (Siemens Medical Solution, Knoxville, TN, USA). The PET scanner was accredited by the Research 4 Life (EARL) initiative for quantitative FDG-PET/CT studies (19). Before image acquisition, patients fasted for at least six hours and blood glucose levels were lower than 8.2 mmol L^{-1} in all patients. The amount of activity administered to the patient was adjusted to the patient's weight and was 3.45 MBq kg^{-1}. Details regarding the PET acquisition protocol are summarised in *Table 1*. No respiratory gating was performed. For the purpose of attenuation correction and anatomical reference, a low dose (LD) CT scan was acquired with a reference tube current time product of 40 mA s. LDCT scans were acquired during timed unforced expiration breath-hold. Modulation of X-ray tube current was performed using CARE Dose 4D. Reconstruction of PET images was performed with a 2D ordered subset expectation maximization (2DOSEM) algorithm using a matrix size of 128 × 128, 4 iterations and 16 subsets. Post-reconstruction filtering was performed using a three-dimensional Gaussian filter kernel with a full width at half maximum of 5 mm.

Image segmentation

The primary tumour and FDG positive lymph nodes were delineated on the pre-treatment and interim PET images. Firstly, delineation was performed using a fixed threshold region growing segmentation at 40% (T40) and 50% (T50) of the maximum standardised uptake value (SUV_{max}) value. Furthermore, adaptive threshold algorithms were used for image segmentation. These included the iterative relative-threshold-level (RTL) (20) and signal-to-background ratio (SBR) (21) approach. For the SBR method, the background for segmentation of the primary tumour was defined by placing a volume of interest (VOI) in the parenchyma of the contralateral lung. For lymph node segmentation, the background was defined by placing a VOI near the aortic root in the mediastinum. The seed-point for the T40, T50, RTL, and SBR segmentation was the SUV_{max} voxel of either the primary tumour ($SUV_{T,max}$) or the corresponding lymph nodes ($SUV_{LN,max}$). The threshold-based segmentations were performed using the Inveon Research Workplace (IRW) 4.1 Software (Preclinical Solutions, Siemens Medical Solutions USA, Knoxville Tennessee, USA). In addition to threshold-based segmentation, image segmentation was performed using the fuzzy locally adaptive Bayesian (FLAB) algorithm (22). Segmentation with this algorithm is performed using custom in-house developed software (ImageD, LaTIM Université de Bretagne Occidentale, Brest, France). The number of classes for segmentation was limited to two and parameters were automatically determined by the software.

Image analysis

The TLG of the primary tumour (TLG_T), defined as the product of the mean tumour FDG uptake ($SUV_{T,mean}$) and metabolic tumour volume (MTV), was calculated on the pre-treatment and interim PET images. Similarly, lymph node TLG (TLG_{LN}) was defined as the mean uptake of the lymph nodes ($SUV_{LN,mean}$) and the corresponding metabolic volumes of the lymph nodes. Furthermore, a summed TLG ($TLG_S = TLG_T + TLG_{LN}$) was calculated. Evaluation of therapy response was performed by calculating the fractional decrease in TLG between pre-treatment and interim PET images (ΔTLG). Segmentation performance of the different algorithms was evaluated through visual assessment by a nuclear medicine physician experienced in thoracic imaging. Segmentation failures were visually identified and were defined as the propagation of segmentation into other anatomical structures, or premature termination of the algorithm resulting in only partial segmentation of the primary tumour and lymph nodes. Lesions that could not be properly segmented according to these criteria were omitted from the analysis. In addition, the similarity between MTVs obtained with different segmentation algorithms was quantified by calculating the spatial overlap using a generalization of the Jaccard Index (JI), as described in *Eq. (1)*.

Eq. (1)

$$JI(A, B, \ldots, n) = \frac{|A \cap B \cap \ldots \cap n|}{|A \cup B \cup \ldots \cup n|}$$

Here the numerator $|A \cap B \cap \ldots \cap n|$ denotes the intersection between segmented volumes (in this study, five in total), whilst the denominator $|A \cup B \cup \ldots \cup n|$ represents the union of the segmented volumes. Perfect spatial overlap is indicated by a value for the JI of 1.0, whilst a value of 0 indicates no spatial overlap of the volumes.

Clinical outcome and statistical analysis

Statistical analysis was performed using SPSS Statistics 20 (IBM, Armonk, New York, USA) and GraphPad Prism, version 4.0c (GraphPad Software Inc, La Jolla, California, USA). PFS was defined as the interval between the start of treatment and the date of documented disease progression as confirmed by imaging or biopsy. If a patient was progression-free at the closeout-date (January 2015), the patient was censored for PFS at that date. Similarly, if patients were still alive at the closeout-date, patients were censored for OS. The predictive value of pre-treatment TLG and ΔTLG was determined for different segmentation algorithms using univariate Cox regression analysis. Correlation between the MTVs and TLGs of different segmentation algorithms was calculated using Spearman rank correlation. Statistical significance was defined for $P < 0.05$.

RESULTS

The median follow-up time for this patient population was 23.4 months (range 3.5–61.9). During follow-up eighteen patients died, all related to cancer progression. Three patients were lost during follow-up. A total of twenty patients developed disease recurrence during follow-up; seven patients developed progression of local disease, whilst metastases were seen in 13 patients. Median time to disease progression was 21 months. PFS after study-baseline at 1 year was 63% (17 out of 27).

Of the 27 patients, 25 had a visible primary tumour. For the other two patients, there was no radiological evidence for a primary tumour (i.e. cT_0). The smallest pre-treatment MTVs were obtained when segmentation was performed with the T50 segmentation algorithm (24.7 ± 30.8 mL), compared to T40 (34.8 ± 39.1 mL), SBR (38.7 ± 42.4 mL) RTL (30.7 ± 34.0 mL). Segmentation with FLAB resulted in the largest MTVs (42.3 ± 42.1 mL). Interim PET MTVs showed similar trends with the smallest MTV for the T50 (20.8 ± 32.6 mL) method, followed by T40 (31.6 ± 44.6 mL), RTL (26.8 ± 37.0 mL), SBR (36.2 ± 50.2 mL) and FLAB (37.6 ± 48.2 mL). For the pre-treatment PET images, an excellent correlation was found between delineation methods for MTV (range ϱ 0.97–1.0, $P < 0.0005$), TLG_T (range ϱ 0.95–1.0, $P < 0.0005$) and $SUV_{T,mean}$ (range ϱ 0.98–1.0, $P < 0.0005$). Similarly, for in-treatment PET images, an excellent correlation was found between delineation methods for MTV (range ϱ 0.93–1.0, $P < 0.0005$), TLG_T (range ϱ 0.94–1.0, $P < 0.0005$) and $SUV_{T,mean}$ (range ϱ 0.94–1.0, $P < 0.0005$).

Quantitative and visual analysis of the MTVs obtained with different segmentation algorithms revealed that the MTVs were highly similar regarding the shape and spatial overlap. Furthermore, the algorithms revealed a similar trend in $SUV_{T,mean}$ and MTV

change between pre-treatment and interim FDG-PET (Supplementary data). The T50 volumes were always entirely enveloped by the other volumes. The generalised JI for all MTVs on the pre-treatment and interim PET was 0.58 ± 0.13 (range 0.31–0.78) and 0.53 ± 0.16 (range 0.20–0.86). When the T50 volumes were omitted from the analysis, the mean JI for pre-treatment and interim PET volumes was 0.74 ± 0.12 (range 0.46–0.89) and 0.71 ± 0.14 (range 0.47–0.96). In tumours with heterogeneous FDG uptake, the T50 algorithm yielded contours that were more erratic and sensitive to discontinuities within the tumour, whilst FLAB, SBR, RTL, and T40 algorithms would segment patches with FDG-uptake continuously throughout the entire lesion, giving an improved representation of the total volume with FDG-uptake.

In the pre-treatment PET images, FLAB segmentation resulted in one segmentation failure of the primary tumour in one patient due to the small size and low contrast. In this patient, all segmentation methods failed to segment the primary tumour in the interim PET images. Furthermore, the T40, T50, RTL, and SBR methods failed to segment the primary tumour in an additional patient that presented with a large lesion with extended growth into the central mediastinum on interim PET images. The FLAB algorithm could segment the primary tumour in this patient and did not show uncontrolled propagation of segmentation into the mediastinal background.

Of the 27 patients, 18 patients had FDG positive lymph nodes on the pre-treatment PET images. Given the smaller volumes and in general lower contrast of mediastinal and hilar lymph nodes, there were considerably more segmentation failures when performing automatic segmentation of lymph nodes. The T40 and RTL algorithms failed to segment 14 and 17 of the 41 lymph nodes on the pre-treatment PET images, respectively. The number of segmentation failures for the T50 and FLAB algorithms in the pre-treatment PET images was 9 and 8, respectively. The SBR algorithm had the fewest segmentation failures, with only 6 lymph node segmentation failures in the pre-treatment PET images.

Reduction of lymph node contrast due to therapy effects on the interim PET images resulted in more segmentation failures for the T40, T50, RTL and FLAB algorithms. Of the 41 lymph nodes in the interim PET, there were 24 segmentation failures for the T40 and RTL algorithms. For the T50 and FLAB method, 12 and 14 lymph node segmentation failures occurred in the interim PET, respectively. Similar to the pre-treatment PET, the SBR algorithm had the fewest segmentation failures, with 5 segmentation failures. Failure of lymph node segmentation was usually due to uncontrolled propagation of the segmentation algorithm in the mediastinal background or primary tumour. *Figure 1* depicts the TLG_S on pre-treatment and interim PET images in box-whisker plots.

FIGURE 1. Box and whisker plots of summed total lesion glycolysis (TLG_S) of the primary tumour and the lymph nodes in pre-treatment and interim ^{18}F-fluorodeoxyglucose (FDG) positron emission tomography (PET) scans obtained with different segmentation algorithms. Bottom and top of each box are lower and upper quartiles. The horizontal line near middle of the box is median. Whiskers are drawn down to the 5% percentile up to the 95% percentile, whilst the outliers are indicated by a dot. T40 = Fixed level threshold segmentation at 40% of the maximum standardised uptake value (SUV_{max}), T50 = Fixed level threshold segmentation at 50% of SUVmax, RTL = Relative level thresholding, SBR = Signal-to-background segmentation, FLAB = Fuzzy locally adaptive Bayesian segmentation.

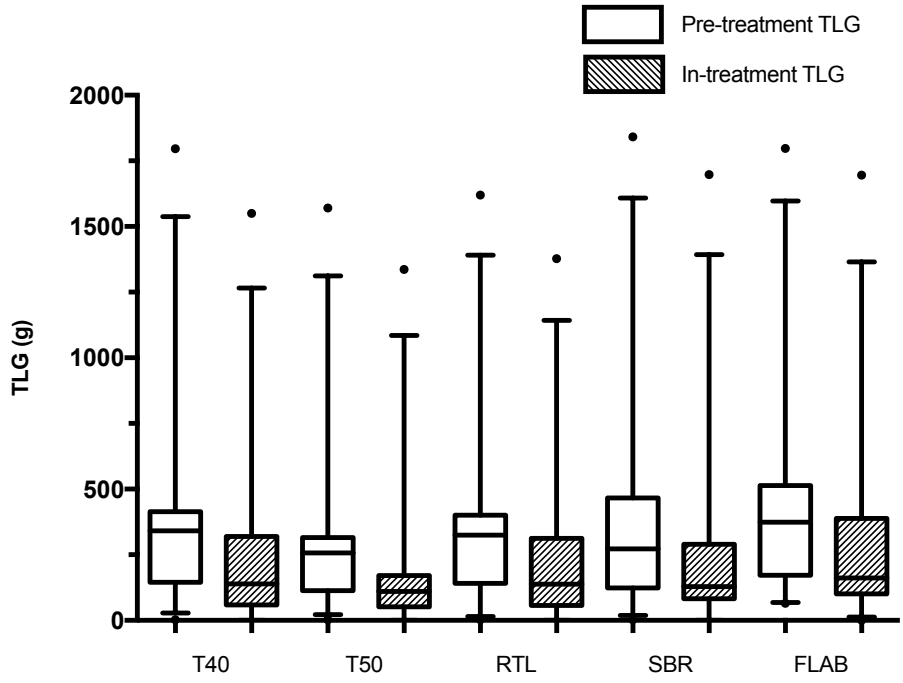

Pre-treatment $SUV_{T,max}$, interim $SUV_{T,max}$, and a relative decrease in $SUV_{T,max}$ was not significantly predictive for PFS and OS. Similarly, pre-treatment $SUV_{T,mean}$, interim $SUV_{T,mean}$, and a relative decrease in $SUV_{T,mean}$ of the primary tumour was not significantly predictive for PFS and OS in this cohort. However, pre-treatment TLG_T was significantly associated with PFS and OS for all segmentation methods. The ΔTLG_T was significantly predictive with PFS for all methods except for FLAB. Furthermore, ΔTLG_T was significantly associated with OS for the T50 and SBR methods. Hazard ratios (HRs) and

corresponding 95% confidence interval (CI) of TLG_T and ΔTLG_T in the univariate Cox regression analysis for PFS and OS are summarised in *Table 2*.

Only TLG_{LN} obtained with the SBR and T50 methods was significantly predictive for PFS and OS. Furthermore, the inclusion of TLG_{LN} improved early response assessment using PET, with pre-treatment TLG_S more strongly associated with PFS and OS than TLG_T. *Figure 2* depicts pre-treatment and interim FDG-PET images of two patients with a different lymph node response, as reflected by ΔTLG_S.

The differences in lymph node segmentation performance were reflected in the significance levels of TLG_S measurements in the univariate analysis for PFS and OS. The HRs and corresponding 95% CI of TLG_S and ΔTLG_S in the univariate Cox regression analysis for PFS and OS are summarised in *Table 3*.

DISCUSSION

In this study we showed that TLG is a robust metric to monitor early therapy response in patients undergoing concomitant chemoradiotherapy for locally advanced NSCLC. Furthermore, the inclusion of TLG_{LN} improves early assessment of treatment response in this patient population. Results of this study are in line with available data in the literature and emphasise the role of FDG-PET imaging for early response monitoring NSCLC (10-14). In particular, TLG outperformed the more traditional $SUV_{T,max}$ and $SUV_{T,mean}$ for predicting PFS and OS. This is probably due to the fact that TLG contains information about disease load as well as the metabolic activity of involved lesions.

In general, all segmentation algorithms had similar performance for segmenting the primary tumour in different anatomical locations. The presence of adjacent anatomical structures (e.g. lymph nodes, mediastinum, liver), did not result in large differences in segmentation performance. Furthermore, lower contrast of the interim PET images resulted in a minimal increase in the number of segmentation failures.

Absolute differences in TLG obtained by the different segmentation methods did not influence its predictive value. Due to the limited size and lower contrast, there were considerably more lymph node segmentation failures. The number of lymph node segmentation failures increased in the interim PET images owing to a further reduction in image contrast. Nevertheless, adequate lymph node segmentation is of importance, with TLG_S having a stronger association with PFS and OS. Out of all the segmentation algorithms, the SBR method demonstrated the lowest number of segmentation failures. The number of FLAB lymph node segmentation failures could be reduced by using a supervised input, with equal performance to that of the SBR method, which is in line with results from another study (23). However, in view of standardising response measurements,

FIGURE 2. Baseline (a + c) and interim (b + d) ^{18}F-fluorodeoxyglucose (FDG) positron emission tomography (PET) images of two non-small cell lung cancer (NSCLC) patients. The first patient (a + b) showed a good response to treatment on both the primary tumour and lymph nodes. Although the primary tumour of the second patient (c + d) showed a good response to treatment, there was a limited response considering the lymph nodes, with more FDG positive lymph nodes in the interim PET. The mean summed fractional decrease of total lesion glycolysis (ΔTLG) of the first patient for the different segmentation methods was 76 ± 6%, with a progression free survival (PFS) of 11 months and overall survival (OS) of 24 months. For the second patient, mean ΔTLG was 38 ± 6% with a PFS and OS of 7 and 21 months, respectively.

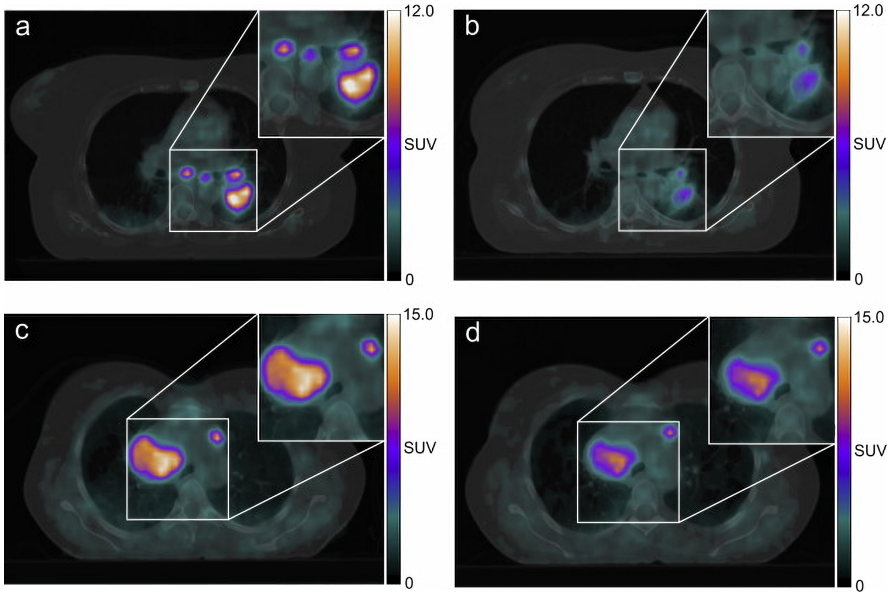

TABLE 2. Hazard ratios (HRs) and 95% confidence interval (CI) of pre-treatment primary tumour total lesion glycolysis (TLG_T) and relative TLG decrease (ΔTLG_T) between pre-treatment and interim ^{18}F-fluorodeoxyglucose (FDG) positron emission tomography (PET) in a univariate Cox regression analysis for progression-free survival (PFS) and overall-survival (OS).

	HR (95% CI) per unit change for PFS	Significance level
Pre-treatment TLG_T		
T40	1.002 (1.000–1.004)	0.02*
T50	1.002 (1.000–1.004)	0.03*
RTL	1.002 (1.000–1.004)	0.03*
SBR	1.002 (1.000–1.003)	0.02*
FLAB	1.002 (1.000–1.003)	0.03*
ΔTLG_T		
T40	1.02 (1.003–1.03)	0.03*
T50	1.02 (1.003–1.03)	0.03*
RTL	1.02 (1.003–1.04)	0.03*
SBR	1.02 (1.004–1.04)	0.02*
FLAB	1.02 (1.000–1.04)	0.07

	HR (95% CI) per unit change for OS	Significance level
Pre-treatment TLG_T		
T40	1.002 (1.001–1.004)	0.004*
T50	1.003 (1.001–1.004)	0.005*
RTL	1.002 (1.001–1.004)	0.004*
SBR	1.002 (1.001–1.003)	0.004*
FLAB	1.002 (1.001–1.003)	0.006*
ΔTLG_T		
T40	1.02 (1.00–1.03)	0.05
T50	1.02 (1.00–1.03)	0.02*
RTL	1.02 (1.00–1.03)	0.08
SBR	1.02 (1.00–1.03)	0.04*
FLAB	1.01 (0.99–1.03)	0.3

T40 = fixed level threshold at 40% of the maximum standardised uptake voxel (SUV_{max}), T50 = fixed level threshold at 50% of SUV_{max}, RTL = relative level thresholding, SBR = signal-to-background-ratio, FLAB = fuzzy locally adaptive Bayesian segmentation. Statistical significance is indicated by an asterisk '*'

TABLE 3. Hazard ratios (HRs) and 95% confidence interval (CI) of pre-treatment summed total lesion glycolysis (TLG_S) and relative TLG decrease (ΔTLG_S) between pre-treatment and interim ^{18}F-fluorodeoxyglucose (FDG) positron emission tomography (PET) in a univariate Cox regression analysis for progression-free survival (PFS) and overall-survival (OS). TLG_S is the sum of primary tumour TLG (TLG_T) and lymph node TLG (TLG_{LN}).

	HR (95% CI) per unit change for PFS	Significance level
Pre-treatment TLG_S		
T40	1.003 (1.001–1.005)	0.002*
T50	1.003 (1.001–1.005)	0.004*
RTL	1.003 (1.001–1.005)	0.003*
SBR	1.002 (1.001–1.004)	0.004*
FLAB	1.002 (1.001–1.004)	0.004*
ΔTLG		
T40	1.02 (1.00–1.05)	0.03*
T50	1.03 (1.02–1.05)	0.001*
RTL	1.01 (1.00–1.02)	0.2
SBR	1.04 (1.02–1.06)	0.001*
FLAB	1.02 (1.00–1.04)	0.04*

	HR (95% CI) per unit change for OS	Significance level
Pre-treatment TLG_S		
T40	1.003 (1.001–1.004)	0.001*
T50	1.003 (1.001–1.005)	0.002*
RTL	1.003 (1.001–1.005)	0.001*
SBR	1.002 (1.001–1.004)	0.001*
FLAB	1.002 (1.001–1.004)	0.002*
ΔTLG_S		
T40	1.01 (1.00–1.03)	0.4
T50	1.02 (1.00–1.04)	0.02*
RTL	1.00 (1.00–1.01)	0.9
SBR	1.02 (1.00–1.04)	0.03*
FLAB	1.01 (1.00–1.03)	0.02*

T40 = fixed level threshold at 40% of the maximum standardised uptake voxel (SUV_{max}), T50 = fixed level threshold at 50% of SUV_{max}, RTL = relative level thresholding, SBR = signal-to-background-ratio, FLAB = fuzzy locally adaptive Bayesian segmentation. Statistical significance is indicated by an asterisk '*'

such a user dependency should be avoided and we chose only to include the results of automatic FLAB segmentation.

Although the results emphasise that PET could be used for prediction of early treatment response in patients with locally advanced NSCLC treated with concomitant chemoradiotherapy, employment of PET-guided decisions for personalising treatment was not explored. Particularly, the strong association of pre-treatment TLG with PFS and OS might merit the choice for treatment intensification in patients with a high pre-treatment TLG such as proposed in the PET-boost dose-escalation trial (24). Furthermore, one might also consider treatment intensification when interim PET images demonstrate a limited decrease in TLG, for instance by dose escalation to metabolically active sub volumes the primary tumour (25, 26), in order to improve loco-regional tumour control. However, standardising PET-based dose painting approaches is of utmost importance. This is emphasised in a study by Knudtsen *et al.* where the used PET reconstruction algorithm and choice of segmentation thresholds significantly influenced treatment plans incorporating these dose painting concepts (27). Although threshold-based segmentation is frequently used for defining subvolumes for dose painting, the stability of different algorithms under varying imaging conditions for this purpose has yet to be investigated. Interestingly, studies emphasise that there is high stability of FDG uptake in tumour areas during the course of the treatment that can be identified on pre-treatment FDG-PET images (28). Although useful, interim PET imaging in a molecularly image-guided ART (IGART) setting would still be of great interest to monitor changes during radiotherapy (2). Indeed, the employment of IGART using FDG-PET has been shown to be of potential value, where the GTV is adapted according to interim FDG-PET imaging (2). Furthermore, results from a study conducted by Nygård *et al.* emphasise that FDG-PET might identify lesion-specific response after a single series of chemotherapy in NSCLC and could be a useful addition to guide and individualise radiotherapy strategy (29). Although dose redistribution might be useful for improving loco-regional tumour control, systemic disease control is also an important aspect in this patient group (30). In this setting, interim PET imaging might identify a failure of systemic disease control at an early stage (i.e. detection of additional lymph node or distant metastasis), making it possible to adapt treatment accordingly.

A limitation of the current study is that only a small patient cohort was considered. However, the advantage is that TLG measurements using different automatic segmentation algorithms showed consistent results, with most algorithms yielding TLG values that had a similar predictive value in this patient cohort.

This study emphasises that adequate lymph node segmentation in PET images improves the assessment of early treatment response in NSCLC patients treated with concomitant chemoradiotherapy. In this regard, given the relative ease of implementation and the high number of successful lymph node segmentations, SBR is the method of choice

for calculation of TLG in FDG-PET images of patients with locally advanced NSCLC for the purpose of assessment of early treatment response.

References

1. Aupérin A, Le Péchoux C, Rolland E, et al. Meta-analysis of concomitant versus sequential radiochemotherapy in locally advanced non-small-cell lung cancer. J Clin Oncol 2010;28:2181–90.
2. Grootjans W, de Geus-Oei L-F, Troost EGC, Visser EP, Oyen WJG, Bussink J. PET in the management of locally advanced and metastatic NSCLC. Nat Rev Clin Oncol 2015;12:395–407.
3. van Baardwijk A, Bosmans G, Boersma L, et al. PET-CT-based auto-contouring in non-small-cell lung cancer correlates with pathology and reduces interobserver variability in the delineation of the primary tumor and involved nodal volumes. Int J Radiat Oncol Biol Phys 2007;68:771–8.
4. De Ruysscher D, Nestle U, Jeraj R, MacManus M. PET scans in radiotherapy planning of lung cancer. Lung Cancer 2012;75:141–5.
5. Chirindel A, Adebahr S, Schuster D, et al. Impact of 4D-18FDG-PET/CT imaging on target volume delineation in SBRT patients with central versus peripheral lung tumors multi-reader comparative study. Radiother Oncol 2015;115:335–41.
6. Kepka L, Socha J. PET-CT use and the occurrence of elective nodal failure in involved field radiotherapy for non-small cell lung cancer: a systematic review. Radiother Oncol 2015;115:151–6.
7. Aerts HJWL, Bussink J, Oyen WJG, et al. Identification of residual metabolicactive areas within NSCLC tumours using a pre-radiotherapy FDG-PET-CT scan: a prospective validation. Lung Cancer 2012;75:73–6.
8. Calais J, Thureau S, Dubray B, et al. Areas of high 18F-FDG uptake on preradiotherapy PET/CT identify preferential sites of local relapse after chemoradiotherapy for non-small cell lung cancer. J Nucl Med 2015;56:196–203.
9. Bentzen SM. Theragnostic imaging for radiation oncology: dose-painting by numbers. Lancet Oncol 2005;6:112–7.
10. Usmanij EA, de Geus-Oei L-F, Troost EGC, et al. 18F-FDG PET early response evaluation of locally advanced non-small cell lung cancer treated with concomitant chemoradiotherapy. J Nucl Med 2013;54:1528–34.
11. Im H-J, Pak K, Cheon G, et al. Prognostic value of volumetric parameters of 18FFDG PET in non-small-cell lung cancer: a meta-analysis. Eur J Nucl Med Mol Imaging 2015;42:241–51.
12. Yossi S, Krhili S, Muratet J-P, Septans A-L, Campion L, Denis F. Early assessment of metabolic response by 18F-FDG PET During concomitant radiochemotherapy of non-small cell lung carcinoma is associated with survival: a retrospective single-center study. Clin Nucl Med 2015;40:e215–21.

13. Hyun S, Ahn H, Kim H, et al. Volume-based assessment by 18F-FDG PET/CT predicts survival in patients with stage III non-small-cell lung cancer. Eur J Nucl Med Mol Imaging 2014;41:50–8.
14. de Geus-Oei L-F, Oyen WJG. Predictive and prognostic value of FDG-PET. Cancer Imaging 2008;8:70–80.
15. Zaidi H, El Naqa I. PET-guided delineation of radiation therapy treatment volumes: a survey of image segmentation techniques. Eur J Nucl Med Mol Imaging 2010;37:2165–87.
16. Lee JA. Segmentation of positron emission tomography images: some recommendations for target delineation in radiation oncology. Radiother Oncol 2010;96:302–7.
17. Visser EP, Boerman OC, Oyen WJG. SUV: from silly useless value to smart uptake value. J Nucl Med 2010;51:173–5.
18. Konert T, Vogel W, MacManus MP, et al. PET/CT imaging for target volume delineation in curative intent radiotherapy of non-small cell lung cancer: IAEA consensus report 2014. Radiother Oncol 2015;116:27–34.
19. Boellaard R, Willemsen AT, Arends B, Visser EP. EARL procedure for assessing PET/CT system specific patient FDG activity preparations for quantitative FDG PET/CT studies. Accessed Oct 2015.
20. van Dalen JA, Hoffmann AL, Dicken V, et al. A novel iterative method for lesion delineation and volumetric quantification with FDG PET. Nucl Med Commun 2007;28:485–93.
21. Daisne J-F, Sibomana M, Bol A, Doumont T, Lonneux M, Grégoire V. Tridimensional automatic segmentation of PET volumes based on measured source-to-background ratios: influence of reconstruction algorithms. Radiother Oncol 2003;69:247–50.
22. Hatt M, Cheze le Rest C, Turzo A, Roux C, Visvikis DA. Fuzzy locally adaptive bayesian segmentation approach for volume determination in PET. IEEE Trans Med Imaging 2009;28:881–93.
23. Arens AIJ, Troost EGC, Hoeben BAW, et al. Semiautomatic methods for segmentation of the proliferative tumour volume on sequential FLT PET/CT images in head and neck carcinomas and their relation to clinical outcome. Eur J Nucl Med Mol Imaging 2014;41:915–24.
24. van Elmpt W, De Ruysscher D, van der Salm A, et al. The PET-boost randomized phase II dose-escalation trial in non-small cell lung cancer. Radiother Oncol 2012;104:67–71.
25. Ingerid Skjei K, JrG Svestad, Erlend Peter Skaug S, et al. Validation of dose painting of lung tumours using alanine/EPR dosimetry. Phys Med Biol 2016;61:2243.

26. EvenAJG, van der Stoep J, Zegers CML, et al. PET-based dose painting in non-small cell lung cancer: comparing uniform dose escalation with boosting hypoxic and metabolically active sub-volumes. Radiother Oncol 2015;116:281–6.
27. Knudtsen IS, van Elmpt W, Öllers M, Malinen E. Impact of PET reconstruction algorithm and threshold on dose painting of non-small cell lung cancer. Radiother Oncol 2014;113:210–4.
28. Gao A, Wang S, Fu Z, Sun X, Yu J, Meng X. (18)F-FDG avid volumes on preradiotherapy FDG PET as boost target delineation in non-small cell lung cancer. Int J Clin Exp Med 2015;8:7561–8.
29. Nygård L, Vogelius IR, Fischer BM, et al. Early lesion-specific 18F-FDG PET response to chemotherapy predicts time to lesion progression in locally advanced non-small cell lung cancer. Radiother Oncol 2016;118:460–4.
30. van Diessen JNA, Chen C, van den Heuvel MM, Belderbos JSA, Sonke J-J. Differential analysis of local and regional failure in locally advanced non-small cell lung cancer patients treated with concurrent chemoradiotherapy. Radiother Oncol 2016;118:447–52.

Supplementary data

The relative decrease in MTV and SUV_{mean} are depicted in *Supplementary Figure 1*.

(a) T40 = fixed level threshold at 40% of the maximum standardised uptake voxel (SUV_{max}),

(b) T50 = fixed level threshold at 50% of SUV_{max}, (c) RTL = relative level thresholding,

(d) SBR = signal-to-background-ratio, (e) FLAB = fuzzy locally adaptive Bayesian segmentation.

Supplementary Figure 1

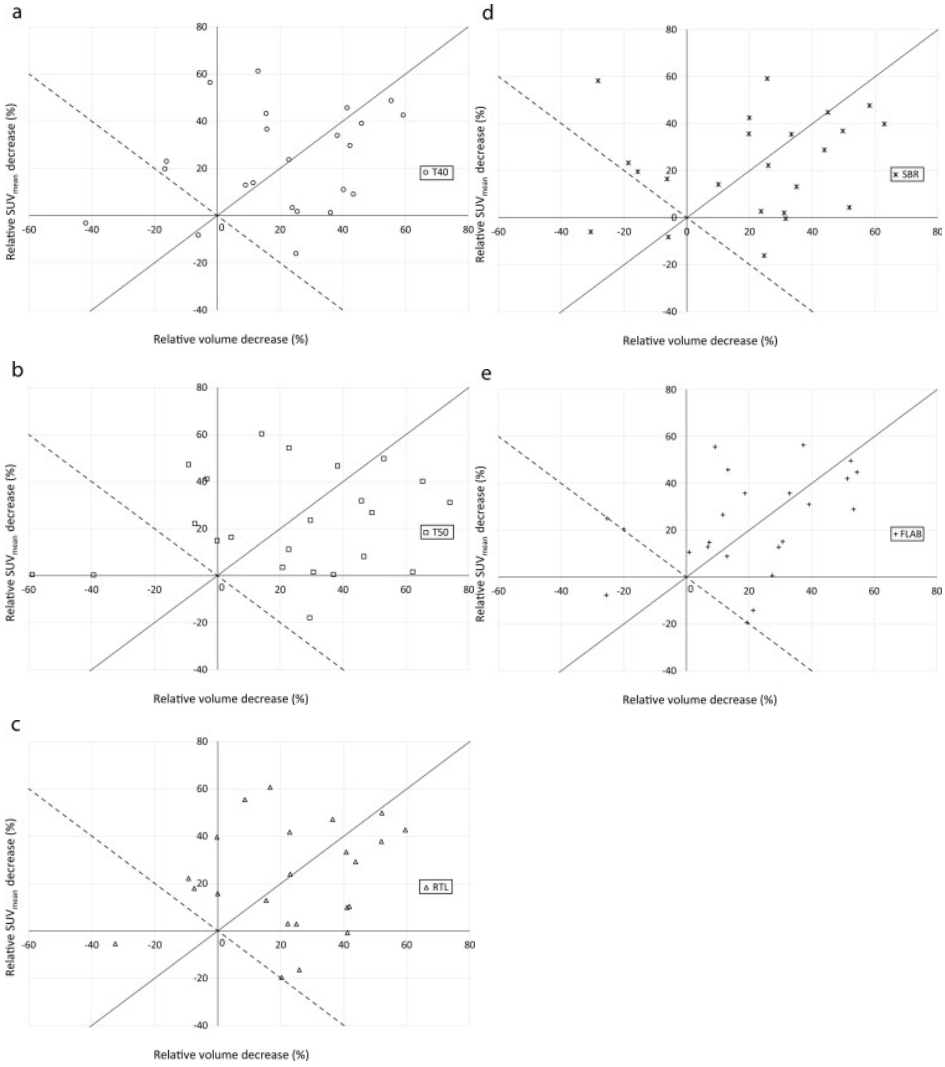


Read online

CHAPTER VI

Stereotactic radiotherapy boost after definite chemoradiation for non-responding locally advanced NSCLC based on early response monitoring ^{18}F-FDG-PET

Tineke W.H. Meijer, Robin Wijsman, Edwin A. Usmanij, Olga C.J. Schuurbiers, Peter van Kollenburg, Liza Bouwmans, Johan Bussink, Lioe-Fee de Geus-Oei

Adapted from: Physics and Imaging in Radiation Oncology, July 2018(7):16-22

6

ABSTRACT

Objectives

Prognosis of locally advanced non-small cell lung cancer remains poor despite chemoradiation. This planning study evaluated a stereotactic boost after concurrent chemoradiotherapy (30 × 2 Gy) to improve local control. The maximum achievable boost directed to radioresistant primary tumour subvolumes based on pre-treatment fluorine-18 fluorodeoxyglucose positron emission tomography/computed tomography (^{18}F-FDG-PET/CT) (pre-treatment-PET) and on early response monitoring ^{18}F-FDG-PET/CT (ERM- PET) was compared.

Materials and Methods

For ten patients, a stereotactic boost (VMAT) was planned on ERM-PET ($PTV_{boost;ERM}$) and on pre-treatment-PET ($PTV_{boost;pre\text{-}treatment}$), using a 70% SUVmax threshold with 7 mm margin to define radioresistant subvolumes. The dose was escalated till organ at risk (OAR) constraints were met, aiming to plan at least 18 Gy in 3 fractions (EQD_2 84 Gy/BED 100.8 Gy).

Results

In five patients, $PTV_{boost;ERM}$ was 9–40% smaller relative to $PTV_{boost;pre\text{-}treatment}$. Overlap of $PTV_{boost;ERM}$ with OARs decreased also compared to the overlap of $PTV_{boost;pre\text{-}treatment}$ with OARs. However, any overlap with OAR remained in 4/5 patients resulting in minimal differences between planned dose before and during treatment. Median dose (EQD_2) covering 99% and 95% of $PTV_{boost;ERM}$ was 15 Gy and 18 Gy respectively. Median boost volume receiving a physical dose of ≥ 18 Gy (V18) was 88%. V18 was ≥ 80% for PTV_{boost} in six patients.

Conclusion

A significant stereotactic boost to volumes with high initial or persistent ^{18}F-FDG-uptake could be planned above 60 Gy chemoradiation. Differences between planned dose before and during treatment were minimal. However, as an ERM-PET also monitors changes in tumour position, we recommend planning the boost on the ERM-PET.

Key Words

Early response prediction, locally advanced non-small lung cancer, radiotherapy, stereotactic boost

INTRODUCTION

Dose escalation up to a total dose of 60 Gy yields a greater proportion of disease control and better survival compared to 40–50 Gy for the treatment of irresectable locally advanced non-small cell lung cancer (NSCLC) (1). However, about 30% of patients treated with 60 Gy radiotherapy have a locoregional recurrence in the absence of distant metastasis (2). A meta-analysis showed that with combined sequential or concurrent chemoradiotherapy, dose escalation beyond 60 Gy does not lead to further improvements in overall survival (3). The RTOG 0617 trial demonstrated that 74 Gy in 2 Gy fractions concurrent chemoradiation might even result in a survival decrement compared to 60 Gy in 2 Gy fractions (4). In the case of radiation therapy alone, higher radiation dose results in longer survival without an upper dose level above which there is no further benefit (3). Therefore, radiation dose intensification combined with chemotherapy should not be discouraged based on the RTOG 0617 results. Especially since in RTOG 0617 compliance with normal tissue dose constraints was not mandatory, older (less conformal) radiotherapy techniques were allowed, and the prolonged overall treatment time could be associated with poorer survival because of accelerated repopulation (4,5).

Intensity-modulated radiation therapy (IMRT) and volumetric- modulated arc therapy (VMAT) enable more conformal irradiation, thereby lowering dose to organs at risk (OAR) (6). Currently, it is possible to identify subvolumes within the planning target volume (PTV) that are more radioresistant (7–9). Usmanij *et al.* (8) demonstrated that NSCLC metabolic non-responders, as determined by a poor decrease in total lesion glycolysis (TLG) on fluorine-18-fluorodeoxyglucose positron emission tomography/computed tomography (^{18}F- FDG-PET/CT) at the beginning of the third week of radiotherapy, have a worse progression-free survival compared to early metabolic responders (8). Thus, early response measurement using ^{18}F-FDG-PET/CT enables the identification of patients that may benefit most from dose escalation.

Stereotactic body radiotherapy (SBRT) delivers very conformal high radiation doses resulting in excellent local control rates (> 90%) with low toxicity in inoperable stage I-II NSCLC patients (10). It was shown that a biologically effective dose (BED) prescription of at least 100 Gy is required for acceptable tumour control probability (11). Therefore, an SBRT radiation boost directed towards ^{18}F-FDG-PET/CT defined radioresistant subvolumes may increase local control in locally advanced NSCLC. Furthermore, by using SBRT, high maximum dose (D_{max}) within the PTV is achieved with limited dose to OAR due to steep dose decline just outside the PTV, enabling higher dose escalation compared to other approaches. Limiting prolongation of overall treatment time (OTT) is another advantage of SBRT boosting as the booster dose is delivered in only a few fractions.

The aim of this study was to compare the maximum achievable dose escalation for locally advanced NSCLC treated with concurrent chemoradiation by using a stereotactic boost directed to radioresistant subvolumes of the primary tumour as determined by an ^{18}F-FDG-PET/CT before start of chemoradiation (pre-treatment PET) and an early response monitoring ^{18}F-FDG-PET/CT (ERM-PET).

MATERIALS AND METHODS

Patients

^{18}F-FDG-PET/CTs acquired for the ERM study by Usmanij *et al.* were used for this planning study (8). This ERM study was approved by the Institutional Review Board of the Radboud university medical centre. All patients gave written informed consent. Twenty-eight patients with stage IIIA-B NSCLC eligible for concomitant chemoradiotherapy were enrolled in this study. A prescription dose of 60 Gy in 2 Gy fractions was applied in this planning study for the entire tumour and involved lymph nodes with margin (PTV_{60Gy}). Detailed information upon radiation treatment planning for PTV_{60Gy} is described in *Supplementary material 1*.

For every patient, a pre-treatment ^{18}F-FDG-PET/CT was acquired with a median interval of 11 days (range 1–27 days) before the start of chemoradiation and an ERM ^{18}F-FDG-PET/CT was performed at the beginning of the third week of treatment (after a median dose of 20 Gy; range 20–24 Gy). The timing of the ERM-PET was specifically chosen at the beginning of the third week of treatment. A decrease in uptake early during chemoradiation reflects tumour response, whereas this decrease in uptake may disappear later in the course of chemoradiation due to the onset of treatment-induced inflammation (8).

We selected those fourteen patients with a poor response to treatment as assessed by a TLG decrease < 45% on the ERM-PET relative to the pre-treatment PET. These poor responders showed worse disease-free survival, possibly due to the fact that they harbour more radioresistant tumours (8). Three patients were ineligible for this planning study because they had only a small primary tumour with the bulk of gross tumour volume (GTV) located in the mediastinum. Furthermore, one radiotherapy CT and radiation treatment plan could not be restored. So, ten patients were included in this planning study. Patient characteristics are listed in *Table 1*.

^{18}F-FDG-PET/CT image acquisition

All PET scans were performed with a hybrid PET/CT scanner (Biography Duo Siemens Medical Solutions, USA, Inc.). Patients fasted for at least six hours. A venous blood sample was drawn to measure blood glucose level (< 8.2 mmol/L in all patients, mean 6.0 mmol/L). Prior to the PET scan, a low dose CT during free-breathing was acquired for PET attenuation correction and anatomical matching. Sixty minutes after intravenous injection of ^{18}F-FDG (3.45MBq/kg; Covidien) and furosemide (10 mg), static emission scans in a three-dimensional mode were obtained with an acquisition time of four minutes per bed position. Images were iteratively reconstructed in 128x128 matrices by ordered subsets expectation maximisation (OSEM) algorithm using four iterations/sixteen subsets (4i/16 s) with a 5 mm Gaussian filter. Correction for photon attenuation (by using the low dose CT) and decay of ^{18}F-FDG was performed for images. Rigid co-registration (starting with a bone match and visually checking the plausibility of the match regarding tumour and surrounding normal tissue) of the PET scans to the radiotherapy planning CT was performed.

Boost volume definition

Radioresistant subvolumes of the primary tumour, to which the boost must be directed, were delineated on the pre-treatment PET and ERM-PET. For automated segmentation of biological target boost volumes (BTV_{boost}), a threshold of 70% of maximum intensity level was used to identify tumour subvolumes at greatest risk of relapse (9). Adding a 7 mm circumferential margin to BTV_{boost} created PTV_{boost}. Volumes (cm^3) of PTV_{boost} based on the pre-treatment PET ($PTV_{boost;pre\text{-}treatment}$) and ERM-PET ($PTV_{boost;ERM}$) were recorded. To assess the effect of timing of PET scans on the planned dose to PTV_{boost}, a stereotactic boost was planned for all ten patients on both the pre-treatment PET and the ERM-PET.

Organs at risk definition and constraints

The bronchial tree (up to and including lobar bronchi), heart, great vessels, oesophagus, lungs minus GTV_{60Gy} (i.e., lung volume minus the volume of the GTV planned to receive 60 Gy), spinal cord and brachial plexus were considered OAR. Adding a 5 mm margin to the first four OAR contours created the planning OAR volumes (PRV) (12). For the latter two OAR, PRVs were created adding a 2 mm margin as breathing induced movement is assumed to be smaller/absent for this nerve tissue. No PRV margin was used for the lungs. The following constraints were applied: Lungs minus GTV_{60Gy}: mean lung dose < 20 Gy, V20 < 35% (Vx is the relative volume receiving x Gy); V5 < 65–70% for lungs minus

GTV_{60Gy} and V5 < 55% for contralateral lung ('soft' constraint) (13–15). PRV oesophagus: D_{max} 70 Gy equivalent dose in 2 Gy fractions (EQD_2) (α/β-value 3 Gy) (16) PRV brachial plexus: D_{max} 66 Gy EQD_2 (α/β-value 2 Gy) (12). PRV heart, great vessels, bronchial tree: D_{max} 94 Gy EQD_2 (α/β-value 3 Gy) (12). PRV spinal cord: D_{max} 53 Gy EQD_2 (α/β-value 2 Gy) (12).

Boost planning

Doses to OARs were determined for the 60Gy treatment plan. Except for the Vx doses and mean dose to the lungs, these doses can be converted into EQD_2 doses using the formula EQD_2 = total dose*((- fraction dose+ α/β)/(2+α/β)). Thereafter, the extra allowed EQD_2 dose to OAR was calculated (i.e., maximum allowed EQD_2 minus maximum EQD_2 delivered after 60 Gy). Subsequently, this extra allowed EQD_2 was converted into a physical dose (planned to be delivered in three fractions). This physical dose was calculated for every separate OAR and used as maximum allowed dose for boost treatment planning. This strategy was performed for both the whole OAR and the part of the OAR in close proximity to the boost volume, to take into account the spatial component of the maximum dose of the 60 Gy treatment plan. So, also the maximum dose of the OAR subvolume near PTV_{boost} was determined in the conventionally fractionated 60 Gy radiotherapy plan. This dose was used to calculate the maximum tolerable dose for that subvolume of the OAR bordering the PTV_{boost}. Higher dose escalation of the boost volume could be achieved with this strategy. Boosts were planned using the Pinnacle^3 (Version 8.0–9.2; Philips Radiation Oncology Systems, Fitchburg, WI) treatment planning system.

A BED prescription dose of at least 100 Gy is required for acceptable tumour control probability (11). A dose of 60 Gy in 2 Gy fractions is 60 Gy EQD_2 and is equal with a BED of 72 Gy (α/β-value = 10 Gy for tumour). Delivering 18 Gy in three fractions results in a boost of 24 Gy EQD_2 (total EQD_2 84 Gy) and a BED of 28.8 Gy (total BED 100.8 Gy). Therefore, it was attempted to plan a boost with a minimum dose of 18 Gy in three fractions. The final planned dose to PTV_{boost} depended on the maximum tolerable dose for the OAR. The majority of tumours in this study were located near critical organs at risk, as is often the case in irresectable stage III NSCLC, resulting in a small therapeutic window for planning a stereotactic radiation boost. Radiation dose was escalated till OAR constraints were met. In case a higher dose than 18 Gy could be planned this was done. However, in case 18 Gy could not be planned due to critical OAR, a lower dose had to be accepted.

All boost plans were generated using a single VMAT arc avoiding the contralateral lung. To ensure a rapid dose decline outside the PTV, a ring contour (1 cm) around the

PTV was created. In case of overlap of PTV_{boost} with PRV, two separate PTVs were created: PTV inside PRV and PTV outside PRV. This enabled better dose coverage for the PTV outside the PRV, thereby limiting suboptimal dosage of the PTV. The optimisation objectives for the PTV_{boost} and the ring contours were individually set according to calculated constraints for OAR. No hard constraints were set for the maximum allowed dose within PTV_{boost}, because the maximum doses reached in this setting will never approach the maximum allowed (EQD_2) dose that is clinically accepted in SBRT for limited stage lung cancer. We allowed a maximum dose as high as needed to enable a steep dose decline outside PTV_{boost}, without exceeding the maximum total dose (EQD_2) accepted in SBRT for limited stage lung cancer.

RESULTS

PTV_{boost} volumes

In only two of ten patients, PTV_{boost} volumes did not overlap with any of the PRVs (*Table 1*). In five of ten patients, $PTV_{boost;ERM}$ was 9–40% smaller relative to $PTV_{boost;pre\text{-}treatment}$. However, for the other five patients, $PTV_{boost;ERM}$ remained stable or increased compared to PTVboost;pre-treatment (range 0–50%) (*Table 2*).

Furthermore, it was examined whether the changes in PTV_{boost} resulted in less overlap with PRVs (*Supplementary material 2*). Overlap did decrease in five patients with 6–100%. Unfortunately, overlap with PRVs disappeared in only one of these five patients (*Figure 1, Supplementary material 2*). Overlap with PRVs increased for two patients (*Supplementary material 2*). Dose-limiting OAR for boost planning allowed dose to OAR and planned dose to OAR are shown in *Table 3* and *Supplementary material 3*.

PTV_{boost} and CTV_{boost} dose

The dose delivered to 99% of PTV_{boost} (D99; EQD_2), dose delivered to 95% of PTVboost (D95; EQD_2), Dmax (EQD_2), and percentage of PTVboost receiving ≥ 18 Gy (V18; physical dose) were assessed for $PTV_{boost;pre\text{-}treatment}$ and $PTV_{boost;ERM}$. Median D99 and D95 of $PTV_{boost;pre\text{-}treatment}$ were 17 Gy (range 4–31) and 19 Gy (range 7–42), respectively.
Median V18 of $PTV_{boost;pre\text{-}treatment}$ was 93% (range 56–100). Median D99 and D95 of $PTV_{boost;ERM}$ was 15 Gy (range 3–30) and 18 Gy (range 6–32), respectively. Median V18 of $PTV_{boost;ERM}$ was 88% (range 51–100).

TABLE 1. Patient characteristics

Patient	Sex	Age	cTNM	Pathology	Location Primary tumour
1	F	55	T2N2M0	AC	RUL; PTV_0 and PTV_2 not near OAR
2	M	61	T2N2M0	SCC	LLL; PTV_0 and PTV_2 overlay aorta PRV, near spinal cord and bronchial tree
3	M	49	T2N2M0	AC	ML; PTV_0 and PTV_2 overlay heart PRV
4	M	60	T3N2M0	SCC	RUL; PTV_0 overlays bronchial tree PRV
5	F	49	T3N2M0	AC	LUL; PTV_0 and PTV_2 overlay heart, aorta and bronchial tree PRV
6	F	52	T4N3M0	NSCLC NOS	LH; PTV_0 and PTV_2 overlay heart, aorta and bronchial tree PRV
7	M	70	T3N2M0	AC	RUL; PTV_0 and PTV_2 overlay heart PRV
8	M	66	T4N0M0	SCC	LUL; PTV_0 and PTV_2 overlay brachial plexus and great vessels PRVs. Near spinal cord and oesophagus
9	M	61	T1N2M0	AC	ML; PTV_0 and PTV_2 not near OAR
10	F	49	T2N2M0	NSCLC NOS	LUL; PTV_0 and PTV_2 overlay heart PRV

Abbreviations: AC: adenocarcinoma; cTNM: clinical tumour node metastasis staging system; LLL: left lower lobe; LUL: left upper lobe; LH: left hilum; ML: middle lobe; NOS: not otherwise specified; OAR: organ at risk; PTV_0: boost planning target volume determined on pre-treatment PET; PTV_2: boost planning target volume determined on the early response monitoring PET; PRV: planning organ at risk volume; RUL: right upper lobe; SCC: squamous cell carcinoma;

FIGURE 1. Boost PTVs of two patients delineated on ^{18}F-FDG-PET/CT scans before start of treatment and at the beginning of week 3 during treatment. ^{18}F-FDG-PET/CT scans of patient number 4 and 8. The green line represents PTV_{boost} before start of treatment (upper panel), the red line represents PTV_{boost} at the beginning of third week of treatment (lower panel). For patient number 4 (left), there was a remarkable decrease in PTV_{boost} volume in contrast to PTV_{boost} volume of patient number 8 (right) whose PTV_{boost} volume was similar for both time points. The blue line indicates the planning organs at risk volumes.

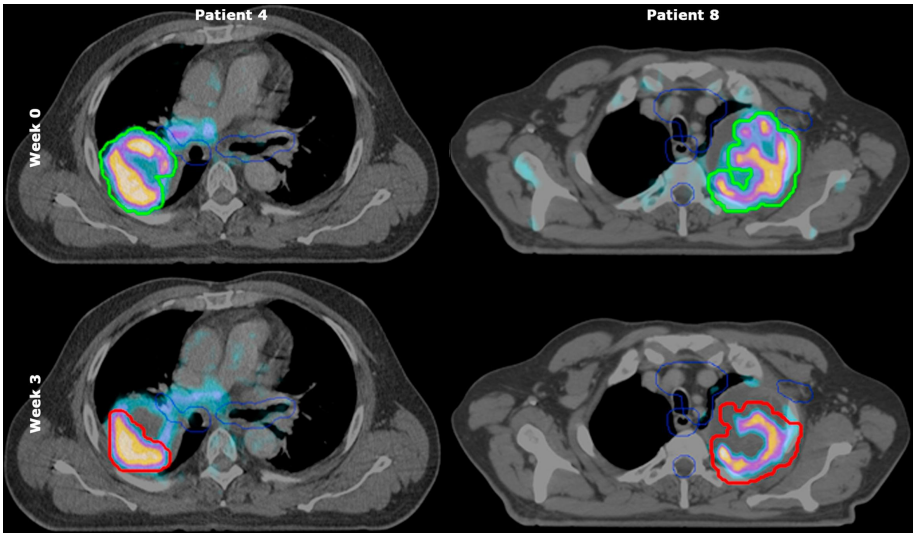

Differences between the planned dose in week 0 and 3 were minimal due to the fact that overlap of $PTV_{boost;ERM}$ with PRVs remained in most patients. V18 in week 3 was higher in five patients compared to V18 in week 0. However, planning results were somewhat worse for four patients in week 3 relative to week 0. For patient number 3, differences in coverage of $PTV_{boost;pre\text{-}treatment}$ and $PTV_{boost;ERM}$ were very large due to changes in atelectasis and thereby a shift in tumour position towards the heart in week 3, resulting in overlap of $PTV_{boost;ERM}$ with heart PRV limiting dose escalation (*Table 4; Figure 2; Supplementary material 2*).

In seven patients, D95 PTV_{boost} was substantially higher than the prescribed dose (74 Gy) of the RTOG 0617 study. The total D95 $PTV_{boost;pre\text{-}treatment}$ was $\geq$ 80 Gy in five patients

TABLE 2. Boost planning target volume determined on pre-treatment PET and on ERM-PET

Patient	PTV_0 (cm^3)	PTV_2 (cm^3)	Absolute difference (cm^3)	Relative difference (%)
1	19	19	0	0
2	214	183	-31	-15
3	14	21	7	50
4	164	98	-66	-40
5	94	56	-38	-40
6	127	133	6	5
7	43	34	-9	-21
8	208	189	-19	-9
9	14	15	1	7
10	15	16	1	7

Abbreviations: PTV_0: boost planning target volume determined on pre-treatment PET; PTV_2: boost planning target volume determined on the early response monitoring PET; Absolute difference: PTV_2 volume minus PTV_0 volume; Relative difference: (absolute difference/PTV_0)*100

and for four patients a total D95 $PTV_{boost;ERM} \geq 80$ Gy could be planned (*Figure 2A; Table 4*). The summed D95 of PTV_{boost} minus overlap with PRV was ≥ 80 Gy in seven patients and for another patient this summed D95 was 79 Gy (*Figure 2B*).
V18, which equals an ablative dose, was ≥ 80% for the whole PTV_{boost} in six patients (*Figure 2D*) and ≥ 80% in eight patients for PTV_{boost} minus overlap with PRV (*Figure 2E*).

In clinical practice, clinical target volume (CTV) coverage is also evaluated in case of overlap with OAR. D95 BTV_{boost} (considering BTV_{boost} as CTV) was considerably larger than D95 PTV_{boost} (*Figure 2C*): for seven patients a summed BTV dose of ≥ 80 Gy could be planned. $BTV_{boost;ERM}$ V18 was (almost) 100% in six patients (*Figure 2F*). In the other patients, BTV-PRV overlap hampered planning of an ablative dose for the complete BTV_{boost}.

FIGURE 2. SBRT dose planned to $PTV_{boost;pre\text{-}treatment}$ and $PTV_{boost;ERM}$. (A) Dose (EQD_2) planned to 95% of PTV_{boost}(D95) for individual patients. (B) Dose (EQD_2) planned to 95% of PTV_{boost} (D95) minus overlap with planning organ at risk volume for individual patients. (C) Dose (EQD_2) planned to 95% of BTV_{boost} (D95) for individual patients. (D) Percentage of PTV_{boost} volume planned to receive ≥18 Gy (V18; physical dose) for individual patients. (E) Percentage of PTV_{boost} volume minus overlap with planning organ at risk volume planned to receive ≥18 Gy (V18; physical dose) for individual patients. (F) Percentage of BTV_{boost} volume planned to receive ≥18 Gy (V18; physical dose) for individual patients. Grey bars indicate dose planned to PTV_{boost} based on early response monitoring ^{18}F-FDG-PET/CT ($PTV_{boost;ERM}$). Black bars indicate dose planned to PTVboost based on pre-treatment ^{18}F-FDG-PET/CT ($PTV_{boost;pre\text{-}treatment}$). X-axis represents individual patients. SBRT: stereotactic body radiotherapy.

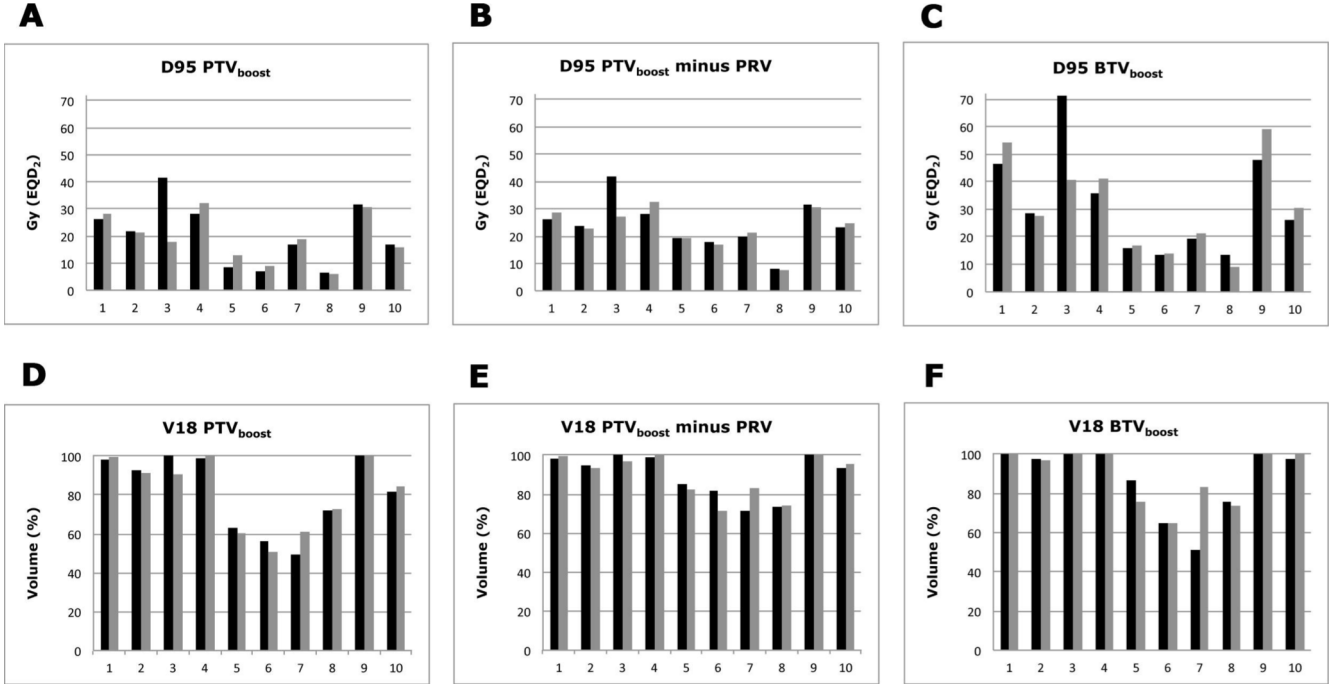

TABLE 3. Dose limiting organs at risk for boost planning

Patient	Dose limiting OAR
1	Oesophagus
2	Oesophagus
3	Heart
4	Lungs
5	Heart, bronchial tree and oesophagus
6	Oesophagus
7	Heart
8	Heart, oesophagus, brachial plexus and spinal cord
9	Lungs
10	Heart

DISCUSSION

This study compared the maximum achievable dose escalation for locally advanced NSCLC treated with concurrent chemoradiation by using a stereotactic boost directed to radioresistant subvolumes of the primary tumour as determined by a pre-treatment PET and an ERM-PET. In five of ten patients, $PTV_{boost;ERM}$ was 9−40% smaller relative to $PTV_{boost;pre\text{-}treatment}$. However, differences between the planned dose before and during treatment were minimal because the overlap of $PTV_{boost;ERM}$ with PRVs remained in most patients. V18, which equals an ablative dose, was ≥ 80% for PTV_{boost} in six patients.

Some studies have investigated the feasibility of dose escalation in locally advanced NSCLC, all with different treatment strategies (12,17,18). For example, a prospective single institution trial examined stereotactic boosting (two fractions of 10 Gy, or three fractions of 6.5 Gy) of residual primary tumour < 5 cm 1−2 months after chemoradiation (60 Gy). Mean coverage of SBRT boost was 96.4% but was not described for patients individually (17). A disadvantage of this strategy is prolonging of OTT, which is biologically less effective. Furthermore, only small tumours were eligible. Delivering three additional SBRT boost fractions immediately after 60 Gy results in a minimal prolongation of the OTT and the boost dose is not delivered simultaneously with chemotherapy.

Another study, the RTOG 1106 study, is an ongoing phase 2 randomised trial comparing 60 Gy in 30 fractions (IMRT) versus adaptive radiotherapy to residual tumour

TABLE 4. Dose delivered to PTV_{boost}.

	D99 (EQD_2)		**D95 (EQD_2)**		**D_{max} (EQD_2)**		**V18**	
Patient	week 0	week 3	week 0	week 3	week 0	week 3	week 0	week 3
1	24	25	28	28	92	85	99	100
2	18	19	22	21	41	41	93	91
3	31	13	42	18	87	80	100	91
4	23	30	28	32	51	48	99	100
5	5	11	8	13	68	55	63	60
6	5	7	7	9	55	41	56	51
7	17	18	17	19	48	59	49	61
8	4	3	7	6	47	51	72	73
9	30	28	32	31	75	77	100	100
10	15	12	17	16	66	66	82	84

Dose in EQD_2, except for V18. Abbreviation: PTV_{boost}: boost planning target volume; D99: dose planned to 99% of PTV_{boost} (EQD_2); D95: dose planned to 95% of PTVboost (EQD_2); D_{max}: maximum dose (EQD_2); V18: percentage of planning target volume receiving ≥18 Gy (physical dose); week 0: boost plan based on pre- treatment ^{18}F-FDG-PET/CT; week 3: boost plan based on early response monitoring ^{18}F-FDG-PET/CT.

based on during-treatment ^{18}F-FDG- PET (fraction 18–19) to deliver a boost in the final nine fractions (2.2–3.8 Gy/fraction) to a maximum total physical dose of 80.4 Gy in thirty fractions. The primary goal of this study is to determine whether the dose can be escalated to improve locoregional control. Contrary to our study, a simultaneously integrated boost (SIB) is planned. The SBRT boost may be advantageous over this SIB procedure due to its dose inhomogeneity with high D_{max} resulting in a higher biologically effective tumour dose.

Van Elmpt *et al.* reported on the PET-boost randomised phase II trial that randomised patients between dose-escalation (IMRT-SIB) of the entire primary tumour or dose-escalation of the high FDG-uptake region (> 50% SUV_{max}) inside the primary tumour (12). Mean boost dose was 79.2 Gy for the entire tumour and 86.9 Gy for the high FDG-uptake area (P = 0.001). However, in case of overlap of PTV with an OAR, PTV was allowed to have reduced coverage for 15% of the volume. D95-99 for boost volumes were not described.

In general, the feasibility of dose escalation entirely depends on the accepted dose to OAR and related toxicity. For example, it is suggested that the negative result of the RTOG 0617 trial is due to cardiac toxicity as compliance with normal tissue dose constraints was encouraged but not necessary. The effect of heart dose on overall survival is complex. It is advised to keep heart V50 < 25% (19). This constraint was met in our study (*Supplementary material 4*). Hepel *et al.* tried to deliver an SBRT boost in two fractions with a total boost dose of 16–28 Gy on primary and nodal disease after 50.4 Gy concurrent chemoradiation (phase I dose escalation trial) (18). There was no dose constraint for the proximal bronchial-vascular tree. One of twelve patients (8.3%) died due to fatal bronchopulmonary haemorrhage. The dose delivered to 4 cm^3 of the bronchial-vascular tree was substantially higher in this patient: 20.3 Gy (EQD_2 53.4 Gy, α/β-value 3 Gy) for SBRT boost and total dose of 73.5 Gy (EQD_2 105.5 Gy, α/β-value 3 Gy). So, a mediastinal SBRT boost may increase the risk of fatal toxicity substantially and therefore a dose constraint to the bronchial-vascular tree is mandatory. Our maximum dose of 94 Gy (EQD_2) delivered to the bronchial-vascular tree PRV is considered safe (12). Severe late oesophageal toxicity (stenosis and fistula) is observed in 6% of patients receiving a maximum dose of ≥ 70 Gy (16). Based on these results we set a maximum of 70 Gy to the oesophagus with 0.5 cm margin. However, the RTOG 1106 protocol allows a maximum dose of 74–76 Gy.

Besides the issue as mentioned earlier regarding treatment-related toxicity, some technical aspects such as boost volume definition and tumour motion management need further discussion. It is not known which segmentation method is optimal for boost volume segmentation. Aerts *et al.* conclude that residual metabolic-active areas after (chemo)radiation have a high overlap with pre-treatment volume defined by 50% SUV_{max} (7). However, defining the boost volume using a threshold of 50% SUV_{max}

may result in too large boost volumes because this threshold is in general regarded as a segmentation method to quantify ^{18}F-FDG-avid areas of the entire tumour (20). Therefore, it is likely that residual metabolic active disease remains within this 50% SUV_{max} volume. Calais *et al.* propose a 70% SUV_{max} threshold on pre-treatment ^{18}F-FDG-PET/CT scans to define treatment-resistant tumour subvolumes (9). This smaller volume will facilitate radiotherapy dose escalation. Therefore, we decided to use this segmentation method notwithstanding that a threshold of 80–90% could be sufficient as well resulting in even smaller boost volumes.

For adequate radiotherapy delivery, determination of tumour movement is important. The ERM study by Usmanij *et al.*, however, was performed when four-dimensional planning CT was not standard of care yet. Therefore, for this planning study, three-dimensional planning CTs were used. It was therefore not possible to assess individual PTV margins for BTV_{boost} such as with the mid-ventilation approach in stereotactic radiotherapy (21). We decided to use a 7 mm PTV margin for BTV_{boost}, as this is a fair PTV margin for the mid-ventilation concept in our experience. However, in case of implementation of this stereotactic boost planning study into clinical practice, a four-dimensional CT should be performed for all patients to assess individual PTV margins for the BTV_{boost} (21).

In conclusion, a stereotactic boost to primary tumour subvolumes with initially high or persistent ^{18}F-FDG uptake (poor-responding areas) could be planned in combination with 60 Gy concurrent chemoradiation. V18, which equals an ablative dose, was ≥ 80% for PTV_{boost} in six out of ten patients. Therefore, a stereotactic boost to regions with high ^{18}F-FDG-uptake is an attractive treatment strategy to optimise NSCLC therapy. Differences between the planned dose before and during treatment were minimal since overlap of $PTV_{boost;ERM}$ with PRVs remained in most patients. However, as an ERM-PET also monitors changes in tumour position, planning the boost on the ERM- PET should be considered.

References

1. Perez CA, Bauer M, Edelstein S, Gillespie BW, Birch R. Impact of tumor control on survival in carcinoma of the lung treated with irradiation. Int J Radiat Oncol Biol Phys 1986;12(4):539–47.
2. Kalman NS, Weiss E, Walker PR, Rosenman JG. Local radiotherapy intensification for locally advanced non-small-cell lung cancer – a call to arms. Clin Lung Cancer 2018;19:17–26.
3. Ramroth J, Cutter DJ, Darby SC, Higgins GS, McGale P, Partridge M, et al. dose and fractionation in radiation therapy of curative intent for non-small cell lung cancer: meta-analysis of randomized trials. Int J Radiat Oncol Biol Phys 2016;96(4):736–47.
4. Bradley JD, Paulus R, Komaki R, Masters G, Blumenschein G, Schild S, et al. Standard-dose versus high-dose conformal radiotherapy with concurrent and consolidation carboplatin plus paclitaxel with or without cetuximab for patients with stage IIIA or IIIB non-small-cell lung cancer (RTOG 0617): a randomised, two-by- two factorial phase 3 study. Lancet Oncol 2015;16(2):187–99.
5. Belderbos J, Walraven I, van Diessen J, Verheij M, de Ruysscher D. Radiotherapy dose and fractionation for stage III NSCLC. Lancet Oncol 2015;16(4):e156–7.
6. Grills IS, Yan D, Martinez AA, Vicini FA, Wong JW, Kestin LL. Potential for reduced toxicity and dose escalation in the treatment of inoperable non-small-cell lung cancer: a comparison of intensity-modulated radiation therapy (IMRT), 3D con- formal radiation, and elective nodal irradiation. Int J Radiat Oncol Biol Phys 2003;57(3):875–90.
7. Aerts HJ, Bussink J, Oyen WJ, van Elmpt W, Folgering AM, Emans D, et al. Identification of residual metabolic-active areas within NSCLC tumours using a pre-radiotherapy FDG-PET-CT scan: a prospective validation. Lung Cancer 2012;75(1):73–6.
8. Usmanij EA, de Geus-Oei LF, Troost EG, Peters-Bax L, van der Heijden EH, Kaanders JH, et al. 18F-FDG PET early response evaluation of locally advanced non-small cell lung cancer treated with concomitant chemoradiotherapy. J Nucl Med 2013;54(9):1528–34.
9. Calais J, Thureau S, Dubray B, Modzelewski R, Thiberville L, Gardin I, et al. Areas of high 18F-FDG uptake on preradiotherapy PET/CT identify preferential sites of local relapse after chemoradiotherapy for non-small cell lung cancer. J Nucl Med 2015;56(2):196–203.
10. Grills IS, Mangona VS, Welsh R, Chmielewski G, McInerney E, Martin S, et al. Outcomes after stereotactic lung radiotherapy or wedge resection for stage I non-small-cell lung cancer. J Clin Oncol 2010;28(6):928–35.

11. Brown JM, Brenner DJ, Carlson DJ. Dose escalation, not "New Biology," can account for the efficacy of stereotactic body radiation therapy with non-small cell lung cancer. Int J Radiat Oncol Biol Phys 2013;85(5):1159–60.
12. van Elmpt W, De Ruysscher D, van der Salm A, Lakeman A, van der Stoep J, Emans D, et al. The PET-boost randomised phase II dose-escalation trial in non-small cell lung cancer. Radiother Oncol 2012;104(1):67–71.
13. Khalil AA, Hoffmann L, Moeller DS, Farr KP, Knap MM. New dose constraint reduces radiation-induced fatal pneumonitis in locally advanced non-small cell lung cancer patients treated with intensity-modulated radiotherapy. Acta Oncologica 2015;54(9):1343–9.
14. Yom SS, Liao Z, Liu HH, Tucker SL, Hu CS, Wei X, et al. Initial evaluation of treatment-related pneumonitis in advanced-stage non-small-cell lung cancer pa- tients treated with concurrent chemotherapy and intensity-modulated radio- therapy. Int J Radiat Oncol Biol Phys 2007;68(1):94–102.
15. Jiang ZQ, Yang K, Komaki R, Wei X, Tucker SL, Zhuang Y, et al. Long-term clinical outcome of intensity-modulated radiotherapy for inoperable non-small cell lung cancer: the MD Anderson experience. Int J Radiat Oncol Biol Phys 2012;83(1):332–9.
16. Chen C, Uyterlinde W, Sonke JJ, de Bois J, van den Heuvel M, Belderbos J. Severe late esophagus toxicity in NSCLC patients treated with IMRT and concurrent chemotherapy. Radiother Oncol 2013;108(2):337–41.
17. Feddock J, Arnold SM, Shelton BJ, Sinha P, Conrad G, Chen L, et al. Stereotactic body radiation therapy can be used safely to boost residual disease in locally advanced non-small cell lung cancer: a prospective study. Int J Radiat Oncol Biol Phys 2013;85(5):1325–31.
18. Hepel JT, Leonard KL, Safran H, Ng T, Taber A, Khurshid H, et al. Stereotactic body radiation therapy boost after concurrent chemoradiation for locally advanced non-small cell lung cancer: a phase 1 dose escalation study. Int J Radiat Oncol Biol Phys 2016;96(5):1021–7.
19. Speirs CK, DeWees TA, Rehman S, Molotievschi A, Velez MA, Mullen D, et al. Heart dose is an independent dosimetric predictor of overall survival in locally advanced non-small cell lung cancer. J Thorac Oncol 2017;12:293–301.
20. Boellaard R, Delgado-Bolton R, Oyen WJ, Giammarile F, Tatsch K, Eschner W, et al. FDG PET/CT: EANM procedure guidelines for tumour imaging: version 2.0. Eur J Nucl Med Mol Imaging 2015;42(2):328–54.
21. Wolthaus JW, Sonke JJ, van Herk M, Belderbos JS, Rossi MM, Lebesque JV, et al. Comparison of different strategies to use four-dimensional computed tomography in

treatment planning for lung cancer patients. Int J Radiat Oncol Biol Phys 2008;70(4):1229–38.

Supplementary data 1

Radiation treatment planning for PTV_{60Gy}

Both ^{18}F-FDG-PET/CTs were transferred to the Pinnacle^3 treatment planning system (Version 9.10; Philips Radiation Oncology Systems, Fitchburg, WI) and rigid fusion of these images with the initial radiotherapy planning CT was performed. The initial gross target volume (GTV) had been depicted on the 3-dimensional (3D) radiotherapy planning CT using the information of the pre-treatment ^{18}F-FDG-PET/CT and consisted of the primary tumour and involved lymph nodes. The clinical target volume (CTV) enclosed the GTV of the primary tumour and lymph nodes with 10 mm and 5 mm margins, respectively. Isotropic expansion of 5 mm of the CTVs created the planning target volume (PTV). Dose coverage for all the initially created PTVs was re-planned by an experienced radiation treatment planning technician (PvK, 25 years of experience in radiation treatment planning). Using a VMAT technique, a prescription dose of 60 Gy in 30 fractions was applied, based on our national treatment protocol and ESMO guideline (1). A standard 10 MV photon arc beam set-up was used avoiding the contralateral uninvolved lung. Predicted dose deposition was calculated using a 3D collapsed-cone convolution superposition algorithm. According to the ICRU 50/62 guidelines, the -5% and +7% dose heterogeneity criteria for the PTV were aimed for (2, 3). Planning parameters for PTV_{60Gy} are described in the table below.

1. Eberhardt WEE, De Ruysscher D, Weder W, et al. 2nd ESMO Consensus Conference in Lung Cancer: locally advanced stage III non-small-cell lung cancer. *Annals of Oncology* 2015;26(8):1573-1588
2. Prescribing, recording and reporting photon beam therapy. Report 50. Bethesda: International Commission on Radiation Units and Measurements; 1993.
3. Prescribing, recording and reporting photon beam therapy. Report 62; supplement to report 50. Bethesda: International Commission on Radiation Units and Measurements; 1999.

Supplementary data 2. Pre-treatment and early response monitoring ^{18}F-FDG-PET/CT based boost target volumes and their overlap with PRVs.

Pt	PTV_0 in PRV (cm^3)	PTV_3 in PRV (cm^3)	Absolute difference (cm^3)	Relative difference (%)	PTV_0 min PRV (cm^3)	PTV_3 min PRV (cm^3)	Absolute difference (cm^3)	Relative difference (%)
1	-	-	-	-	-	-	-	-
2	4	3.5	-0.5	-12.5	208.8	179.1	-29.7	-14.2
3	0	1	1	100	13.5	19.5	6	44.4
4	0.3	0	-0.3	-100.0	163.5	98.4	-65.1	-39.8
5	21.8	13.7	-8.1	-37.2	70	40.9	-29.1	-41.6
6	37.3	35	-2.3	-6.2	86.7	94.2	7.5	8.7
7	11.80	7.8	-4	-33.9	29.30	24.9	-4.4	-15.0
8	2.2	3.7	1.5	68.2	205.5	184.9	-20.6	-10.0
9	-	-		-	-	-	-	-
10	1.6	1.6	0	0	12.7	13.9	1.2	9.4

Patient 1 and 9 did not have an overlap of boost planning target volume with planning organ at risk volume.

Abbreviations: PRV: planning organ at risk volume; PTV_0 in PRV: overlap of boost planning target volume determined on pre-treatment ^{18}F-FDG-PET/CT with planning organ at risk volume; PTV_0 min PRV: part of boost planning target volume determined on pre-treatment ^{18}F-FDG-PET/CT without overlap with planning organ at risk volume; PTV_3 in PRV: overlap of boost planning target volume determined on early response monitoring ^{18}F-FDG-PET/CT with planning organ at risk volume; PTV_3 min PRV: part of boost planning target volume determined on early response monitoring ^{18}F-FDG-PET/CT without overlap with planning organ at risk volume; Absolute difference: PTV_3 volume minus PTV_0 volume; Relative difference: (absolute difference/PTV_0)*100

Supplementary data 3. Allowed and planned dose to organs at risk based on planning on early response monitoring ^{18}F-FDG-PET/CT

	Heart		*Bronchial tree*		*Oesophagus*		*Brachial plexus*	
Pt	**Allowed D_{max}**	**Planned D_{max}**	**Allowed D_{max}**	**Planned D_{max}**	**Allowed D_{max}**	**Planned D_{max}**	**Allowed D_{max}**	**Planned D_{max}**
1	27.1	13.6	31.5	9.7	8.7	8.7	6.9	3.8
2	29.7	26.7	30.6	23.1	6.6	6.6	N/A	N/A
3	29.3	29.3	28.9	23.8	7.0	2.6	N/A	N/A
4	27.6	11.1	27.1	18.8	7.9	5.1	N/A	N/A
5	30.6	30.6	30.6	30.4	8.3	7.9	8.2	0.5
6	28.0	26.5	28.0	25.1	7.0	7.0	7.3	0.7
7	31.0	30.9	30.6	18.9	7.0	3.0	N/A	N/A
8	30.6	30.6	33.2	11.2	10.0	9.7	4.6	4.3
9	39.4	9.1	33.6	1.9	22.1	2.3	N/A	N/A
10	29.3	29.2	29.3	6.8	11.7	4.7	N/A	N/A

	Spinal cord		*Lungs minus GTV_{60Gy}*			*Contralateral lung*
Pt	**Allowed D_{max}**	**Planned D_{max}**	**MLD 60 Gy plus boost**	**V20 60 Gy plus boost**	**V5 60 Gy plus boost**	**V5 60 Gy plus boost**
1	17.3	4.4	15.7	26.3	53.6	54.2
2	29.9	15.2	16.1	22.6	68.8	64.5
3	14.7	3.6	18.3	30.3	66.6	52.2
4	5.8	4.3	20.4	33.9	49.7	15.5
5	15.1	7.5	18.4	28.4	61.8	54.9
6	11.7	3.8	14.9	24.5	46	36.3
7	20.1	1.8	13.2	22	46.8	40.6
8	3.8	3.6	11.2	16.6	40.9	36.3
9	13.6	1.1	19.9	38.8	80.8	64.5
10	7.4	2.0	16.5	25.2	57.6	54.5

Allowed and planned dose in EQD_2 (except for mean lung dose) for stereotactic boost planning based on early response monitoring ^{18}F-FDG-PET/CT. Abbreviations: D_{max}: maximum dose; MLD: mean lung dose; GTV_{60Gy}: gross target volume receiving 60 Gy; PRV: planning organ at risk volume; V20: percentage receiving ≥20 Gy; V5: percentage receiving ≥5 Gy; 60 Gy plus boost: summed physical dose of the total radiation treatment plan (60 Gy plus stereotactic boost).

Supplementary data 4

Heart dose

Patient	Heart V50	Heart D_{mean}
1	4.5	7.9
2	6.6	32.4
3	15.0	19.3
4	7.7	17.6
5	5.2	11.3
6	9.4	11.2
7	5.6	7.5
8	0.0	2.1
9	5.7	17.0
10	12.0	16.1

Mean dose (D_{mean}) and percentage of heart receiving ≥50 Gy (V50) (summed physical dose) for individual patients of total radiation plan (60 Gy treatment plan plus boost planned on early response monitoring ^{18}F-FDG-PET/CT).


Read online

CHAPTER VII

The predictive value of early in-treatment FDG-PET/CT response to chemotherapy in combination with bevacizumab in advanced non-squamous non-small cell lung cancer

Edwin A. Usmanij, Tinatin Natroshvili, Johanna N.H. Timmer-Bonte, Wim J.G. Oyen, Miep A. van der Drift, Johan Bussink, Lioe-Fee de Geus-Oei

Adapted from: Journal of Nuclear Medicine 2017; Aug;58(8):1243-1248.

Financial support: research grants Roche BV, the Netherlands
A. Timmer-Bonte, M. van der Drift: Roche paid a fee to the pulmonology ward where this author worked at the time of this study.

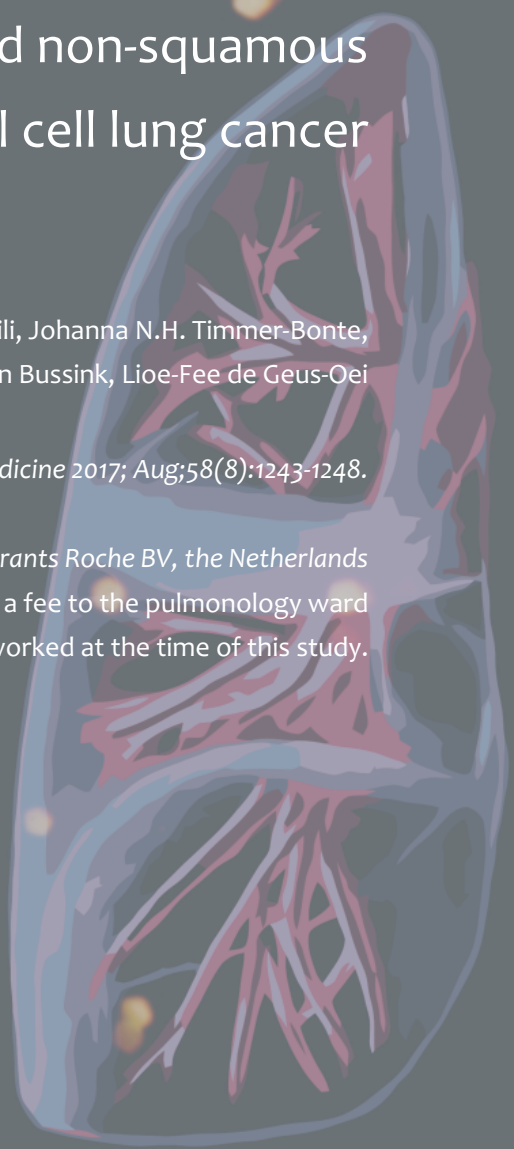

7

ABSTRACT

Objective

^{18}F-fluorodeoxyglucose-positron emission tomography/computed tomography (^{18}F-FDG-PET/CT) is potentially applicable to predict response to chemotherapy in combination with bevacizumab in patients with advanced non-small cell lung cancer (NSCLC).

Materials and Methods

In 25 patients with advanced non-squamous NSCLC, ^{18}F-FDG-PET/CT was performed before treatment and after two weeks, at the end of the second week of first cycle carboplatin – paclitaxel and bevacizumab (CPB) treatment. Patients received up to a total of 4 cycles of CPB treatment. Maintenance treatment with bevacizumab monotherapy was continued until progressive disease without significant treatment-related toxicities of first-line treatment. In the case of progressive disease, bevacizumab was combined with erlotinib. Standardised uptake value (SUV) corrected for lean body mass (SUL and SUL_{peak}) were obtained. PET response criteria in solid tumours (PERCIST) were used for response evaluation. These semi-quantitative parameters were correlated with progression-free survival (PFS) and overall survival (OS).

Results:

A metabolic response, defined by a significant reduction in SUL_{peak} ≥30% after two weeks of CPB, was predictive of PFS and OS. For partial metabolic responders (n = 19) median OS was 22.8 months. One year and 2-y OS were 79% and 47%, respectively. Non-metabolic responders (n = 6) (stable metabolic disease or progressive disease) showed a median OS of 4.4 months (1-y, and 2-y OS was 33% and 0% respectively) ($P < 0.001$).

Conclusion

^{18}F-FDG-PET/CT after one treatment cycle is predictive of outcome to first-line chemotherapy with bevacizumab in patients with advanced non-squamous NSCLC. This enables identification of patients at risk of treatment failure, permitting treatment alternatives such as an early switch to a different therapy.

Key Words

Early response prediction, advanced non-small cell lung cancer; carboplatin-paclitaxel chemotherapy; bevacizumab, ^{18}F-FDG PET/CT, PERCIST

INTRODUCTION

Lung cancer is the major cause of cancer-related death in the Western World (1). Non-small cell lung cancer (NSCLC) represents about 80% of all lung cancer. In the majority of cases, patients already have locally advanced or metastatic disease at presentation. Vascular endothelial growth factor (VEGF) is an important mediator in tumour angiogenesis, which plays an essential role in cancer cell survival in local tumour growth and the development of distant metastases. A strongly increased expression of VEGF has been found in non–small-cell lung cancers (2) and is associated with an unfavourable impact on survival (3). Bevacizumab, a monoclonal antibody against VEGF-A, interacts with this pathway by blocking the effect of VEGF. A landmark phase 3 trial has shown that the addition of bevacizumab to carboplatin and paclitaxel in NSCLC improved overall survival (4). Recent American Society of Clinical Oncology guideline recommends adding bevacizumab to carboplatin plus paclitaxel (5). One explanation is that bevacizumab leads to vascular normalisation of tumour vasculature (6), thus increasing delivery and of cytotoxic therapy to the tumour leading to improved treatment efficacy. The evaluation of tumour volume response by conventional imaging techniques using Response evaluation criteria in solid tumours (RECIST) criteria has its limitations in detection of early therapy response (7), especially in the case of targeted treatment. FDG-PET/CT provides rapid, non-invasive, in vivo assessment and quantification of glucose metabolism and might be a powerful tool for measurement of treatment response. Changes in tumour glucose metabolism precede changes in tumour size and can possibly reflect drug effects at a cellular level, resulting in a potential advantage over morphological imaging. Molecular imaging using FDG-PET/CT has shown in NSCLC patients to be a valuable tool for early detection of treatment response in chemotherapy (8), chemo-radiotherapy (9-13) and targeted treatment (14-19). The prediction of response using FDG-PET/CT may enable a distinction between patients who are going to benefit from treatment. Early detection of non-responders allows for treatment adaptation or earlier switch to other treatment lines. Ultimately, this can lead to a reduction in ineffective and potentially toxic therapy, a reduction in costs and a more personalised tumour-oriented approach. Few FDG-PET/CT response-monitoring studies have been performed to evaluate anti-angiogenic treatment in NSCLC (20,21). To address this issue, a side-study for early FDG-PET/CT response monitoring study was performed, alongside a phase 2 trial in patients with newly diagnosed advanced NSCLC treated with first-line chemotherapy carboplatin, paclitaxel and bevacizumab (CPB). We explored the value of FDG-PET/CT to predict clinical outcome by using an early in-treatment FDG-PET/CT.

MATERIALS AND METHODS

Patients

From January 2009 to January 2013, patients with newly diagnosed locally advanced or metastatic NSCLC without prior systemic treatment were enrolled in this prospective single centre study. Patients with histologically or cytologically confirmed non-squamous NSCLC (stage IIIB or stage IV) and at least one measurable lesion (based on RECIST 1.1) were eligible. Exclusion criteria were previous chemotherapy or systemic anti-tumour therapy, previous radical radiotherapy, performance score ≥2 (Eastern Co-operative Oncology Group) or another active malignancy except for non-melanoma skin cancers in the last five years. This study was approved by the institutional review Board of the Radboud university medical centre Nijmegen. All patients provided written informed consent.

Treatment

Patients were treated with bevacizumab (15 mg/kg every three weeks), paclitaxel (200 mg/m^2 body surface area on day 1 every three weeks) and carboplatin (area under concentration-time curve of 6, on day 1 every three weeks). Patients received a maximum of 4 cycles of therapy, after which monotherapy of bevacizumab was continued as long as patients had no evidence of progressive disease and no significant treatment-related toxicities. In the case of progressive disease bevacizumab 15 mg/kg every 3 weeks continued and erlotinib 150 mg/day (second-line treatment) added. Both epidermal growth factor receptor (EGFR) mutated and EGFR wild type genotypes were included in the study.

Study design

The primary objective of this phase II study was to monitor the efficacy of erlotinib plus bevacizumab (BE) subsequent to a progressive disease on CPB as determined by the maximum achieved disease control rate. One of the secondary objectives was the determination of early response, and FDG-PET/CT was performed before treatment and after one cycle of treatment (before the second cycle of treatment). Other secondary objectives were to monitor disease control rate and time to progression of CPB and BE respectively, and overall survival. The study design is shown in *Figure 1*. Clinicians were blinded to the results of the in-treatment FDG-PET/CT. Standard clinical response evaluation was done using contrast-enhanced computed tomography (CT) every 6 weeks

until disease progression. A response was assessed according to RECIST 1.1 (22) every 6 weeks (or every 9 weeks after week 18 in the BE treatment phase), at the onset of clinical signs of progression and in case of premature discontinuation of study treatment. Partial response (PR) or complete response, had to be confirmed after a minimum of 4 weeks. In case of stable disease (SD), follow-up measurements must have met the stable disease criteria at least once after study entry at a minimal interval of 6 weeks.

FDG-PET/CT

For each patient baseline and in-treatment FDG-PET/CT was performed with the same hybrid PET/CT scanner (Siemens Biograph Duo or Siemens Biograph 40 mCT, Siemens Medical Solutions USA, Inc.) according to the guidelines of the European Association of Nuclear Medicine (23). At least 6 hours before ^{18}F-FDG injection, the patients fasted,

FIGURE 1. Study design.

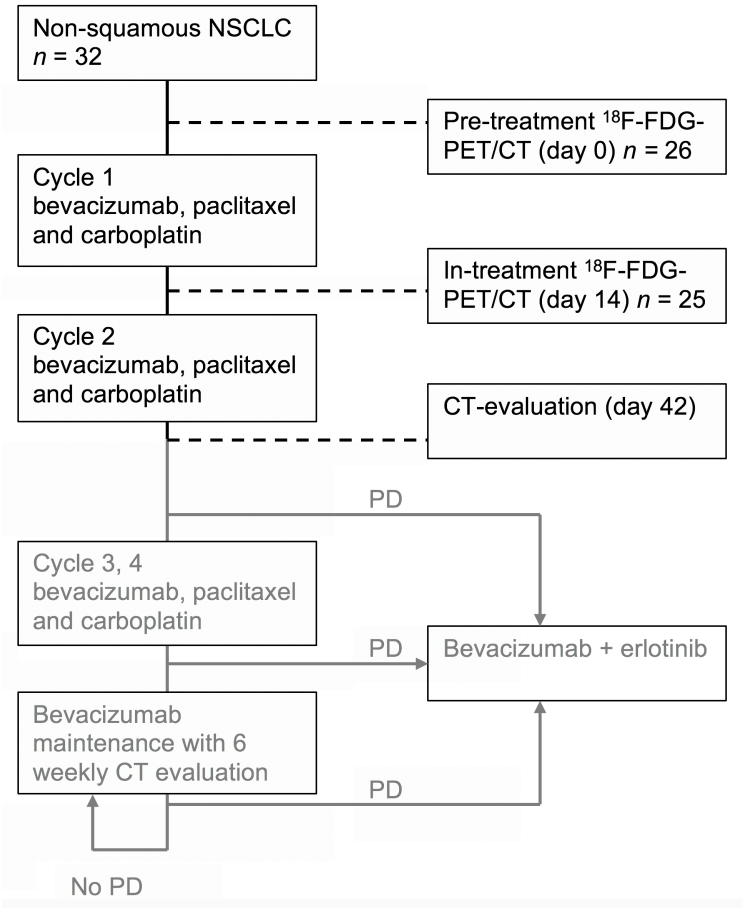

including discontinuation of any tube or PEG-feeding and any glucose-containing i.v. fluids. Immediately before ^{18}F-FDG injection, the blood glucose level was checked. According to protocol FDG-PET/CT scans were performed at mean 66 minutes (range 58 – 73) after ^{18}F-FDG injection and furosemide 10 mg, covering the neck, thorax, abdomen and pelvis. The PET acquisition time was 4 minutes per bed position. PET scans from the Siemens Biograph Duo were processed using iterative reconstruction with the ordered subsets expectation maximisation algorithm (image matrix size, 128 x 128, 4 iterations, 16 subsets; and a 5-mm 3-dimensional Gaussian filter). PET images from the Siemens Biograph 40 mCT were reconstructed with the TrueX algorithm (with a spatially varying point spread function and the incorporation of time-of-flight measurements (Ultra-HD PET). Image reconstruction was performed with three iterations, 21 subsets, and a matrix size of 400 × 400 (pixel spacing of 2.04 mm). Reconstructed images were corrected for injected dose, the decay of ^{18}F-FDG, patient body weight, and attenuation using a low-dose CT scan. Correction for breathing motion using a 4D mode was not used.

Analysis of FDG-PET

FDG-PET/CTs were analysed on Pinnacle^3 (version 8.0d; Philips Radiation Oncology Systems). At baseline, FDG-PET/CT was analysed visually (number and localisation of lesions) and quantitatively. SUV was normalised by lean body mass using Janmahasatian formula (24). The SUL_{peak} of target lesions at baseline was at least 1.5× mean liver SUL + 2 standard deviations of mean SUL. At follow-up, FDG-PET/CT was analysed visually (number and localisation of lesions, new lesions, visual change in uptake and size) and quantitatively (SUV, SUL, SUL_{peak}). A maximum of five target lesions was selected and delineated using a 50% iso-contour threshold, according to PERCIST criteria (up to a maximum of two lesions per organ). New FDG-avid lesions, suspect for metastasis, were considered progressive disease. For evaluation of response predefined response criteria (PERCIST criteria) were used (25): A complete metabolic response (CMR) was defined as a complete resolution of FDG-uptake within the measurable target lesions and other lesions (less than mean liver activity and at the level of surrounding background blood pool activity) without the advent of new suspicious FDG-avid lesions. Partial metabolic response (PMR) was defined as a reduction of ≥30% in the target tumour SUL_{peak} (and an absolute drop of at least 0.8 SUL). PMD was a ≥30% increase in SUL_{peak} or advent of new FDG-avid lesions typical of cancer. Stable metabolic disease (SMD) (reduction < 30% and increase < 30%) was disease other than CMR, PMR or PMD. Two independent readers, blinded to the results of the CT-scans, performed reading of the FDG-PET/CTs and vice versa.

Statistical analysis

Patients were considered evaluable for analysis if they underwent both pre-treatment FDG PET/CT and in-treatment FDG PET/CT. OS was measured from the date of treatment start to time to disease-related death. PFS was measured from the date of treatment start to time of disease progression on contrast-enhanced CT. In-treatment response evaluation on CT was measured at 6-weeks after treatment start. On FDG-PET/CT (measured 2 weeks in-treatment) metabolic response was defined as CMR or PMR and metabolic non-response was defined as SMD or PMD. Concordance between in-treatment PERCIST and RECIST was assessed using Cohen's κ coefficient and Wilcoxon's signed-ranks test. OS and PFS survival analysis were performed using Kaplan-Meier-method. Responders and non-responders were compared using log-rank statistics. Statistical analysis was performed using SPSS 22.0 (SPSS Inc.) for Windows (IBM Corp, Armonk, NY). The level of statistical significance was defined as a $P < 0.05$ based on two-sided tests. No time-dependent adjustment was needed because no progression or death was observed before the RECIST assessment.

RESULTS

Patients Characteristics and Follow-up

Thirty-two patients were enrolled in the phase 2 study, of which 26 patients had a baseline FDG-PET/CT. Patient characteristics are shown in *Table 1*. One patient did not receive in-treatment FDG-PET/CT after the first treatment cycle and therefore was excluded from further analysis. Of the remaining 25 patients, 22 patients (88%) received 4 cycles (out of 4) CBP, while three patients (12%) received only 2 cycles first-line treatment, due to early disease progression. 21 patients (84%) continued monotherapy bevacizumab. 19 patients (76%) received second-line treatment of erlotinib plus bevacizumab after they progressed on (CP)B. One patient receiving second-line erlotinib and bevacizumab had an EGFR mutation. In the present study, an EGFR mutation was found in two patients. Baseline FDG-PET/CT was always performed before treatment; the median time of baseline FDG-PET/CT was 13 days (range 2 – 35d) before treatment. There was no relation between delay on treatment start and outcome (PFS or OS) in Cox proportional hazards analysis (hazard ratio of 0.997 (0.963 – 1.033) ($P = 0.871$) for OS and hazard ratio of 0.987 (0.952 – 1.023) for PFS ($P = 0.470$). The in-treatment FDG-PET/CT was performed after one cycle of treatment at day 14 (13 – 20 d), always before the second cycle of treatment. Median time to second-line treatment was 9.3 months (range 1.4 – 21.9 mo). Kaplan Meier analysis for PFS and OS stratified using RECIST (6-weeks after

treatment start) is shown in *Figure 2*, no significant difference between response groups was found (log-rank P = 1.000 and P = 0.468 for PFS and OS, respectively). During follow-up, all 25 patients died due to disease progression.

TABLE 1. Patient Characteristics

Characteristics	Value
Median age (y) (range)	54 (42 - 81)
Gender	
Male	15 (47%)
Female	17 (53%)
EGFR mutation status	
EGFR mutation	2 (6%)
No EGFR mutation	30 (94%)
TMM-stage (7th edition)	
IIIB	1 (4%)
IV	31 (96%)
Smoking status	
Current smoker	15 (47%)
Former smoker	17 (53%)
Previous malignancy	
No	6 (19%)
Yes	26 (81%)
CPB treatment cycles	
<4	6 (19%)
4	26 (81%)
Maintenance bevacizumab cycles	
0	6 (19%)
≥ 1	26 (81%)
BE maintenance cycles	
0	11 (34%)
≥ 1	21 (66%)

FIGURE 2. Kaplan-Meier analysis of progression free survival (PFS) and overall survival (OS) stratified using in-treatment CT (RECIST). For SD median PFS was 8.4; median OS was 14.5 months; For PR median PFS was 7.4 months; median OS was survival was 17.6 months. Log-rank test, P = *NS*.

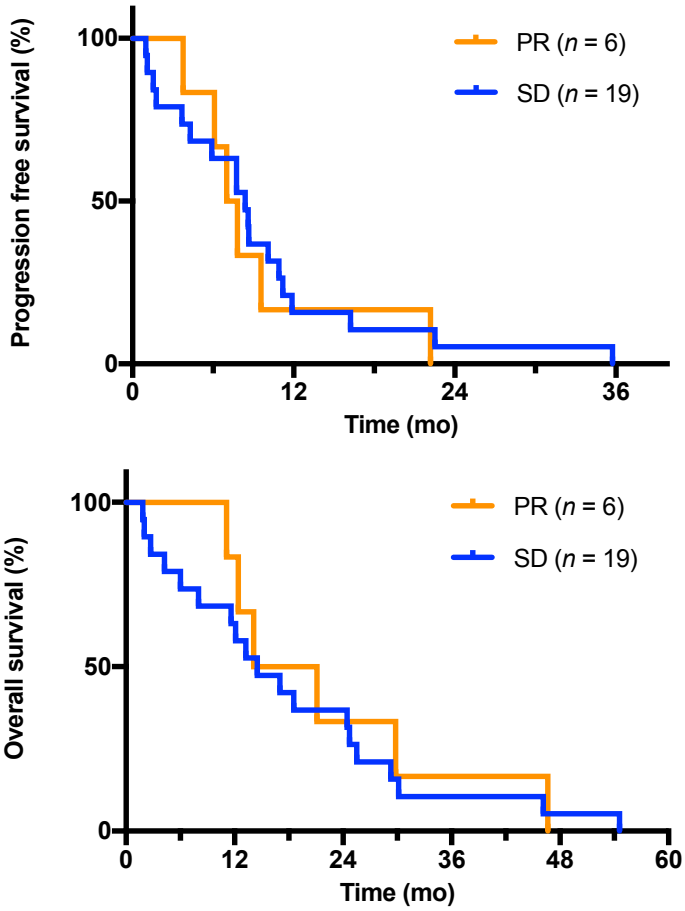

Predictive value of FDG-PET/CT

Median baseline SUV was 6.8, and after 15 days of CPB treatment, median SUV was 5.0 in the target lesions. In all cases, SUL versus SUV response categories (using the same cut-off levels of 30%) were 100% concordant. According to PERCIST, no patient had CMR, 2 (8%) patients had PMD, while 4 (16%) patients had stable metabolic disease (SMD). 19 (76%) patients had PMR. For non-responders (both PMD and SMD) median PFS was 1.7 months (range 1.0 – 6.1 mo). For patients with PMR median PFS was 8.7 months (range 3.7 – 35.7 mo), 1-y and 2-y PFS were 21% and 5%, respectively. For SMD and PMD

median OS was 4.4 months (range 1.7 – 14.1 mo); 1-y and 2-y OS was 33% and 0% respectively. For PMR median OS was 22.8 months (range 4.3 – 54.6 mo), 1-y and 2-y OS were 79% and 47%, respectively. The Kaplan-Meier analysis of PFS and OS stratified using PERCIST is shown in *Figure 3*. Two examples of patients with stage IV disease are shown in *Figure 4 and 5*, with their baseline and in-treatment FDG-PET/CT.

Comparison of treatment response between RECIST and PERCIST

Nineteen patients were classified as SD on CT (6-weeks in-treatment), while four patients were classified as SMD according to FDG-PET/CT. 15 patients were classified as PMR. RECIST and PERCIST classifications are shown in *Table 2*. PERCIST and RECIST were discordant in 16 patients (64%). Of the 19 patients having SD according to RECIST, 14 patients were reclassified as having PMR according to PERCIST. One patient was classified as PMD due to the advent of new FDG-avid lesions suspected of bone metastasis. However, these lesions were not detected on the 6-week in-treatment CT (patient died 52 days after treatment start). Cohen's coefficient $\varkappa = 0.023$ was indicating minimal agreement between RECIST and PERCIST. Wilcoxon's signed-ranks test was $P < 0.01$ indicating a significant difference between RECIST and PERCIST.

TABLE 2. Comparison of in-treatment response between PERCIST and RECIST

	RECIST			
PERCIST	CR ($n = 0$)	PR ($n = 6$)	SD ($n = 19$)	PD ($n = 0$)
CMR ($n = 0$)	0	0	0	0
PMR ($n = 19$)	0	5	14	0
SMD ($n = 4$)	0	1	3	0
PMD ($n = 2$)	0	0	2	0

FIGURE 3. Kaplan-Meier analysis of progression free survival (PFS) and overall survival (OS) stratified using PERCIST criteria. For SMD and PMD median PFS was 1.7 months; median OS was 4.4 months; For PMR median PFS was 9.1 months; OS was 22.8 months; Log-rank test, $P < 0.001$.

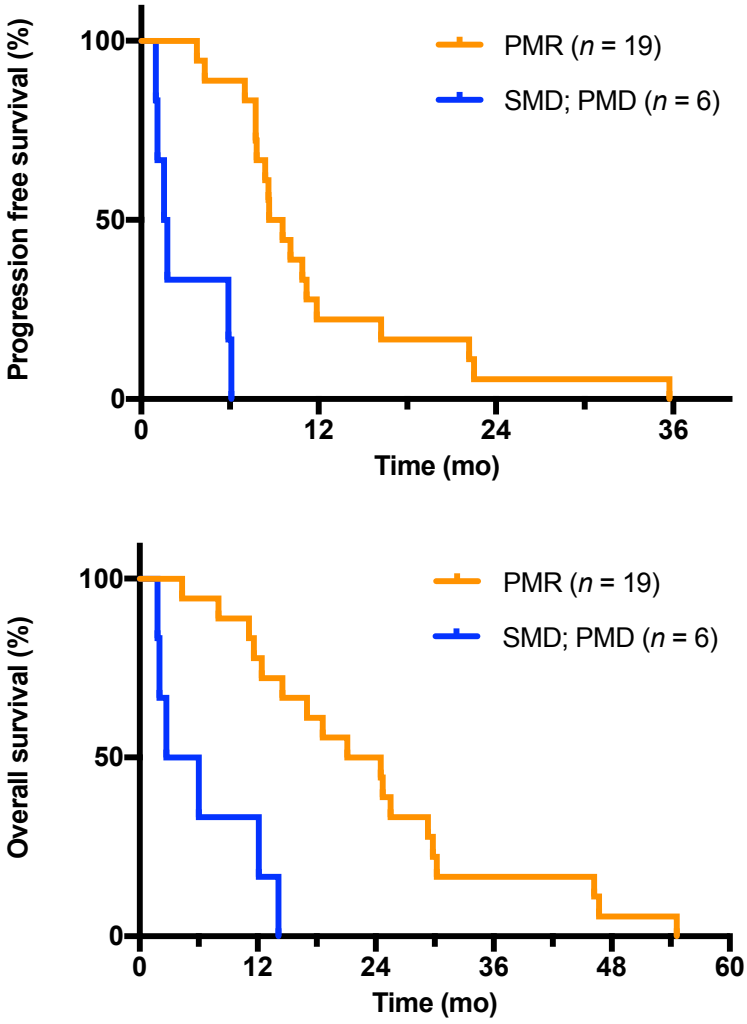

FIGURE 4. Baseline (A) and in-treatment (B) FDG-PET/CT in a 51-year-old female patient with NSCLC, stage IVB, with a Pancoast tumour in the left lung with metastasis in the right adrenal gland (white and black arrows). In-treatment FDG-PET/CT showed apparent decrease in uptake classified as partial metabolic response. Survival was 12.4 months.

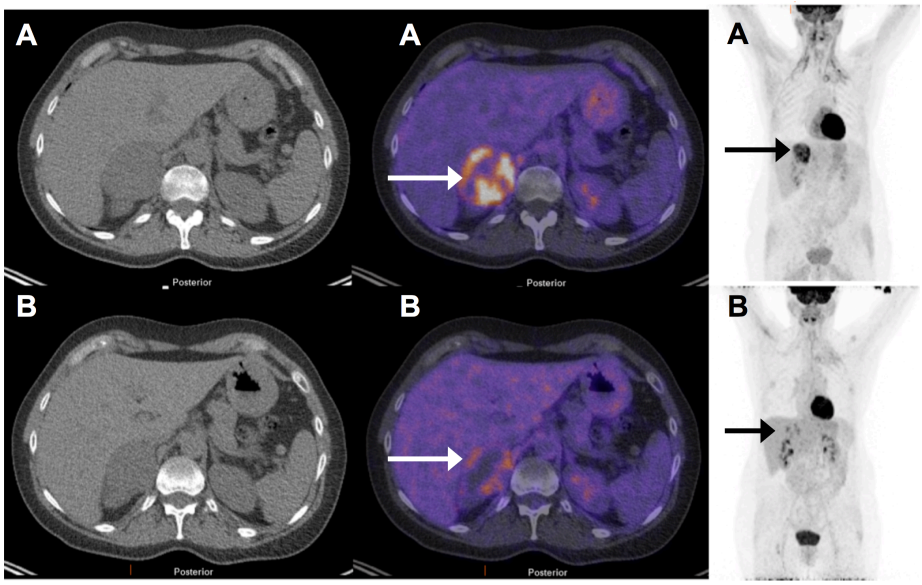

DISCUSSION

This prospective study showed that early in-treatment FDG-PET/CT in advanced NSCLC after two weeks of first chemotherapy and bevacizumab is predictive of PFS and OS. Compared to CT, PET detected response earlier during treatment and more frequently. Therefore, the predictive potential of an early in-treatment FDG-PET/CT, performed at two weeks after the start of treatment, is better than measurement of size changes on CT according to RECIST at six weeks after the start of treatment. This resulted in discordance between PERCIST and RECIST in 16 patients (64%). These differences can only partially be explained by the difference in timing of the response evaluation of FDG-PET/CT (2 weeks in-treatment) and diagnostic CT (6 weeks in-treatment). Early after treatment initiation, tumour size changes as a result of, both tumour reduction (i.e. mitotic cell death and cell loss) and tumour growth (i.e. cell division). As a result, small size changes, i.e. actual response or actual tumour growth or progression are underestimated when tumour

FIGURE 5. Baseline (A) and in-treatment (B) FDG-PET/CT in a 67-year-old female patient with NSCLC, stage IVB, with a tumour in the left lower lobe with metastases in lymph nodes, lung, liver and bones. In-treatment FDG-PET/CT showed apparent increase in uptake (open arrows) and new FDG-avid bone lesions (black arrows), classified as progressive metabolic disease. Survival was 1.7 months.

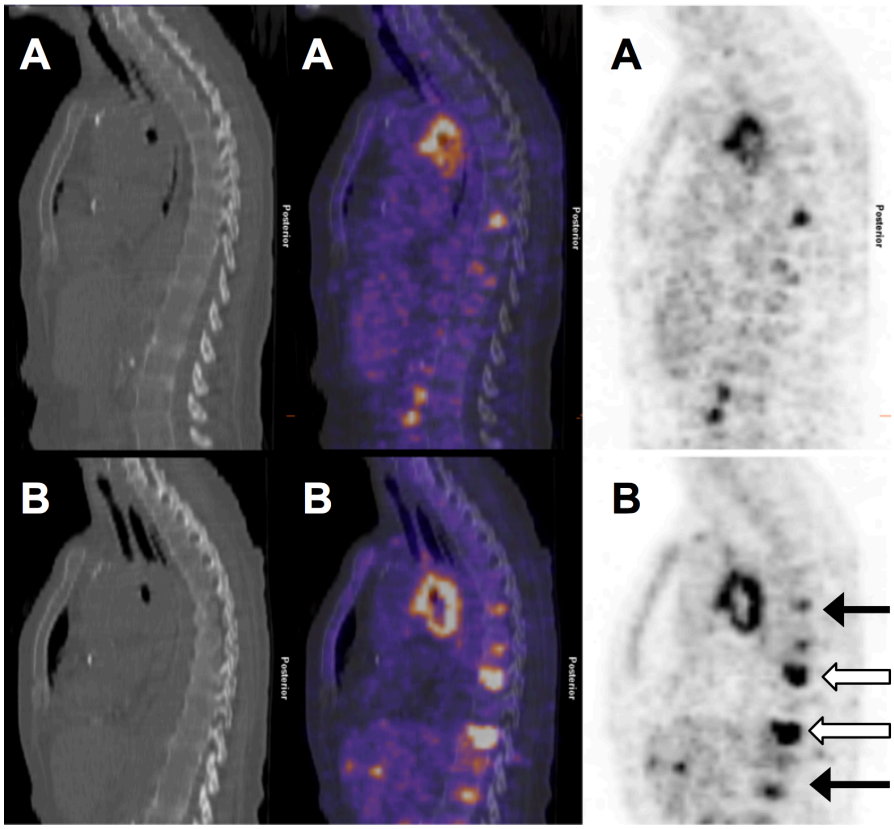

size is used as an early predictive marker. According to PERCIST, a significant reduction in FDG-uptake after one treatment cycle was associated with favourable outcome in terms of both PFS and OS. In this study, 6 out of 25 patients (24%) were classified as non-responders (SMD or PMD), showing significantly lower median OS and PFS when compared to patients with a PMR ($P < 0.001$). Of the 19 patients having SD according to RECIST, 14 patients were reclassified as having PMR according to PERCIST, showing that metabolic changes exceeded the threshold criteria earlier than morphological changes. A prospective study by Shang *et al.* (26) comparing RECIST, EORTC and PERCIST criteria for evaluation of early response (after two weeks) to chemotherapy in NSCLC patients showed that both EORTC and PERCIST criteria were more accurate in predicting early response to treatment.

Studies addressing response prediction in advanced NSCLC treated with first-line chemotherapy and bevacizumab are limited. De Langen *et al.* (21) demonstrated in (locally) advanced NSCLC patients treated with erlotinib and bevacizumab that a decrease in SUV of more than 20% after three weeks was associated with increased progression-free survival. In oncology practice, it is important to identify effective biomarkers for prediction of failure or success of treatment. In contrast to our study, other response-monitoring studies (9-14) did not use PERCIST criteria for response evaluation (25). Predefined response criteria, are not only essential tools to assess an objective early response but are also crucial in the harmonisation of FDG-PET/CT studies and facilitate reproducibility across response assessment trials.

A major concern during anti-VEGF treatment is tumour evasion and resistance from VEGF blockage, involving several possible escapes mechanisms (27). An apparent increase in FDG-uptake during treatment might suggest resistance mechanisms resulting in an increase in anaerobic metabolism and an increase in glycolysis. Alternatively, the decrease of tumour vascularity due to anti-angiogenic agents could also lead to an increase in hypoxia and glycolysis. However, ^{18}F-FDG alone is not capable of discriminating between hypoxic and non-hypoxic regions. Tumour hypoxia and metabolism are independent events, which was shown in a study comparing ^{18}F-FAZA and ^{18}F-FDG in NSCLC (28). The effects of anti-angiogenic treatment could negatively affect the efficacy of FDG-PET/CT early response monitoring in NSCLC. However, in our report, we show that early response monitoring in NSCLC patients treated with chemotherapy the addition of bevacizumab seems feasible. Another entirely different approach is ^{89}Zr-bevacizumab to visualise targeting of VEGFR for prediction of treatment efficacy (*29*), however further studies are needed to establish a potential role for ^{89}Zr-bevacizumab in NSCLC.

A limitation of our study is the relatively small number of patients. For the development of a clinical application of metabolic treatment response studies, larger series are necessary. In our analysis, PMD and SMD patients were defined as non-metabolic responders. These two categories may have outcome differences can only be detected by a much larger study population. When effective surrogates for early prediction are established, treatment decision-making based on the early in-treatment FDG-PET/CT seems feasible. In our study, we showed that as early as two weeks into first-line treatment, early metabolic changes predict clinical outcome. The majority of other FDG-PET/CT response assessments studies were performed at relative late time-point during treatment, not allowing any treatment adaptation based on the response assessment (30-32). Early discontinuation of an ineffective treatment regimen can possibly prevent unnecessary treatment toxicity. Moreover, earlier switch to a potentially beneficial different therapy could result in early tumour consolidation, better outcomes and better cost-effectiveness.

Another limitation of our study is the second line bevacizumab and erlotinib therapy started after progression on CPB or on bevacizumab maintenance. This investigational second line approach (given in 76% of the patients) showed only modest clinical benefit (33), where OS and PFS on first line CPB were in line with published data (4). However, the optimal strategy of anti-angiogenic therapy in the treatment of advanced NSCLC is still subject to randomised trials and large observational studies. Continuation of bevacizumab treatment in the absence of disease progression is a new treatment strategy in NSCLC, which is less toxic than traditional chemotherapy agents (34) and well tolerated (35). The concept of continuing bevacizumab treatment beyond progression is under investigation (36). More recently, the role of erlotinib with bevacizumab as first-line therapy is being explored (37).

CONCLUSION

The current study in advanced non-squamous NSCLC patients treated with first-line chemotherapy and bevacizumab showed that early in-treatment FDG-PET/CT is predictive of response to treatment and overall survival, already after two weeks of therapy. This enables identification of patients at risk of treatment failure, permitting an early and more individualised treatment modification.

References

1. Jemal A, Bray F, Center MM, Ferlay J, Ward E, Forman D. Global cancer statistics. *CA Cancer J Clin.* 2011;61:69-90.
2. Fontanini G, Boldrini L, Chine S, et al. Expression of vascular endothelial growth factor mRNA in non-small-cell lung carcinomas. *Br J Cancer.* 1999;79:363-369.
3. Zhan P, Wang J, Lv XJ, et al. Prognostic value of vascular endothelial growth factor expression in patients with lung cancer: a systematic review with meta-analysis. *J Thorac Oncol.* 2009;4:1094-1103.
4. Sandler A, Gray R, Perry MC, et al. Paclitaxel-carboplatin alone or with bevacizumab for non-small-cell lung cancer. *N Engl J Med.* 2006;355:2542-2550.
5. Masters GA, Temin S, Azzoli CG, et al. Systemic therapy for stage IV non-small-cell lung cancer: American Society of Clinical Oncology clinical practice guideline update. *J Clin Oncol.* 2015;33:3488-3515.
6. Shih T, Lindley C. Bevacizumab: an angiogenesis inhibitor for the treatment of solid malignancies. *Clin Ther.* 2006;28:1779-1802.
7. Birchard KR, Hoang JK, Herndon JE, Jr., Patz EF, Jr. Early changes in tumor size in patients treated for advanced stage nonsmall cell lung cancer do not correlate with survival. *Cancer.* 2009;115:581-586.
8. Ordu C, Selcuk NA, Erdogan E, et al. Does early PET/CT assesment of response to chemotherapy predicts survival in patients with advanced stage non-small-cell lung cancer? *Medicine (Baltimore).* 2014;93:e299.
9. Usmanij EA, de Geus-Oei LF, Troost EG, et al. 18F-FDG PET early response evaluation of locally advanced non-small cell lung cancer treated with concomitant chemoradiotherapy. *J Nucl Med.* 2013;54:1528-1534.
10. Dong X, Sun X, Sun L, et al. Early change in metabolic tumor heterogeneity during chemoradiotherapy and its prognostic value for patients with locally advanced non-small cell lung cancer. *PLoS One.* 2016;11(6):e0157836.
11. Roy S, Pathy S, Kumar R, et al. Efficacy of 18F-fluorodeoxyglucose positron emission tomography/computed tomography as a predictor of response in locally advanced non-small-cell carcinoma of the lung. *Nucl Med Commun.* 2016;37:129-138.
12. Yossi S, Krhili S, Muratet JP, Septans AL, Campion L, Denis F. Early assessment of metabolic response by 18F-FDG PET during concomitant radiochemotherapy of non-small cell lung carcinoma is associated with survival: a retrospective single-center study. *Clin Nucl Med.* 2015;40:e215-221.
13. Toma-Dasu I, Uhrdin J, Lazzeroni M, et al. Evaluating tumor response of non-small cell lung cancer patients with (1)(8)F-fludeoxyglucose positron emission tomography: potential for treatment individualization. *Int J Radiat Oncol Biol Phys.* 2015;91:376-384.

14. Mileshkin L, Hicks RJ, Hughes BG, et al. Changes in 18F-fluorodeoxyglucose and 18F-fluorodeoxythymidine positron emission tomography imaging in patients with non-small cell lung cancer treated with erlotinib. *Clin Cancer Res.* 2011;17:3304-3315.
15. Aukema TS, Kappers I, Olmos RA, et al. Is 18F-FDG PET/CT useful for the early prediction of histopathologic response to neoadjuvant erlotinib in patients with non-small cell lung cancer? *J Nucl Med.* 2010;51:1344-1348.
16. Riely GJ, Kris MG, Zhao B, et al. Prospective assessment of discontinuation and reinitiation of erlotinib or gefitinib in patients with acquired resistance to erlotinib or gefitinib followed by the addition of everolimus. *Clin Cancer Res.* 2007;13:5150-5155.
17. Zander T, Scheffler M, Nogova L, et al. Early prediction of nonprogression in advanced non-small-cell lung cancer treated with erlotinib by using [(18)F]fluorodeoxyglucose and [(18)F]fluorothymidine positron emission tomography. *J Clin Oncol.* 2011;29:1701-1708.
18. Benz MR, Herrmann K, Walter F, et al. (18)F-FDG PET/CT for monitoring treatment responses to the epidermal growth factor receptor inhibitor erlotinib. *J Nucl Med.* 2011;52:1684-1689.
19. Takahashi R, Hirata H, Tachibana I, et al. Early [18F]fluorodeoxyglucose positron emission tomography at two days of gefitinib treatment predicts clinical outcome in patients with adenocarcinoma of the lung. *Clin Cancer Res.* 2012;18:220-228.
20. Dingemans AM, de Langen AJ, van den Boogaart V, et al. First-line erlotinib and bevacizumab in patients with locally advanced and/or metastatic non-small-cell lung cancer: a phase II study including molecular imaging. *Ann Oncol.* 2011;22:559-566.
21. de Langen AJ, van den Boogaart V, Lubberink M, et al. Monitoring response to antiangiogenic therapy in non-small cell lung cancer using imaging markers derived from PET and dynamic contrast-enhanced MRI. *J Nucl Med.* 2011;52:48-55.
22. Eisenhauer EA, Therasse P, Bogaerts J, et al. New response evaluation criteria in solid tumours: revised RECIST guideline (version 1.1). *Eur J Cancer.* 2009;45:228-247.
23. Boellaard R, O'Doherty MJ, Weber WA, et al. FDG PET and PET/CT: EANM procedure guidelines for tumour PET imaging: version 1.0. *Eur J Nucl Med Mol Imaging.* 2010;37:181-200.
24. Janmahasatian S, Duffull SB, Ash S, Ward LC, Byrne NM, Green B. Quantification of lean bodyweight. *Clin Pharmacokinet.* 2005;44:1051-1065.
25. Wahl RL, Jacene H, Kasamon Y, Lodge MA. From RECIST to PERCIST: Evolving Considerations for PET response criteria in solid tumors. *J Nucl Med.* 2009;50 Suppl 1:122S-150S.
26. Shang J, Ling X, Zhang L, et al. Comparison of RECIST, EORTC criteria and PERCIST for evaluation of early response to chemotherapy in patients with non-small-cell lung cancer. *Eur J Nucl Med Mol Imaging.* 2016; 43:1945-1953.

27. Abdollahi A, Folkman J. Evading tumor evasion: current concepts and perspectives of anti-angiogenic cancer therapy. *Drug Resist Updat.* 2010;13:16-28.
28. Kerner GS, Bollineni VR, Hiltermann TJ, et al. An exploratory study of volumetric analysis for assessing tumor response with (18)F-FAZA PET/CT in patients with advanced non-small-cell lung cancer (NSCLC). *EJNMMI Res.* 2016;6:33.
29. Bahce I, Huisman MC, Verwer EE, et al. Pilot study of (89)Zr-bevacizumab positron emission tomography in patients with advanced non-small cell lung cancer. *EJNMMI Res.* 2014;4:35.
30. Fledelius J, Khalil AA, Hjorthaug K, Frokiaer J. Using positron emission tomography (PET) response criteria in solid tumours (PERCIST) 1.0 for evaluation of 2'-deoxy-2'-[18F] fluoro-D-glucose-PET/CT scans to predict survival early during treatment of locally advanced non-small cell lung cancer (NSCLC). *J Med Imaging Radiat Oncol.* 2016;60:231-238.
31. Ding Q, Cheng X, Yang L, et al. PET/CT evaluation of response to chemotherapy in non-small cell lung cancer: PET response criteria in solid tumors (PERCIST) versus response evaluation criteria in solid tumors (RECIST). *J Thorac Dis.* 2014;6:677-683.
32. Han EJ, Yang YJ, Park JC, Park SY, Choi WH, Kim SH. Prognostic value of early response assessment using 18F-FDG PET/CT in chemotherapy-treated patients with non-small-cell lung cancer. *Nucl Med Commun.* 2015;36:1187-1194.
33. Van Groningen H, Timmer-Bonte A, Hurk DV, Dohmen M, Graaf CS, Van der Drift M. 171P: Carboplatin-paclitaxel bevacizumab followed by the addition of erlotinib to bevacizumab beyond progression in patients with advanced NSCLC. *J Thorac Oncol.* 2016;11:S132.
34. Sandler A, Yi J, Dahlberg S, et al. Treatment outcomes by tumor histology in Eastern Cooperative Group Study E4599 of bevacizumab with paclitaxel/carboplatin for advanced non-small cell lung cancer. *J Thorac Oncol.* 2010;5:1416-1423.
35. Lopez-Chavez A, Young T, Fages S, et al. Bevacizumab maintenance in patients with advanced non-small-cell lung cancer, clinical patterns, and outcomes in the Eastern Cooperative Oncology Group 4599 Study: results of an exploratory analysis. *J Thorac Oncol.* 2012;7:1707-1712.
36. Gridelli C, Bennouna J, de Castro J, et al. Randomized phase IIIb trial evaluating the continuation of bevacizumab beyond disease progression in patients with advanced non-squamous non-small-cell lung cancer after first-line treatment with bevacizumab plus platinum-based chemotherapy: treatment rationale and protocol dynamics of the AvaALL (MO22097) trial. *Clin Lung Cancer.* 2011;12:407-411.
37. Seto T, Kato T, Nishio M, et al. Erlotinib alone or with bevacizumab as first-line therapy in patients with advanced non-squamous non-small-cell lung cancer

harbouring EGFR mutations (JO25567): an open-label, randomised, multicentre, phase 2 study. *Lancet Oncol.* 2014;15:1236-1244.

7

CHAPTER VIII

Gender and histological subtype account for differences in the metastatic pattern of non-small cell lung cancer: a nationwide autopsy study

Edwin A. Usmanij, Anne Posthuma, Niek Hugen, Roy P.J. van den Ende,
Iris D. Nagtegaal, Johan Bussink, Lioe-Fee de Geus-Oei

Manuscript in preparation

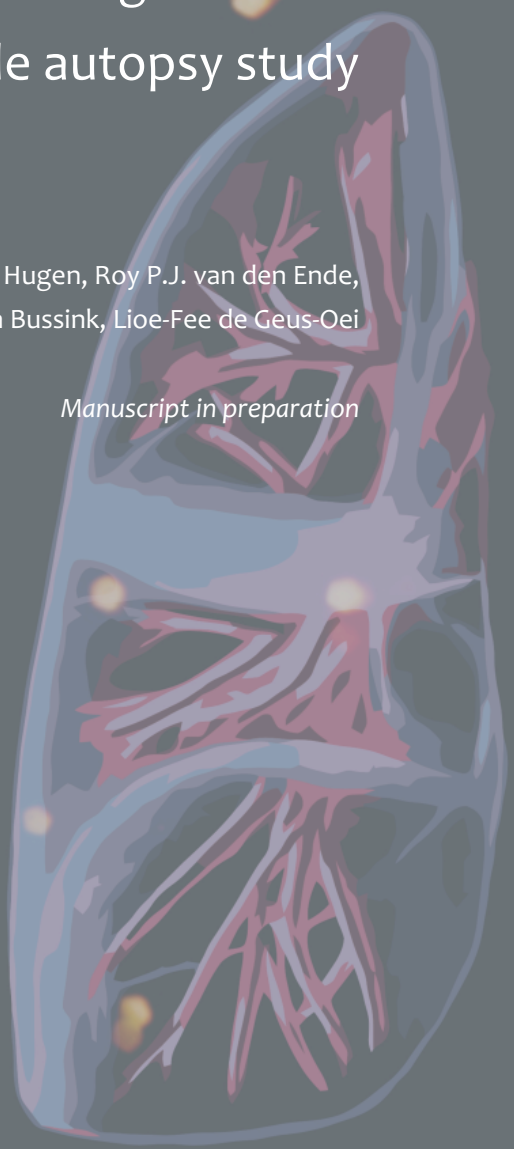

ABSTRACT

Background

Clinical studies in non-small cell lung cancer (NSCLC) have suggested a difference in metastatic patterns between adenocarcinoma (AC) and squamous cell carcinoma (SCC), which might be relevant for treatment and follow up.

Methods

A nationwide retrospective review was performed of pathology records in the Netherlands of all patients with NSCLC who underwent an autopsy between January 2001 and December 2010. These autopsies were selected from the Dutch pathology registry (PALGA) and the presence and location of metastatic disease were retrieved. Clinical relevance of these findings was validated in a single centre cohort on all patients with NSCLC who underwent ^{18}F-fluoro-deoxy-glucose positron emission tomography/computed tomography (FDG PET/CT) between January 2012 and May 2013 for initial staging workup.

Results

From the total of 2798 NSCLC patients, 1128 were diagnosed as AC and 875 as SCC. Patients with AC more frequently developed metastases (49.7% versus 24.8% in SCC, $P < 0.001$) and had metastases at multiple sites more often (77.2% versus 66.8%, $P = 0.004$). Especially metastases to the adrenal gland and bone were more common in AC. SCC metastasised twice as often to the kidney compared with AC (23.2% vs 12.8%) ($P < 0.001$). Female AC patients developed significantly more lung metastases compared with male AC patients. Liver metastases were observed more frequently in female AC patients (49.1% vs 40.5%, $P = 0.044$). Validation with the FDG-PET/CT cohort was performed in a total of 143 NSCLC patients, of which 42 had metastases. Results from this cohort confirmed our findings from the autopsy study.

Conclusion

There are differences in metastatic patterns between AC and SCC. Also, gender-specific differences in AC were found. Both histopathological and gender-specific risks should be considered a stratification factor in future research initiatives focusing on advanced disease and should be routinely considered during future staging and follow-up of NSCLC.

Key Words

nationwide autopsy, non-small-cell lung cancer, metastasis, gender specific risks

INTRODUCTION

Lung cancer is the most common cancer worldwide, with about 1.8 million new cases and 1.6 million deaths in 2012 (1). In women, it is the leading cause of cancer-related death in developed countries (2). It is estimated that with the rise of lung cancer in women, the incidence rates of lung cancer might be identical in both sexes in the next decade. Approximately 83% of lung cancers are non–small cell lung cancer (NSCLC) of which adenocarcinoma (AC) and squamous cell carcinoma (SCC) are the two most common types, accounting for 43% and 23% of all lung cancers (3). Lung cancer most commonly metastasises to the lymph nodes, brain, adrenal glands, bones and liver (4-6). A majority of NSCLC patients presented with (locally) advanced disease. The addition of ^{18}F-fluoro-deoxy-glucose positron emission tomography / computed tomography (FDG-PET/CT) in the workup of patients with lung cancer has improved staging, re-staging and detection of recurrent disease (7-10).

Knowledge of clinical characteristics of metastatic disease is important to inform clinical decision-making. Previous single-centre studies showed data on metastatic patterns in different histological subtypes of NSCLC (11-15), suggesting that the metastatic pattern is influenced by histological subtype (11-15). AC developed more distant metastases compared to other NSCLC subtypes (15). Gender-specific differences in lung cancer development have been reported, including more women with AC and more lung cancer in female non-smokers, which can possibly be attributed to genetic and biologic factors. Especially due to the rise of lung cancer in women, predictive factors for metastatic patterns in lung cancer need to be updated, since historical data are based on a predominantly male population.

Post-mortem studies offer a possibility to register both the extent and the location of metastatic disease in different subtypes of NSCLC. Here, we analysed data from the nationwide network and registry of histopathology and cytopathology Dutch Pathology Registry (PALGA) (16), which is used for all pathology data collection in the Netherlands. This provides a unique opportunity for complete nationwide assessment metastatic NSCLC. The pathology data were compared with the distribution of metastasis at the time of diagnosis based on a single-centre retrospective cohort of patients receiving FDG-PET/CT for initial staging of lung cancer.

MATERIALS AND METHODS

A nationwide retrospective review was performed of pathological and autopsy records of 3489 patients diagnosed with lung cancer between January 2001 and December 2010. In the Netherlands, a post-mortem examination is performed at the request of the family or treating physician. All autopsies included in this study were performed in order to obtain information on the medical status of the deceased or to determine the exact cause of death. Only whole-body autopsies were included in this study, and no forensic autopsies were included. Small-cell lung cancer was excluded. Tumour histology had been assessed by different pathologists in all cases. Local staging according to the TNM classification (7th edition of the American Joint Committee on Cancer) was reconstructed from the reports of the pathology records. No clinical information on patient characteristics and treatment was available. To validate the clinical relevance of the autopsy results, the pathology data were compared with a single centre retrospective cohort of patients receiving FDG-PET/CT for initial staging of lung cancer.

FDG-PET/CT Cohort

A retrospective review was performed on all consecutive patients with a non-small cell lung carcinoma who underwent a (standard work-up) FDG-PET/CT scan for initial staging at the Radboud University Medical Centre between November 2011 and May 2013. The reports of the FDG-PET/CT scans and the pathological analyses were evaluated. The reports of the FDG-PET/CT scans were generated by different nuclear medicine physicians in all cases. Exclusion criteria were: patients with NSCLC other than AC or SCC, patients with inconclusive pathological data and patients with a synchronous double tumour (with different histology). Histological subtype was determined by the pathologist according to the IASCL revised 2011 criteria (17) in this cohort. Staging using the PET/CT scan was determined according to TNM staging 7th edition (18). This study was approved by the regional medical ethical review board.

Statistical analysis

Differences between categorical variables were calculated using the chi-squared test for normally distributed variables or the Fisher exact test for not normally distributed variables. All statistical analyses were performed using SPSS 23.0 (SPSS, Inc., Chicago, IL, USA). Two-sided P-values of < 0.05 were considered significant.

RESULTS

A total of 3489 autopsies was available of lung cancer patients in the PALGA database: 691 patients presented with small cell lung cancer and were excluded from the analysis. Patients with large cell carcinoma (LCC) (676 patients, 24.2%), carcinoid (97 patients, 3.5%), giant-cell carcinoma (4 patients, 0.1%) and other NSCLC histology (9 patients, 0.2%) were excluded from the analysis. In AC distant metastases were found in 561 out of 1128 (49.7%) versus 220 out of 875 (24.8%) in SCC ($P < 0.001$). In *Figure 1*. the selection of NSCLC with AC and SCC is shown. For AC and SCC clinicopathological data are summarised in *Table 1*. Metastases were found in 781 out of 2003 autopsies in AC and SCC patients (39.0%). The median age of all patients at autopsy with metastases was 68 years (range 33 – 92), the median age at initial diagnosis was 68 years. Brain autopsy was performed in 230 patients (of 781), of which 140 with AC and 90 with SCC.

FIGURE 1. Diagram with selection of stage IV non-small cell lung cancer (NSCLC) patients between 2001 and 2010 from the Nationwide Histopathology and cytopathology data network in the Netherlands. Small cell lung cancer (SCLC), adenocarcinoma (AC), squamous cell carcinoma (SCC).

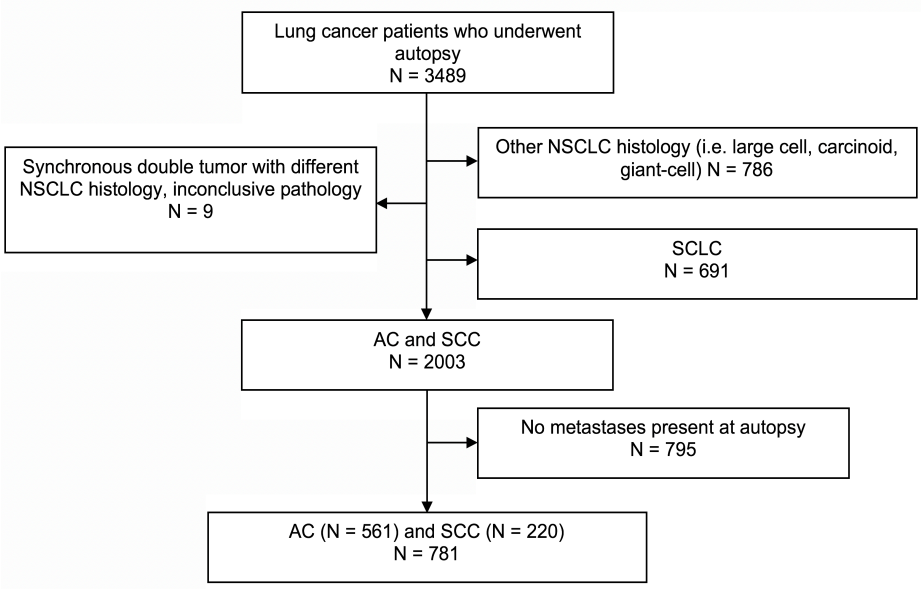

TABLE 1. Clinicopathological features of AC versus SCC

Features	AC (*n* = 1128)	%	SCC (*n* = 875)	%	P
Sex					< 0.001
Men	709	62.9	710	81.1	
Women	419	37.1	165	18.9	
Age at autopsy					
Median (range)	70 (33-96)		72 (39-95)		NS
< 45	29	2.6	9	1.0	
45 - 59	222	19.7	87	9.9	
60 - 74	473	41.9	430	49.1	
≥ 75	404	35.8	349	39.9	
Stage at autopsy (TNM7)					
M0	567	50.3	655	74.9	< 0.001
M1	561	49.7	220	25.1	
no. of metastatic sites					
1	128	11.3	73	8.3	< 0.001
2	140	12.4	60	6.9	
3	112	9.9	39	4.5	
4	80	7.1	16	1.8	
≥ 5	94	8.3	27	3.1	
unknown	7	0.6	5	0.6	

AC: adenocarcinoma, SCC: squamous cell carcinoma

Metastatic patterns between AC and SCC

Single site metastasis was present in 132 out of 561 AC patients (23.5%) and in 73 out of 220 SCC (33.2%). AC more frequently showed metastases at multiple sites (≥ 2) 77.2% (433/561) versus 66.8% (147/220) in SCC, P = 0.004 (*Figure 2*). Different sites of metastasis are summarised in *Table 2*. In AC, 225 out of 561 (40.1%) patients developed pulmonary metastases (one or more pulmonary metastases at a contralateral lobe of the primary tumour), while in SCC 80 out of 220 (36.4%) developed pulmonary metastases. Adrenal gland metastases were found in 240 out of 561 (42.8%) of AC patients, versus 54 out of 220 (24.5%) in SCC patients (P < 0.001). Bone metastases were more frequently detected in AC than in SCC (181 out of 561 (32.3%) versus 43 out of 875 (19.5%) (P = 0.001). Pleural metastases were found in 59 out of 561 (10.5%) in AC, compared with 19 out of 220 (8.9%) in SCC. Kidney metastases were more frequently detected in SCC than

in AC (51 out of 220 (23.2%) versus 72 out of 561 (12.8%), P < 0.001). Brain autopsy was performed in 90 patients with SCC and 140 patients with AC. In AC brain metastases were found in 66 out of 140 brain autopsies (47.1%) compared with 24 out of 90 brain autopsies in SCC (26.7%), P = 0.001.

Uncommon sites of metastases (<5%) in both AC and SCC were small and large intestine and pancreas; there was no significant difference between AC or SCC for these uncommon sites. Rare sites of metastases (<1%) were the stomach, uterus, urinary bladder, gallbladder, ovary, prostate, breast and oesophagus. Gallbladder, ovary and uterus

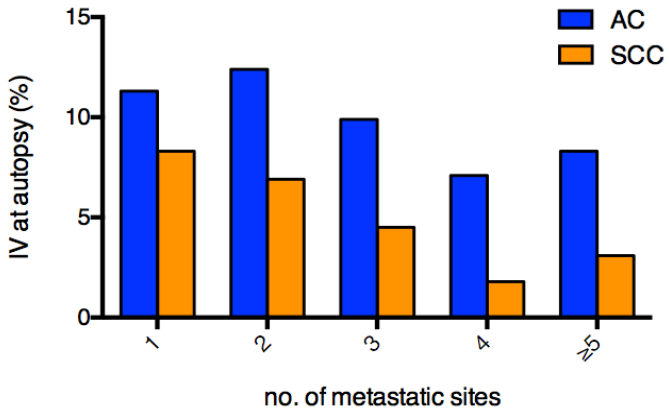

FIGURE 2. Number of metastases in stage IV adenocarcinoma (AC) versus squamous cell carcinoma (SCC)

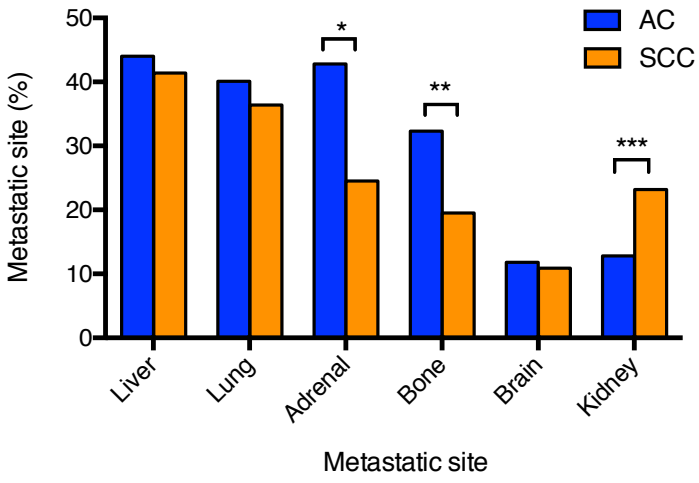

FIGURE 3. Distribution of metastasis in adenocarcinoma (AC) and squamous cell carcinoma (SCC). * P < 0.001, ** P < 0.001, *** P < 0.001

metastases were only found in AC. Rare metastasis in the breast or prostate metastasis were found only in SCC. Differences in metastatic patterns between AC and SCC are shown in *Figure 3*. No significant difference in metastatic site or number of metastases was found between male and female patients with SCC. In contrast, female patients with AC showed significantly more lung metastases (47.0% vs 35.4%, P = 0.006) (*Figure 4*). Liver metastases were also observed more frequently in female AC patients; 49.1% vs; 40.5%, P = 0.044. The combinations of metastasis in AC and SCC are shown in *Table 3*.

Clinical relevance: validation with initial staging FDG-PET/CT

Between November 2011 and May 2013, a total of 143 patients underwent an FDG-PET/CT for initial staging of newly diagnosed NSCLC: 70 patients with AC (49%) and 73 patients with SCC (51%). The PET cohort consisted of 36 (25%) patients with stage I, 17 (12%) stage II, 48 (34%) stage III and 42 (29%) stage IV. Of these 42 patients with metastatic disease, 14 patients had SCC and 28 had AC. In stage IV patients the most common metastatic sites were bones, adrenal gland and liver (*Figure 5*). In the stage IV group, bone metastases were found in 57% of AC patients (16/28) versus (43%) of SCC (6/14) patients (P = 0.02). There was no difference in the incidence of liver metastases. Brain metastases were found in 4 out of 28 patients with AC (14%) versus 0 out of 14 in SCC (P = 0.04). Adrenal gland metastases were found in 16 out of 28 patients with AC (57%) versus 5 out of 14 patients with SCC (36%) (P < 0.01).

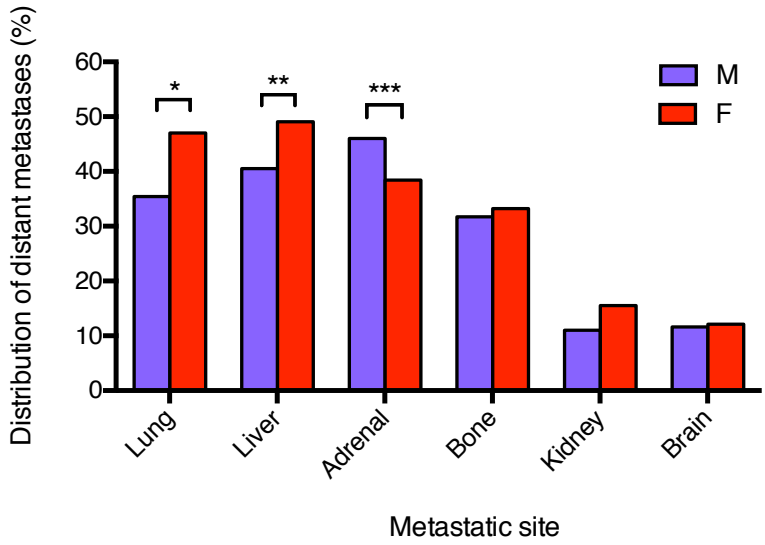

FIGURE 4. Distribution of metastases in adenocarcinoma (AC) in male (M) and female (F). * P = 0.006, ** P = 0.044, *** P = 0.07 (NS)

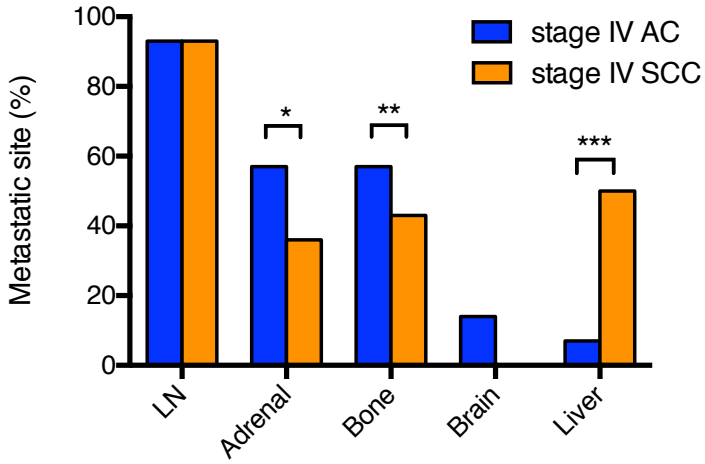

FIGURE 5. Metastases found for each histological subtype in stage IV disease on initial staging; adenocarcinoma (AC) and squamous cell carcinoma (SCC). LN, lymph node. * P = 0.01, ** P = 0.02, *** P = 0.10 (NS)

TABLE 2. Metastatic sites of AC versus SCC

Site of distant metastases	AC (n = 561)	%	SCC (n = 220)	%	P
Liver	247	44.0	91	41.4	NS
Lung	225	40.1	80	36.4	NS
Adrenal	240	42.8	54	24.5	< 0.001
Bone	181	32.3	43	19.5	0.001
Brain*	66	11.8	24	10.9	NS
Kidney	72	12.8	51	23.2	< 0.001
Peritoneum	36	6.4	14	6.4	NS
Pericardium	60	10.7	15	6.8	NS
Pleura	59	10.5	19	8.6	NS
Pancreas	28	5.0	9	4.1	NS
Spleen	32	5.7	10	4.5	NS
Thyroid	30	5.3	8	3.6	NS
Myocardium	19	3.4	13	5.9	NS
Intestine, small	18	3.2	8	3.6	NS
Intestine, large	14	2.5	2	0.9	NS
Stomach	5	0.9	2	0.9	NS
Skin	13	2.3	10	4.5	NS
Uterus	2	0.4	0	0.0	NS
Urinary bladder	1	0.2	1	0.5	NS
Gallbladder	4	0.7	0	0.0	NS
Ovary	5	0.9	0	0.0	NS
Prostate	0	0.0	1	0.5	NS
Oesophagus	1	0.2	0	0.0	NS
Breast	0	0.0	1	0.5	NS

AC: adenocarcinoma, SCC: squamous cell carcinoma

* Brain autopsy was performed in 90 patients with SCC and 140 patients with AC. In AC brain metastases were found in 66 out of 140 (47.1%) brain autopsies compared with 24 out of 90 brain autopsies in SCC (26.7%).

TABLE 3. Combination of metastases in patients with more metastatic sites

Location of metastases in AC

Site of metastases	no. patients	Liver	Adrenal	Lung	Bone	Other
Liver	247		130 (52.6%)	109 (44.1%)	108 (43.7%)	165 (66.8%)
Adrenal	240	130 (54.2%)		83 (34.6%)	99 (41.3%)	183 (76.3%)
Lung	225	109 (48.4%)	83 (36.9%)		89 (39.6%)	142 (63.1%)
Bone	181	108 (59.7%)	99 (54.7%)	89 (49.2%)		135 (74.6%)
Other	392	165 (42.1%)	183 (46.7%)	142 (36.2%)	135 (34.4%)	

Location of metastasis in SCC

Site of metastases	no. patients	Liver	Adrenal	Lung	Bone	Other
Liver	91		47 (51.6%)	35 (38.5%)	47 (51.6%)	33 (36.3%)
Adrenal	54	17 (31.5%)		11 (20.4%)	21 (38.9%)	15 (27.8%)
Lung	80	27 (33.8%)	24 (30.0%)		28 (35.0%)	26 (32.5%)
Bone	43	10 (23.3%)	14 (32.6%)	8 (18.6%)		9 (20.9%)
Other	145	84 (57.9%)	110 (75.9%)	85 (58.6%)	98 (67.6%)	

Percentage given for site-specific metastases indicates how many have also involving other sites.

DISCUSSION

In this nationwide autopsy study, we showed that histological subtypes in NSCLC are important predictors of patterns of metastatic spread. Interestingly, gender-specific differences were revealed, showing women to have adenocarcinoma more frequently with a different distribution of metastatic disease than men.

We showed that differences in metastatic patterns metastases exist between AC and SCC. Compared to SCC, AC metastasised to different sites, in various combinations and was more likely to have a higher number of metastases. Knowledge of these differences has implications for initial staging decisions, selection of appropriate treatment and follow-up. Also, this may have implications for treatment of oligo-metastatic NSCLC. Currently, the influence of histology in metastatic potential in NSCLC is often disregarded when discussing management options in NSCLC. Moreover, historical information and studies are based on a predominantly male population. The incidence in female patients, however, is rapidly rising whereas it is slowly declining in males (2). It is estimated that with the continuing rise of lung cancer in women, the incidence of lung cancer might be identical in both sexes in the next decade. While clinical staging and performance score are significant determinants in the decision making of patients with NSCLC, we demonstrated that histology-specific risks of metastatic potential exist and, surprisingly, the metastatic spread is also gender specific.

Previous studies have shown that most common metastatic sites for NSLSC are liver, bone, brain, pericardium, adrenal glands and pleura (14). However, the size of these studies is often small (with a maximum of several hundred patients), compared with our nationwide study including 2798 NSCLC patients. We demonstrated that differences in the metastatic potential of AC and SCC exist. AC showed significantly more distant metastases compared to SCC. AC presents with a higher incidence of metastases in the adrenal glands and bones, while more kidney metastases were found in SCC. We showed that in SCC kidney metastases occur in up to 23.2% of patients with metastatic disease. While metastases to the kidneys are seldom encountered clinically, renal metastases are found more frequently at autopsy (19). Detection of renal metastases with FDG-PET/CT is limited due to the excretion of FDG in the urinary tract. The autopsy data, however, revealed 123 patients with renal metastases, of which 7 had isolated renal metastasis. In those particular situations, it could have changed treatment decision making, currently unknown due to the inability to detect small renal metastases by CT and/or PET. Metastases often develop late in the course of the disease and small metastases can be detected that might not be clinically relevant.

Currently, FDG-PET/CT is established as the standard of care to characterise mediastinal lymph nodes and detect unexpected extrathoracic metastases. FDG-PET/CT can identify previously unsuspected distant metastases in approximately 10–20% of patients, with high accuracy (20-22). Furthermore, characteristics between lesions allow for a distinction between metastasis and second primary tumours (23). To establish the clinical value of differences in metastatic patterns in autopsy studies, we verified these with initial staging cohort of 143 patients and found a similar difference in metastatic pattern between AC and SCC, with increased bone and adrenal gland metastases for AC.

Gender differences in lung cancer pathogenesis are becoming increasingly important. In male patients, SCC is the main NSCLC, while in females AC is more common. Smoking history may partly explain this difference (24, 25) and several other hypotheses exist for these gender differences: a decreased DNA repair capacity in women, a higher susceptibility of tobacco carcinogens in women and an increased frequency of mutations in tumour suppressor genes (26-30). From a clinical perspective, female patients with NSCLC have favourable survival rates, but different treatment-related toxicity profiles (31, 32). Despite these differences, earlier in the literature, no significant influence of gender on metastatic potential or metastatic locations was found (5, 13, 14), possibly due to smaller cohorts. Absolute differences in the prevalence and locations of the tumours and the significance of variables in other studies might be due to a selected study population with differences in treatment. In our large nationwide autopsy study, we found no significant gender differences in the metastatic pattern in SCC. However, women with metastatic AC had significantly more metastases to both lung and liver, compared to men. It can be hypothesised that a different biological behaviour or a different homing of tumour cells exist in female patients. Hormonal influences may play a role in cancer progression and formation of metastases as well. Oestrogen receptors are frequently present in lung cancer (ERβ expression of 52 – 69% of cases) and have been linked to the pathogenesis of lung cancer (29, 33, 34) and a role of differences in tumour immunology and a difference in oestrogen receptor signalling has been suggested in tumour genesis (35). Also, molecular signatures, like epidermal growth factor receptor (EGFR) mutations in adenocarcinomas, have been found to be present more often in women, but also in Asians and never smokers (36). The microenvironment of the target organ is thought to be an important factor in metastasis. It was hypothesised that tumour-stromal interactions could influence differences in metastatic patterns (37). When tumour cells enter the circulation, they do not spread to every organ randomly, but they tend to seed in selected organs as hypothesised by the "seed and soil" theory. Some histological subtypes may have a better ability to thrive in specific target organs. For example metastases from small cell lung cancer have a predilection for the brain (38). The NSCLC subtypes AC and SCC are distinct

clinical entities that have different embryologic origins and arise in different anatomic locations. However, the difference in the genotype of the tumour cells is not the only explanation for a potential difference in metastatic patterns. As mentioned previously, target organ tumour microenvironment plays a vital role in metastases.

This autopsy study focusing on the metastatic disease from NSCLC showed differences in metastatic patterns between AC and SCC in a large nationwide population. Autopsy studies offer a unique opportunity to study the distribution of metastases and arguably can be seen as the gold standard in the study of cancer metastases. Clinically based studies have the advantage that metastasis at various sites can be analysed as time-dependent variables, allowing for a better evaluation of metastasis as a prognostic factor.

One limitation of an autopsy study is that it unequivocally leads to a biased population, complicated by lead time and length time biases. Secondly, correlation with clinical factors, like treatment regimens, performance score, smoking habits, molecular profiling and clinical outcome were not available, due to the anonymisation of the pathology database. Therefore, a possible effect of specific organ metastasis on overall survival could not be confirmed. Interestingly, previous studies found that bone metastases and liver metastases were associated with shortened survival (39-41). Although we included only whole-body autopsies, metastases outside of routinely examined regions (especially for brain and bone) may have been missed. Brain autopsy was only allowed in a limited number of NSCLC patients (319 out of 2798). The limitation in the number of brain autopsies inevitably leads to an underestimation of brain metastases. Earlier an epidemiological study in a cohort of patients with brain metastasis showed that the incidence of patients with NSCLC was 12.6% out of 742 patients (42). We found a small difference between proven brain metastases in AC and SCC (5.9% vs 2.7%, respectively) (P = 0.07) suggesting that the prevalence of brain metastases might be different between AC and SCC. A possible explanation is that brain metastasis are increasingly seen in adenocarcinomas with EGFR mutations and EML4-ALK1 rearrangements (43). A non-invasive method for staging with FDG PET/CT is becoming widely available and is currently a standard procedure for the staging of lung cancer. While the sensitivity of FDG-PET/CT for brain metastases is 72% (44) current NSCLC guidelines advise screening all stage III patients for brain metastases, preferably by magnetic resonance imaging (MRI), or otherwise a contrast-enhanced CT.

CONCLUSION

In this nationwide autopsy study, we showed that different metastatic patterns exist in NSCLC, that are determined by tumour type and gender. AC showed significantly more metastases in adrenal glands and bone, while SCC showed more kidney metastases. In women with AC liver and lung metastases are more frequently present, compared to men. Biological differences in lung cancer between men and women are increasingly being recognised. Knowledge of these factors is particularly important because of the continuing rise in the incidence of lung cancer in women. Further research on genetic, metabolic, immunogenic and hormonal factors and gender-based clinical trials are warranted since historical data are based on a predominantly male population. Both histopathological and gender-specific risks should be considered for stratification in future research initiatives focusing on advanced disease.

ACKNOWLEDGEMENT

Collaborators in the PALGA-group. Dr. S.H. Sastrowijoto (Orbis Medisch Centrum Sittard), Dr. C. Jansen (Laboratorium Pathologie Oost-Nederland).

FUNDING

This research received no specific grant from any funding agency in the public, commercial, or non-profit sectors.

DISCLOSURE

The authors have declared no conflicts of interest.

References

1. Ferlay J, Soerjomataram I, Ervik M, Dikshit R, Eser S, Mathers C, Rebelo M, Parkin DM, Forman D, Bray, F. GLOBOCAN 2012 v1.0, Cancer Incidence and Mortality Worldwide: IARC CancerBase No. 11 [Internet]. Lyon, France: International Agency for Research on Cancer; 2013. Available from: http://globocan.iarc.fr, accessed on 1-10-2015.
2. Torre LA, Bray F, Siegel RL et al. Global cancer statistics, 2012. CA Cancer J Clin 2015; 65: 87-108.
3. Howlader N, Noone AM, Krapcho M, Garshell J, Miller D, Altekruse SF, Kosary CL, Yu M, Ruhl J, Tatalovich Z,Mariotto A, Lewis DR, Chen HS, Feuer EJ, Cronin KA (eds). SEER Cancer Statistics Review, 1975-2012, National Cancer Institute. Bethesda, MD, http://seer.cancer.gov/csr/1975_2012/, based on November 2014 SEER data submission, posted to the SEER web site, April 2015, accessed on 1-10-2015.
4. Disibio G, French SW. Metastatic patterns of cancers: results from a large autopsy study. Arch Pathol Lab Med 2008; 132: 931-939.
5. Stenbygaard LE, Sorensen JB, Olsen JE. Metastatic pattern in adenocarcinoma of the lung. An autopsy study from a cohort of 137 consecutive patients with complete resection. J Thorac Cardiovasc Surg 1995; 110: 1130-1135.
6. Hess KR, Varadhachary GR, Taylor SH et al. Metastatic patterns in adenocarcinoma. Cancer 2006; 106: 1624-1633.
7. Berlangieri SU, Scott AM, Knight SR et al. F-18 fluorodeoxyglucose positron emission tomography in the non-invasive staging of non-small cell lung cancer. Eur J Cardiothorac Surg 1999; 16 Suppl 1: S25-30.
8. Kalff V, Hicks RJ, MacManus MP et al. Clinical impact of (18)F fluorodeoxyglucose positron emission tomography in patients with non-small-cell lung cancer: a prospective study. J Clin Oncol 2001; 19: 111-118.
9. Schrevens L, Lorent N, Dooms C, Vansteenkiste J. The role of PET scan in diagnosis, staging, and management of non-small cell lung cancer. Oncologist 2004; 9: 633-643.
10. Lee ST, Berlangieri SU, Poon AM et al. Prevalence of occult metastatic disease in patients undergoing 18F-FDG PET for primary diagnosis or staging of lung carcinoma and solitary pulmonary nodules. Intern Med J 2007; 37: 753-759.
11. Quint LE, Tummala S, Brisson LJ et al. Distribution of distant metastases from newly diagnosed non-small cell lung cancer. Ann Thorac Surg 1996; 62: 246-250.
12. Yesner R, Carter D. Pathology of carcinoma of the lung. Changing patterns. Clin Chest Med 1982; 3: 257-289.

13. Stenbygaard LE, Sorensen JB, Olsen JE. Metastatic pattern at autopsy in non-resectable adenocarcinoma of the lung--a study from a cohort of 259 consecutive patients treated with chemotherapy. Acta Oncol 1997; 36: 301-306.
14. Stenbygaard LE, Sorensen JB, Larsen H, Dombernowsky P. Metastatic pattern in non-resectable non-small cell lung cancer. Acta Oncol 1999; 38: 993-998.
15. Martini N, Burt ME, Bains MS et al. Survival after resection of stage II non-small cell lung cancer. Ann Thorac Surg 1992; 54: 460-465; discussion 466.
16. Casparie M, Tiebosch AT, Burger G et al. Pathology databanking and biobanking in The Netherlands, a central role for PALGA, the nationwide histopathology and cytopathology data network and archive. Cell Oncol 2007; 29: 19-24.
17. Travis WD, Brambilla E, Noguchi M et al. International association for the study of lung cancer/american thoracic society/european respiratory society international multidisciplinary classification of lung adenocarcinoma. J Thorac Oncol 2011; 6: 244-285.
18. Edge SB, Compton CC. The American Joint Committee on Cancer: the 7th edition of the AJCC cancer staging manual and the future of TNM. Ann Surg Oncol 2010; 17: 1471-1474.
19. Zhou C, Urbauer DL, Fellman BM et al. Metastases to the kidney: a comprehensive analysis of 151 patients from a tertiary referral centre. BJU Int 2016; 117: 775-782.
20. MacManus MP, Hicks RJ, Matthews JP et al. High rate of detection of unsuspected distant metastases by pet in apparent stage III non-small-cell lung cancer: implications for radical radiation therapy. Int J Radiat Oncol Biol Phys 2001; 50: 287-293.
21. Marom EM, McAdams HP, Erasmus JJ et al. Staging non-small cell lung cancer with whole-body PET. Radiology 1999; 212: 803-809.
22. Pieterman RM, van Putten JW, Meuzelaar JJ et al. Preoperative staging of non-small-cell lung cancer with positron-emission tomography. N Engl J Med 2000; 343: 254-261.
23. Dijkman BG, Schuurbiers OC, Vriens D et al. The role of (18)F-FDG PET in the differentiation between lung metastases and synchronous second primary lung tumours. Eur J Nucl Med Mol Imaging 2010; 37: 2037-2047.
24. de Perrot M, Licker M, Bouchardy C et al. Sex differences in presentation, management, and prognosis of patients with non-small cell lung carcinoma. J Thorac Cardiovasc Surg 2000; 119: 21-26.
25. Egleston BL, Meireles SI, Flieder DB, Clapper ML. Population-based trends in lung cancer incidence in women. Semin Oncol 2009; 36: 506-515.
26. Patel JD. Lung cancer in women. J Clin Oncol 2005; 23: 3212-3218.

27. International Early Lung Cancer Action Program I, Henschke CI, Yip R, Miettinen OS. Women's susceptibility to tobacco carcinogens and survival after diagnosis of lung cancer. JAMA 2006; 296: 180-184.
28. Bain C, Feskanich D, Speizer FE et al. Lung cancer rates in men and women with comparable histories of smoking. J Natl Cancer Inst 2004; 96: 826-834.
29. Stabile LP, Davis AL, Gubish CT et al. Human non-small cell lung tumors and cells derived from normal lung express both estrogen receptor alpha and beta and show biological responses to estrogen. Cancer Res 2002; 62: 2141-2150.
30. Wei Q, Cheng L, Amos CI et al. Repair of tobacco carcinogen-induced DNA adducts and lung cancer risk: a molecular epidemiologic study. J Natl Cancer Inst 2000; 92: 1764-1772.
31. Nakamura H, Ando K, Shinmyo T et al. Female gender is an independent prognostic factor in non-small-cell lung cancer: a meta-analysis. Ann Thorac Cardiovasc Surg 2011; 17: 469-480.
32. Wijsman R, Dankers F, Troost EG et al. Multivariable normal-tissue complication modeling of acute esophageal toxicity in advanced stage non-small cell lung cancer patients treated with intensity-modulated (chemo-)radiotherapy. Radiother Oncol 2015; 117: 49-54.
33. Skov BG, Fischer BM, Pappot H. Oestrogen receptor beta over expression in males with non-small cell lung cancer is associated with better survival. Lung Cancer 2008; 59: 88-94.
34. Kawai H, Ishii A, Washiya K et al. Combined overexpression of EGFR and estrogen receptor alpha correlates with a poor outcome in lung cancer. Anticancer Res 2005; 25: 4693-4698.
35. Patel JD, Bach PB, Kris MG. Lung cancer in US women: a contemporary epidemic. JAMA 2004; 291: 1763-1768.
36. Midha A, Dearden S, McCormack R. EGFR mutation incidence in non-small-cell lung cancer of adenocarcinoma histology: a systematic review and global map by ethnicity (mutMapII). Am J Cancer Res 2015; 5: 2892-2911.
37. Sautes-Fridman C, Cherfils-Vicini J, Damotte D et al. Tumor microenvironment is multifaceted. Cancer Metastasis Rev 2011; 30: 13-25.
38. Lassen U, Kristjansen PE, Hansen HH. Brain metastases in small-cell lung cancer. Ann Oncol 1995; 6: 941-944.
39. Sorensen JB, Hansen HH, Hansen M, Dombernowsky P. Brain metastases in adenocarcinoma of the lung: frequency, risk groups, and prognosis. J Clin Oncol 1988; 6: 1474-1480.
40. Hoang T, Xu R, Schiller JH et al. Clinical model to predict survival in chemonaive patients with advanced non-small-cell lung cancer treated with third-generation

chemotherapy regimens based on eastern cooperative oncology group data. J Clin Oncol 2005; 23: 175-183.

41. Bauml J, Mick R, Zhang Y et al. Determinants of survival in advanced non--small-cell lung cancer in the era of targeted therapies. Clin Lung Cancer 2013; 14: 581-591.
42. Schouten LJ, Rutten J, Huveneers HA, Twijnstra A. Incidence of brain metastases in a cohort of patients with carcinoma of the breast, colon, kidney, and lung and melanoma. Cancer 2002; 94: 2698-2705.
43. Hendriks LE, Smit EF, Vosse BA et al. EGFR mutated non-small cell lung cancer patients: more prone to development of bone and brain metastases? Lung Cancer 2014; 84: 86-91.
44. Hjorthaug K, Hojbjerg JA, Knap MM et al. Accuracy of 18F-FDG PET-CT in triaging lung cancer patients with suspected brain metastases for MRI. Nucl Med Commun 2015; 36: 1084-1090.

CHAPTER IX

GENERAL DISCUSSION AND FUTURE PROSPECTS

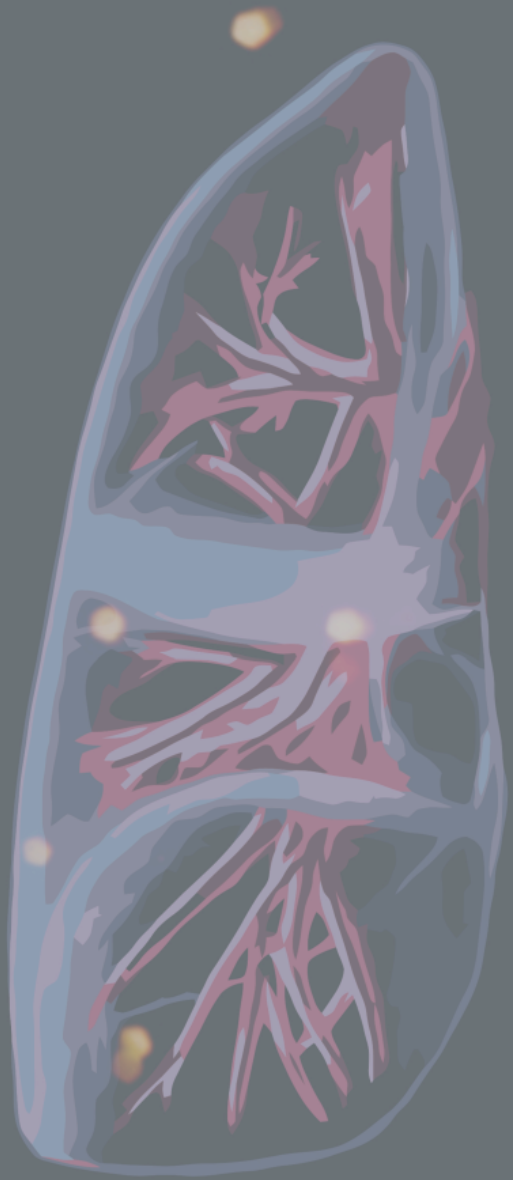

Despite significant changes in diagnosis and treatment of patients with non-small cell lung cancer (NSCLC) over the last decade, NSCLC remains a leading cause of cancer-related mortality worldwide. In an effort to improve survival of NSCLC there has been an emphasis on early diagnosis, selection of optimal treatment and improved radiotherapy planning and more recently, adjuvant treatment with immune checkpoint inhibitors. Advances in conformal radiotherapy techniques allowed high dose irradiation with near-surgical precision. Targeted treatments have considerably expanded treatment options for NSCLC patients. These recent developments emphasise the need to change from 'a one size fits all' treatment paradigm for NSCLC towards a personalised approach of treatment.

Treatment response monitoring in NSCLC

Molecular imaging using FDG-PET/CT provides an opportunity to investigate in a non-invasive way the biology of cancer in vivo and to measure the impact of treatment. The rationale of metabolic imaging is that acquired mutations in oncogenes and tumour suppressor genes and loss of cell viability affects glucose metabolism (1, 2). FDG-PET/CT can provide patient-specific quantitative information of tumour metabolism before, during and after treatment. Molecular imaging can characterise some biological features of malignant tissue and reduction of FDG uptake that often precedes structural changes that are typically correlated with tumour response (3). Individualised treatment strategies become more relevant as our knowledge about tumour-specific drivers and specific tumour targets increases and the choice in anti-tumour agents has expanded considerably. Consequently, there is a rising need to identify pre-treatment factors that can potentially predict outcome. FDG-PET/CT is a non-invasive approach and might overcome issues of intra-tumoural and inter-tumoural heterogeneity, since biomarkers derived from biopsy material of tumour samples may significantly confound the analysis.

Chapter III described a prospective study of the role of early in-treatment response assessment with FDG-PET/CT performed in patients with locally advanced NSCLC. An early in-treatment evaluation was performed after two weeks, after the first treatment cycle of chemoradiation and 10 Gy of radiotherapy. In this study we showed that a decrease in FDG-uptake, calculated as the percentage decrease in total lesion glycolysis (ΔTLG) is a superior predictor of progression-free survival (PFS), compared to RECIST. Unexpectedly, already at an early time point, there were significant morphologic changes resulting in changes in tumour volume on in-treatment low dose CT after two weeks of treatment. However, this was not predictive of long-term PFS. For the definition of metabolic response, only a limited number of semi-quantitative parameters were retrieved using semi-automatic fixed threshold methods. For response calculation, a semi-

quantitative parameter calculated as a percentage change to baseline was used. We showed that ΔTLG performed better in early response prediction than a decrease in standardised uptake value (SUV) or maximum SUV (SUV_{max}); both ΔSUV and ΔSUV_{max} were not a significant predictive factor. Interestingly, in our study, the end-of-treatment FDG-PET/CT (2-5 months after completion of chemoradiotherapy) was not predictive of response. This suggests that persistent FDG-uptake is not always indicative of treatment resistance or associated with a poor clinical outcome. Radiation-induced inflammation could play an important role and mask true biological responders from non-responders. FDG-uptake is not limited to accumulate in tumour tissue, but also accumulates in macrophages, neutrophils and fibroblast. Multiple biological processes, such as proliferation, cell repair and inflammation, may conceal vital tumour residue and non-vital tumour tissue.

In this prospective study, patients with a (pathological) response after chemoradiotherapy with IIIA/N2 disease with a resectable tumour were potential candidates for curative resection. Eight patients received a lobectomy; however, the potential role of surgery in patients who could be downstaged after chemoradiotherapy remains controversial. In a phase III trial induction chemoradiotherapy plus surgery were compared with definitive CRT in patients with stage IIIA/N2 showing no difference in overall survival (OS) between the two groups (4). However, in a subgroup analysis, patients that received a lobectomy had an improved OS compared to patients with only chemoradiotherapy. A considerably high mortality rate was observed in patients undergoing a pneumectomy.

In **Chapter VII** the predictive value of early in-treatment FDG-PET/CT response to chemotherapy in combination with bevacizumab in advanced non-squamous non-small cell lung cancer is demonstrated. The early in-treatment evaluation was performed with FDG-PET/CT after two weeks. In this study, metabolic changes preceded morphologic changes. Many patients with stable disease (SD) according to RECIST could be reclassified as a partial metabolic response (PMR) based on FDG-PET/CT. We showed that only FDG-PET/CT was predictive of overall survival (OS). In this study predefined response criteria were used, the PET response criteria in solid tumours (PERCIST), for evaluation of in-treatment response. To facilitate the clinical implementation of early response studies, the use of predefined criteria is crucial. To establish a role of FDG-PET/CT for bevacizumab and chemotherapy, more studies are needed. The number of response monitoring studies in NSCLC treated with bevacizumab and first-line chemotherapy is still very limited. It could be argued whether a metabolic non-responder in our study had suffered from resistance to anti-VEGF treatment or whether it was caused by a resistance to chemotherapy. However, from a clinical perspective, the addition of bevacizumab to

chemotherapy is of limited value, as it only improved PFS but not OS in the phase II trial AVAiL (5). For therapy response monitoring of bevacizumab specifically, antibody-based positron emission tomography imaging with Zr-89 (^{89}Zr-bevacizumab) could be used to visualise targeting of VEGFR. A limitation of this antibody PET imaging is that targeting does not necessarily imply treatment efficacy. Other VEGF-axis dependent resistance mechanisms (PIGF, VEGB, VEGFC and VEGFD) may contribute to the signalling of VEFGR and ultimately lead to tumour angiogenesis (6).

One limitation of the prospective studies in **Chapter III** and **Chapter VII** is that the number of included patients is limited. This precludes subgroup or multivariate analysis. However, these studies do add to the growing support of evidence in favour of early response monitoring using FDG-PET/CT in NSCLC.

Methodological aspects of response monitoring with FDG-PET/CT

FDG-PET/CT is a suitable non-invasive tool for response evaluation and prediction of response and patient outcome. An increasing number of studies regarding early in-treatment response monitoring in NSCLC using FDG-PET/CT has become available. Papers from 2003 to 2017 with studies involving response monitoring using FDG-PET(/CT) in patients treated with chemotherapy or chemoradiotherapy are summarised in *Table 1*. These studies show that FDG-PET/CT is an effective method for early response prediction in NSCLC patients treated with chemotherapy and chemoradiotherapy. In general, a substantial reduction in FDG-uptake, evaluated with a quantitative or semi-quantitative method, defines a favourable therapeutic response. However, the definition of 'metabolic response' has generally been a matter of post hoc determination, with the use of receiver operating characteristics curves of the threshold of change in parameters that provides the best stratification of the patient population. One important consideration is that there is an intrinsic variability of the quantitative measure, as well as that magnitude of change (i.e., threshold) for defining response. Many differences in 'early metabolic response' can be expected due to a variation in the selected imaging variables and timing of FDG-PET/CT. Identification of predictive metabolic factors for early tumour response is important for exploring the potential role of early in-treatment FDG-PET/CT. However, this also leads to large variability in the definition of early metabolic response in these response monitoring studies. Apart from the differences in the definition of a metabolic response, differences in chemotherapy, radiotherapy schedules, the timing of in-treatment scans and disease stages, make pooling of data very difficult. This hampers a meta-analysis of early response prediction in NSCLC with FDG-PET/CT and can partly explain why early in-treatment response monitoring in current clinical practice is lacking. One technical aspect is to harmonise acquisition processing and analysis of FDG-PET/CT

in clinical trials, earlier been described by Boellaard *et al.* (7). Standardisation of response monitoring for further prospective response monitoring studies is warranted.

Interpretation of FDG-PET/CT

The application of response monitoring studies with FDG-PET/CT has been routine clinical practice for many types of tumours for many years. However, categorisation of response into responders or non-responders has not been that easy. Let alone, exact criteria for early in-treatment response evaluation lack in many solid tumours. An objective and reliable assessment of treatment response require a detailed description of how to perform qualitative or (semi-)quantitative PET response.

The FDG uptake can be assessed by qualitative methods (i.e., visual analysis), semi-quantitative and quantitative methods. When a qualitative assessment is used to decrease the potential of the subjectivity of visual analysis, normalisation to an appropriate reference tissue is needed. Most often the liver is used as a reference since under fastening conditions the hepatic glucose uptake is relatively stable in the non-diseased liver. The mean liver SUV is expected to be within 1.0 and 2.2. Another reference point is the mediastinal blood pool and is often used as a cut-off for normal and pathophysiological uptake. Blood pool SUV measurements are estimated to be around 1.6. For evaluation of malignant lymphoma's, for example, it has been used for the interim and end-of-treatment evaluation of response to therapy (Deauville criteria).

(Semi-)quantitative analysis is one of the assets of FDG-PET/CT to measure changes in tumour metabolism objectively. Uptake measurement using SUV is most widely used. For reproducible data strict adherence to acquisition parameters, patient preparation and image reconstruction is needed. Many factors do have a significant influence on quantitative parameters, like physiologic, technical and biological factors (8). Therefore, adherence to acquisition and analysis protocols, including the use of the same preparation regimen, uptake time and scanning parameters are needed for response monitoring. In an ideal case, the FDG-PET/CT should be performed on the same scanner, maintained with regular quality assurance using calibration phantoms. Variations in acquisition and analysis can introduce changes that do not reflect an underlying biological effect. In other words, differences in scanning acquisition and analysis protocol could induce changes that can falsely be interpreted as a significant decrease or an increase and might cause changes more substantial than shown in repeatability studies. Also, differences between centres, due to different PET/CT systems, differences in acquisition and imaging reconstruction can result in an increase in variability in SUV. Ideally, a comparison from institutions with a uniform approach to imaging procedures is needed. To minimise these differences in performance

between different centres, adherence to EARL accreditation is essential to increases the SUV reproducibility (9).

With regard to response monitoring, full quantitative data is used infrequently. A quantitative method using kinetic modelling or Patlak analysis includes the need for arterial blood sampling or dynamic imaging of the blood pool. These study protocols are very complex and time-consuming and result in much discomfort for the subjects and negatively affect patient throughput. One crucial limitation of dynamic imaging is that it does not include the whole body when using the currently commercially available PET/CT systems. Only one bed position, consisting of a field of view of approximately 15-20 cm, can be measured. This requires prospective determination of the region to be imaged and the target lesions need to fit within one bed position. Previous studies showed that intra-individual comparison of SUV before and during or after the treatment highly correlated with changes in Ki. This correlation has already also been confirmed by Weber *et al.* (10), showing that the changes in Ki and changes in SUV both showed high diagnostic accuracy for the prediction of pathological response and prediction of OS. Additionally, previous chemotherapy response evaluation study in NSCLC showed that ΔSUV and ΔMR_{glu} are predictive of response (11). Concluding, simplified semi-quantitative methods based on static imaging are suitable for response monitoring and has currently replaced complex dynamic quantitative measurements.

Standardised uptake value

Historically, the SUV_{max} reflecting the maximum voxel of the tumour is most often used. It is an intra-observer reproducible parameter and is often used for assessment of therapeutic response. However, this parameter has many limitations. Due to considerable fluctuations in this parameter in repeated measurement studies, it is not useful as a robust response parameter. SUV_{max} can be heavily influenced by variations in acquisition and reconstruction methods and image 'noise' (12). In an attempt to overcome this issue, SUV_{peak} was introduced and is based on the maximum average SUV within a 1 mL spherical volume. Compared to SUV_{max} it can be argued that SUV_{peak} is a more robust alternative and is less dependent on noise typically associated with clinical whole-body studies (12). Nevertheless, even this parameter only reflects a small percentage of the tumour. Weber *et al.* (13) showed in a repeated measurement study that variability in SUV_{max} and SUV_{peak} could decrease by up to 30% or increase up to 40%, while not receiving treatment, showing that repeatability of both SUV_{max} and SUV_{peak} in these repeatability measurements were not fundamentally different. It is important to realise that smaller changes than the measurement error might not reflect biological or predictive significance. One of the limiting factors using SUV_{max} and SUV_{peak} is that changes in the extent of the pathologic metabolic activity are ignored. Especially in tumours with central necrosis, a rapidly growing tumour may show a reduction in SUV_{max} or SUV_{peak} as the thin rim of viable tissue becomes subject to partial volume effects. Also, in tumours with a decrease in metabolism in most parts of the tumour, but a small part with persistently high FDG-uptake resulting in an unchanged SUV_{max} or SUV_{peak}.

In **Chapter III** a simple normalisation method based on 'simple body' weight was performed for calculation of the SUV parameter. This normalisation of SUV using body weight has one potential weakness. Body composition can change significantly during chemotherapy. A normalisation of SUV using body weight seems less suitable since in a fasting state fat accumulates little FDG. To overcome this issue, other methods are introduced for normalisation based on body surface area (BSA) or lean body mass (LBM). SUV corrected for LBM (SUL) is becoming a popular metric for semi-quantitative assessment. Especially in obese patients, SUV normalisation using BSA or LBM have been shown to provide a more reliable estimate of FDG-uptake during significant weight loss (14). In **Chapter VII** we used predefined PERCIST criteria that require these SUV corrections based on LBM. However, in this early response monitoring study, the change in body weight and LBM between baseline and in-treatment FDG-PET/CT was minimal. Consequently, when normalisation was performed based on body weight instead of LBM, it did not affect the classification of metabolic response.

Total lesion glycolysis

For response assessment, volumetric parameters such as metabolic active tumour volume (MTV) and total lesion glycolysis (TLG) (15) are often used. TLG, historically known as the Larson-Ginsberg index, reflects both tumour volume as well as metabolic data and is defined as the product of SUV and MTV. Studies already showed the prognostic value of pre-treatment TLG in osteosarcoma (16), malignant mesothelioma (17, 18) head and neck cancer (19) and multiple myeloma (20). Other studies have shown the usefulness of TLG for evaluating treatment response in different tumours. Both volumetric parameters have resulted in significant predictive factors for outcome in breast cancer (21) and oesophageal cancer (22). However, one crucial factor is that the definition of metabolic tumour volume, i.e., the method of tumour delineation has a significant impact on the absolute value of TLG.

Delineation of Region of Interest

The definition of the metabolic tumour volume, the region of interest (ROI) of the tumour, has a substantial effect on the measurement of SUV, MTV and TLG. Tumours are heterogeneous and can contain non-tumour elements like fibrous tissue and necrosis. During treatment, the distribution of viable tumour and total tumour volume may change over time. This becomes more likely as the period between the pretherapy, and the in-treatment scan is extended, and ROI definition may be further compromised. Especially during treatment non-ideal shapes could be expected with non-uniform FDG-distribution and low tumour-to-background contrast. Different methods for ROI definition exist, and the chosen method could significantly affect the quantification of tumour response. Various approaches exist to delineate metabolic active tumour volume and are ranging from manually drawn ROI's to (semi)automatic methods. A critical limitation of manually defined ROI's is the relatively large inter-observer variability as compared to semi-automatic methods, especially in tumours with surrounding high physiologic FDG-uptake (such as the heart) or low FDG-uptake (such as atelectasis). Therefore, (semi)automatic methods are preferred, ranging from absolute thresholds (e.g., SUV 2.5), a fixed threshold of 41% or 50% of maximum SUV, relative threshold methods or adaptive thresholds.

Chapter V describes the effects of different response delineation methods and the effect on early response parameters. Different segmentation techniques are tested in this prospective response monitoring study and its impact on ΔTLG. This study showed different limitations of relative threshold methods. There was both an association between whole body ΔTLG and outcome, both OS and PFS. The segmentation performance of the primary tumour was analysed between relative threshold segmentation and adaptive

methods. All different ROI methods come with strengths and weaknesses. An absolute threshold method would fail in targets with a high background activity (like liver metastasis) since the threshold would be too low to exclude normal background tissue. On the other hand, lung lesions with a relatively low FDG-uptake delineated with absolute thresholding would only include a small portion of the lesion. For fixed threshold methods (41% or 50% of maximum SUV) the true tumour volume is underestimated since low activity areas in the periphery of the tumour are not included. Also, when FDG-uptake decreases during treatment, a lower SUV_{max} on follow-up would result in a lower absolute threshold, sometimes leading to a paradoxical increase in MTV and possibly a higher TLG. Adaptive methods, such as the fuzzy locally adaptive Bayesian (FLAB) method, try to overcome segmentation problems in heterogeneous metabolic active tumour volumes. Despite these fundamental differences in segmentation, relatively small differences in terms of predictive performance were found between these methods. However, for lymph node segmentation, the signal-to-background (SBR) method outperformed all other methods. This is caused by the relatively high background of the mediastinal blood pool against the affected mediastinal lymph nodes. The inclusion of involved lymph nodes is important since the predictive performance ΔTLG was marginally stronger when affected lymph nodes were included in the analysis. Later during treatment, when the tumour-to-background ratio has further declined, semi-automatic delineation methods become less reliable in the actual delineation of the residual MTV and the SBR method seems to overcome this issue.

Criteria for metabolic tumour response

For response assessment in clinical practice and further clinical trials, a widely accepted definition of metabolic response is of high importance. Different attempts have been made in the past to define metabolic tumour response criteria. Currently, there is a lack of univocal PET parameters for an early in-treatment metabolic response. FDG-PET/CT is a powerful tool for early response monitoring in NSCLC as many exploratory response monitoring studies already have demonstrated (*Table 1*) in many different (post-hoc) definitions of early metabolic response. However, the lack of implementation of predefined criteria for early metabolic response makes adoption in routine clinical practice challenging. Different criteria have been proposed for the definition of metabolic response. As discussed earlier, for measurement of response it is most often quantified by measurement of the relative change in uptake of the lesions. The European Organization for Research and Treatment of Cancer (EORTC) proposed criteria defined a 15% to 25% decrease in SUV as a partial metabolic response after one cycle of chemotherapy and greater than 25% after more than one treatment cycle. However, these criteria do not provide any details on the preferred method of delineation or what PET parameter. As discussed previously, the

delineation method for ROI has a significant effect on the absolute values of SUV_{mean}, MTV or TLG. Also, response calculation in multiple lesions is unclear in EORTC criteria since they lack recommendations for evaluation of the response of multiple lesions. Most studies that examined the role of therapeutic response assessment in NSCLC, focused on a response in either the primary tumour alone or the most metabolically active lymph node. This aggregation process is not always clear in response monitoring studies. Proposed by Wahl *et al.* (23) are PERCIST, which is of great value since it gives more guidance for selection of lesions to include, what measurements to use and added quantification of a complete metabolic response. This can ultimately lead to a lower interobserver variability and higher reproducibility of the results. A short overview of the differences between EORTC and PERCIST criteria is shown in *Table 2*. For routine clinical practice, these response criteria need to be robust, non-laborious and operator-friendly so that results are reliable and reproducible. So, are the PERCIST criteria 'the holy grail'? There are some practical problems with PERCIST that need to be addressed. The selection of tumour lesions is (analogous to RECIST 1.1) a maximum of five lesions (up to two targets in the same organ). One important criterium is to only include lesions with a diameter of at least 1.5 cm. However, it is known that bone metastases on CT cannot always be reliably assessed when they lack sufficient sclerotic or lytic component. Consequently, FDG-avid bone metastases are often ruled out solely based on these size criteria. Also, the criterium that FDG-avidity SUL_{peak} needs to be least 1.5-fold greater than liver SULmean+2SD, this can result in the exclusion of FDG-avid pulmonary lesions due to their low background activity. Due to the selection of highly avid lesions, many liver lesions (with higher FDG-uptake and background activity) are preferred over many lung lesions (with lower absolute FDG-uptake and background activity). For response measurement, it is not necessary to measure the same lesion and different lesions can be considered in the follow-up scans. The selection of measured tumour lesion is a major contributor to variability in the assessment of treatment response with FDG-PET/CT (24).

Timing of in-treatment evaluation

The crucial question is: when is it the most optimal time to examine the reduction in FDG-uptake? Ideally, the timing of in-treatment should be as early during treatment as possible, since it then leaves enough possibility to escalate or de-escalate treatment. On the other hand, it may take some time for the treatment to affect the tumour. Timing FDG-PET/CT relatively short after specific treatments might reflect a temporary phenomenon rather than a true response to treatment. Also, the change in FDG-uptake needs to reflect an actual significant metabolic change rather than measuring a small difference that lies within the measurement error of the PET acquisition. Still, there are few data about the optimal timing

TABLE 1. Overview of response monitoring studies with FDG-PET/CT in NSCLC treated with chemotherapy and/or radiotherapy

Study	No. of patients	Year	Design	Treatment	Clinical Stage	Histology AC(%)/ SCC(%)/ NOS(%)	In-treatment response	ROI delineation	Response criteria	Outcome measure
Weber *et al.* (10)	57	2003	Prospective	CTx	IIIB-IV	31 (54%)/ 18 (32%)/ 8 (14%)	After 1 cycle (21 d)	Unknown	ΔSUV>20%	OS
Hoekstra *et al.* (49)	47	2005	Prospective	CTx	IIIA-IIIB/N2	16 (34%)/ 19 (40%)/ 12 (26%)	After 1 cycle and 3 cycles	50% of SUV_{max}	ΔMR_{glu}>35% SUV_{BSAg}<140	PFS
de Geus-Oei *et al.* (11)	51	2007	Prospective	CTx	IB-IV	24 (47%)/ 21 (41%)/ 6 (12%)	After 2, 3 cycles	50% of SUV_{max}	ΔMR_{glu}>47% ΔSUV>35%	OS
Baardwijk *et al.* (50)	23	2007	Prospective	CRT	IB-IIIB	5 (36%)/ 5 (36%) /4 (29%)	7, 14 d	Manual	ΔSUV_{max} (NS)	PFS
Nahmias *et al.* (25)	15	2007	Prospective	CTx	IIIB-IV	7 (47%)/6 (40%)/2 (13%)	7, 14, 21 d	Fixed SUV=5	ΔSUV >20%	OS
Lee *et al.* (51)	31	2009	Prospective	CTx and EGFR TKI	IIIB-IV	22 (71%)/ 6 (19%)/ 3 (10%)	3 wk after 1st cycle	NA	ΔSUV_{max} >20%	PFS
Zhang *et al.* (52)	46	2011	Prospective	CTx	IIIA-IIIB	21 (46%)/ 25 (54%)/ 0 (%)	After 1 cycle (3 wk)	Manual	ΔSUV_{max} >50%	OS
Van Elmpt *et al.* (26)	34	2012	Prospective	CRT	IIB- IV	unknown	After 1, 3 cycles	Gradient based	ΔSUV_{mean} >20%	OS
Massaccesi *et al.* (53)	25	2012	Prospective	CRT	IIB- IIIB	13 (52%) /10 (40%) /2 (8%)	3 wk	50% of SUV_{max}	EORTC (ΔSUV > 15%)	PFS
Novello *et al.* (30, 54)	22	2013	Prospective	CTx	IIIB-IV	10 (45%)/ 4 (18%) /8 (36%)	2 wk	Manual	EORTC (ΔSUV > 15%) (NS)	PFS, OS
Usmanij *et al.* (55)	28	2013	Prospective	CRT	IIIA-IIIB	14 (50%)/ 11 (39%)/ 3 (11%)	14 d	50% of SUV_{max}	ΔTLG >38%	PFS

Moon *et al.* (56)	52	2013	Prospective	CTx	IV	45 (83%)/ 7(13%)/0 (0%)	After 4 cycles	Relative threshold (blood pool + 2 SD)	ΔTLG >50%, ΔMTV >50%	PFS, OS
Huang *et al.* (57)	63	2014	Prospective	CRT	IIIA-IIIB	19 (36%)/ 30 (57%)/ 4 (8%)	2 cycles / 40 *Gy* / 28 d ± 3d	50% of SUV_{max}	$\Delta SUVmax>37\%$, $\Delta SUV_{mean}>42\%$, ΔMTV >30%	OS
Wang *et al.* (58)	44	2015	Prospective	CRT	I-III	6 (14%)/ 10(23%)/ 28 (64%)	4 wk	Relative threshold (SUV_{max}/ blood pool)	ΔNSUV−A>75%	PFS, OS
Yossi *et al.* (59)	31	2015	Retrospective	CRT	II- IIIB	15 (48%)/ 11 (35%)/ 5 (16%)	After 40 *Gy*	SUV cut-off 3.0	ΔTLG>15%	PFS, OS
Dong *et al.* (60)	58	2016	Prospective	CRT	IIIA-IIIB	25 (43%)/ 30 (52%)/ 3 (5%)	40 *Gy* / 28 d ± 3d	SUV cut-off 3.0	ΔContrast>70%, AUC-CSHΔ>33%	PFS, OS
Shang *et al.* (61)	35	2016	Prospective	CTx	III-IV	22 (63%)/ 13 (37%)/ 0 (0%)	After 2 cycles	Iterative adaptive	PERCIST (ΔSUL_{peak} >30%), EORTC (ΔSUV >25%)	PFS
Fledius *et al.* (62)	21	2016	Retrospective	CRT	IIB-IIB	8 (38%) / 10 (48%)/ 3 (14%)	After 2 cycles	NA	PERCIST (ΔSUL_{peak} >30%)	PFS, OS
Mattoli *et al.* (63)	44	2017	Retrospective	CRT	IIIA-IIIB	25 (57%) / 15 (34%) / 4 (9%)	2 cycles / 4 ± 2.8 weeks	NA	PERCIST (ΔSUL_{peak} >30%)	PFS, OS

CRT: chemoradiotherapy, CTx: chemotherapy, RT: radiotherapy, AC: adenocarcinoma, SCC: squamous cell carcinoma, NOS: non-small cell lung cancer not otherwise specified
OS: overall survival, PFS: progression free survival, SUL: standardised uptake corrected for lean body mass, MTV: metabolic active tumour volume, CMR: complete metabolic response, PMR: partial metabolic response, SMD: stable metabolic disease, PMD: progressive metabolic disease, PERCIST: PET response criteria in solid tumours, EORTC: European Organisation for Research and Treatment of Cancer, TTP: time to progression, NS: not significant, NA: not applicable

TABLE 2. Comparison of response criteria of EORTC and PERCIST

	EORTC (1999)	PERCIST (2009)
Semiquantitative parameter	SUV_{mean}	SUL_{peak}
Normalisation	Body surface area	Lean body mass
Response categories		
Complete metabolic response (CMR)	Resolution of FDG-avid lesions (equal or lower than background tissue)	Complete resolution of FDG-avid lesions, indistinguishable from background tissue, SUL_{peak} less than liver ROI
Partial metabolic response (PMR)	Decrease of SUV_{mean} 15 -25% after 1 cycle or >25% after 2 or more treatment cycles	Decrease of target lesion SUL_{peak} ≥30% and at least 0.8 SUL_{peak} units difference, no increase >30% in SUL_{peak} or size of target and non-target lesions
Stable metabolic disease (SMD)	Increase SUV_{mean} <25% or decrease <15% No increase in extent of FDG-uptake in longest diameter > 20%	Increase <30% or decrease of SUL_{peak} <30%
Progressive metabolic disease (PMD)	New FDG-avid lesions Increase of SUV_{mean} > 25% or increase in extent of FDG-uptake, longest diameter >20%	New FDG-avid lesions Increase target lesions SUL_{peak} ≥30% and at least 0.8 SUL_{peak} units Increase in target lesion extent and no decline in SUL_{peak}

European Organisation for Resarch and Treatment of Cancer (EORTC) and Positron Emission Tomography Response Criteria in Solid Tumours (PERCIST). ROI, Region of interest. SUV Standardised uptake value, SUL standardised uptake value corrected for lean body mass.

for evaluation of in-treatment response in NSCLC and there is no consensus regarding the optimal timing of early in-treatment FDG-PET/CT. While chemotherapy can decrease tumour metabolism during treatment due to direct cytotoxic effects and cell kill, normally in end-of-treatment evaluation it can point to residual or resistant disease. However, when evaluating early during treatment, there is still considerable FDG-uptake is remaining in the tumour, even in patients responding to the treatment (25, 26). When radiation is added, there is also a possible effect of radiation-induced inflammation that can produce possible misinterpretations. In our prospective clinical studies discussed in **Chapter III** and **VII**, the timing of the in-treatment FDG PET was chosen to be as early as two weeks in-treatment. An earlier overview of clinical studies (*Table 1*) concerning early response monitoring reveals a broad range in the timing of interim evaluation, ranging from 1 to 6 weeks in-treatment. The timing of in-treatment evaluation should be dependent on the schedule and type of cytostatic or cytoreductive treatment. Waiting too long for in-treatment response could result in delayed treatment adaptation for the patient or misclassification of patients as responders. Also, a time point chosen too early can reflect a possible flare phenomenon. Assessments performed too early might not correlate with the biological effect, since glucose metabolism can still be present in cells that have received lethal damage. On the other hand, FDG-uptake is also possible in sub-lethal damaged cells which are unable to proliferate but are still viable. It can be expected that at a later time-point during treatment the proportion of surviving clonogenic cells in the entire population of the tumour is still decreasing and differences in measured metabolic activity will be larger as compared to the FDG-PET/CT at baseline. The timing of in-treatment FDG-PET/CT should highly depend on the treatment, and that seems more than reasonable. In a large prospective study of stage IV NSCLC patients treated with paclitaxel-carboplatin and bevacizumab, FDG-PET/CT was performed shortly (within three days) after administration of bevacizumab of the second cycle of chemotherapy (27). Many patients showed a significant decrease in FDG-uptake, however, the response on FDG-PET/CT was not predictive of OS (with or without the use of nitro-glycerine patches). In this specific study, a possible substantial decrease in FDG-uptake might not be related to direct cytotoxic effects or cell kill of treatment, but rather a direct anti-angiogenic effect of bevacizumab resulting in lower tumour perfusion. This finding seems to be inconsistent with the widely accepted mechanism of action of anti-angiogenic drugs that they transiently normalise structurally and functionally abnormal tumour vasculature, improving drug and chemotherapy penetration in tumour tissue (28). Also contrary to this hypothesis, another study showed an adverse effect of bevacizumab on ^{11}C-docetaxel uptake and a reduction of tumour perfusion instead (29). This effect of a decrease in perfusion in tumour tissue was seen within a few hours and persisted for at least four days after bevacizumab administration.

Metabolic response assessment with FDG-PET/CT can also yield false positive results due to inflammation and early post-radiotherapy changes. This is the direct consequence of FDG being an imaging biomarker of metabolism and not a specific tracer for cancer. Especially after radiotherapy, infiltration of lymphoid cells could be responsible for an increase of FDG-uptake. Serial imaging studies during and after radiotherapy suggest that inflammatory FDG uptake in normal tissues only increases after the first few months after treatment rather than occurring early during therapy. Especially inflammatory lung tissue uninvolved with tumour is unable to be separated from viable tumour tissue, possibly limiting an accurate region of interest definition. An in-treatment evaluation after two weeks seems to be a good compromise between early evaluation without a possible confounding effect of tissue inflammation, and it provides a time window for treatment adaptation.

Another important factor is that delineation of metabolic active tumour becomes more problematic later on during treatment. Edit-Sanson *et al.* have demonstrated the time-course of FDG-uptake in 10 NSCLC candidates for curative radiotherapy (60-70 Gy) (30). FDG-PET performed every seven fractions showed that later during the time course of treatment, fixed threshold and adaptive methods failed to delineate the tumour in a significant number of cases. Consequently, SUV and other volumetric parameters like MTV and TLG become more and more unreliable later during the treatment course. Due to the decrease in tumour FDG-uptake later during the treatment, (semi-)automatic delineation methods have more problems in a separation of the tumour volume from background tissue. After two weeks there is still significant FDG-uptake left for automatic segmentation methods to delineate the metabolic active tumour volume. Therefore, a choice for treatment evaluation later than two weeks after the start of treatment can only be based on manual delineation. This comes at the cost of low repeatability since manual delineation is highly subjective, potentially resulting in inconsistent outcomes.

FDG-PET/CT and radiotherapy

Advances in conformal radiotherapy techniques like intensity modulated radiotherapy (IMRT) and volumetric modulated arc therapy (VMAT) combined with FDG-PET/CT allowed precise dose delivery and individualised treatment with near surgical precision. FDG-PET/CT is recommended for radiotherapy planning, since FDG-PET/CT significantly improves target delineation accuracy, especially in specific cases with lung atelectasis and nodal disease. Biologically adaptive radiotherapy is an approach that modifies the initial treatment planning during the course of radiotherapy. Geometrical and biological variations induced by radiotherapy could be accounted for, instead of applying the same baseline characteristics to all radiotherapy fractions. After initial treatment delivery of a specific dose, the treatment plan is re-optimised aiming the boost of radiation therapy to the residual tumour, while sparing healthy tissues. One crucial factor is that the target tissue does not have uniform radiological properties. Differences in sub-volumes can exist due to radio-resistance and hypoxia. Areas of high uptake on pre-treatment FDG-PET/CT identify preferential sites of local relapse after chemoradiotherapy for NSCLC (31).

In **Chapter III** we discussed early response assessment in locally advanced NSCLC and showed that change in TLG was predictive of progression-free survival. In theory, those patients who showed a minimal or no decline in TLG might be candidates for treatment adaptation, i.e., treatment intensification. For dose escalation, it is possible to boost based on the pre-treatment FDG-PET/CT while boosting based on in-treatment FDG-PET/CT allows identification of radio-resistant disease. Careful selection of patients is needed as treatment intensification should only be applied when unnecessary radiation to organs at risk could be avoided. In selected cases, dose escalation was possible for smaller tumour volumes than the original tumour volume. In **Chapter VI** an FDG-PET/CT guided dose escalation study was performed to improve local tumour control in stage III NSCLC. On these patients, who were treated with 60 Gy chemoradiotherapy, dose escalation simulations were performed on subvolumes with markedly increased uptake, based on pre-treatment and early in-treatment FDG-PET/CT. Based on the in-treatment FDG-PET/CT planned target volume could be reduced in 5 out of 10 patients. One limitation is that no respiratory gating was applied during the FDG-PET/CT acquisition. Due to the long acquisition time of FDG-PET/CT with typical acquisition times of 3 to 4 minutes per axial view, motion artefacts due to free breathing can occur. This can result in an underestimation of FDG-uptake and an overestimation of MTV. Optimally respiratory gating (ORG) during acquisition of PET results in a significant increase in SUV_{mean} and a significant decrease in MTV can be used to increase target accuracy further (32). ORG also resulted in a more accurate alignment between PET and

CT and an increase in TLG and SUV_{mean}, compared to non-gated CT (33). Implementation of ORG improves quantitative accuracy however with the targeting of radioresistant disease did not result in a clinically relevant difference in radiation dose to the organs at risk (34).

With an increasing spectrum of developments in treatment strategies and target therapies, personalised decision making is becoming increasingly relevant. With spiralling costs of treatment, this further presses the need to optimally select specific treatments for the individual patient, while minimising the costs and side effects of ineffective treatment. We demonstrated that the concept of early in-treatment response monitoring using FDG-PET/CT in NSCLC is valid and that metabolic changes during the treatment course are predictive of clinical outcome. Measurement of the tumour response to treatment based on metabolic activity, rather than size alone, reflects a fundamental advantage to investigate the biology of cancer in vivo prior to and during treatment. Each of these additional FDG-PET/CT may add significantly to the costs and time of treatment. However, they also might prevent costs by early discontinuation of in-effective treatment. Investigations of the comparative effectiveness and cost-effectiveness of FDG PET/CT in assessing treatment response are still needed.

The methodology of the current early in-treatment response monitoring studies and clinical endpoints are still heterogeneous and uniform quantitative cut-off points are lacking. The sample size is a critical defect in the current early in treatment response monitoring studies. Therefore, it is essential to pool data from multiple centres. In order to compare different results from different studies, more standardisation is needed for image analysis. Currently, there is a consensus in quantitative analysis in FDG-PET/CT and are already described in protocols from Europe (35) and the USA (36). Implementation of predefined criteria, like PERCIST, in response monitoring studies would greatly aid future pooling and meta-analysis of response monitoring studies. With current advances in computing power and (semi)automated quantitative assessment of FDG-PET/CT based on PERCIST criteria may provide an immediate and objective report of treatment response. Prospective adaptive multicentre trails PET-guided treatment needs to be conducted to establish a foundation for clinical practice. Current initiatives of adaptive PET-based studies are being started and the results of these adaptive PET-based studies are waited for with great interest (37).

Other than chemoradiotherapy in NSCLC, there is an increasing body of evidence for early response assessment with FDG-PET/CT in targeted treatments, like EGFR-TKI (38-42) and immune checkpoint inhibitors such as nivolumab (43). Also, the implementation of other PET traces could be more specific for treatment response evaluation. During treatment as the tumour changes, the interplay between proliferation, angiogenesis, and hypoxia will show areas of active tumour repopulation, resistant areas and regressing tumour areas. To visualise tumour resistant areas, hypoxia tracers (like Fluoro-misonidazole, ^{18}F-FMISO) could be used for quantification of hypoxia. For

targeting cell proliferation, Fluoro-thymidine (^{18}F-FLT) has been used for early response assessment in patients treated with EGFR-TKI (44).

Various textural features and parameters reflecting tumour heterogeneity have shown much potential for response assessment (45). Differences in aggressive and heterogeneous features caused by various clones harbouring various mutations can contribute to inter-tumoural and even intra-tumoural heterogeneity. One limiting factor of (semi)quantitative parameters is that they ignore changes not only in the extent of the pathologic metabolic activity but also inadequately describes the heterogeneous distribution of FDG within a tumour. Current research on intra-tumour heterogeneity in solid malignancies is rapidly increasing. In particular, there is an increasing interest in using intra-tumour heterogeneity to correlate with tumour type, aggressiveness, tumour grade, metastatic potential, hypoxia and treatment resistance. This concept of radiogenomics is aimed at developing tools for non-invasive genotyping by identifying imaging biomarkers. Different parameters could be correlated to different aspects of the tumour microenvironment, such as proliferation, angiogenesis, hypoxia, inflammation, and expression of specific receptors or mutations. Identification of a subset of features that are most relevant to the underlying biological mechanism can improve our understanding of tumour response. Eventually, we hope to find radiomic features that can serve as predictive markers similar to CT based radiomic features (46). It is increasingly recognised that genetic heterogeneity exists within the tumour and between metastatic sites in the individual patient. As many different features have been described and as more different samples are tested, the need for large patient datasets are a necessity.

Current practice for treatment selection in NSCLC has evolved from a mostly empiric method, based on known prognostic factors like performance status, weight loss, and stage to a more integrated approach where clinical factors, histological and molecular factors are included. Especially with a sustained increase in lung cancer rates in females, further research on the effect of gender and outcome in NSCLC is important. Gender is not only a prognostic factor, but there might be differences in response to targeted treatments in females, compared to men (47). With modern techniques, the identification of specific genetic factors that may play a role in disease progression should direct research to identify the clinical predictors of outcome for NSCLC. Ultimately, all known prognostic factors like performance status, weight loss, stage and metabolic parameters, gender, histology, mutation status together with in-treatment parameters should lead to an integrated and personalised approach. Pooling of relevant patient data into large (nationwide) sets of 'big data' can eventually lead to more predictive models to forecast clinical outcome and optimise treatment strategy (48).

Measurement of the tumour response to treatment based on metabolic activity, rather than size alone, reflects a fundamental advantage to investigate the biology of cancer in vivo and to measure the impact and change in metabolism. Traditional chemotherapy is still the cornerstone of treatment of NSCLC, but still, the overall survival in advanced stage disease remains dismal. With the advent of tyrosine kinase inhibitors, anaplastic lymphoma kinase and monoclonal antibodies, analysis of underlying mutations, the effective use of treatment combinations and early discontinuation of in-effective treatment are crucial. With this increasing pallet of treatment choices, there is a potential increasing role of PET for early in-treatment response measurement. Selection of highly effective treatments and subsequently early discontinuation of in-effective treatment should ultimately lead to an improved outcome and a reduction of adverse events. Personalised medicine for NSCLC is a reality now, and its use will only increase in the future.

References

1. Lunt SY, Vander Heiden MG. Aerobic glycolysis: meeting the metabolic requirements of cell proliferation. Annu Rev Cell Dev Biol. 2011;27:441-64.
2. DeBerardinis RJ, Lum JJ, Hatzivassiliou G, Thompson CB. The biology of cancer: metabolic reprogramming fuels cell growth and proliferation. Cell Metab. 2008;7(1):11-20.
3. Smith TA. FDG uptake, tumour characteristics and response to therapy: a review. Nuclear medicine communications. 1998;19(2):97-105.
4. Albain KS, Swann RS, Rusch VW, Turrisi AT, 3rd, Shepherd FA, Smith C, et al. Radiotherapy plus chemotherapy with or without surgical resection for stage III non-small-cell lung cancer: a phase III randomised controlled trial. Lancet. 2009;374(9687):379-86.
5. Reck M, von Pawel J, Zatloukal P, Ramlau R, Gorbounova V, Hirsh V, et al. Phase III trial of cisplatin plus gemcitabine with either placebo or bevacizumab as first-line therapy for nonsquamous non-small-cell lung cancer: AVAil. Journal of clinical oncology : official journal of the American Society of Clinical Oncology. 2009;27(8):1227-34.
6. Clarke JM, Hurwitz HI. Understanding and targeting resistance to anti-angiogenic therapies. J Gastrointest Oncol. 2013;4(3):253-63.
7. Boellaard R, Delgado-Bolton R, Oyen WJ, Giammarile F, Tatsch K, Eschner W, et al. FDG PET/CT: EANM procedure guidelines for tumour imaging: version 2.0. European journal of nuclear medicine and molecular imaging. 2015;42(2):328-54.
8. Vriens D, Visser EP, de Geus-Oei LF, Oyen WJ. Methodological considerations in quantification of oncological FDG PET studies. European journal of nuclear medicine and molecular imaging. 2010;37(7):1408-25.
9. Kaalep A, Sera T, Oyen W, Krause BJ, Chiti A, Liu Y, et al. EANM/EARL FDG-PET/CT accreditation - summary results from the first 200 accredited imaging systems. European journal of nuclear medicine and molecular imaging. 2018;45(3):412-22.
10. Weber WA, Petersen V, Schmidt B, Tyndale-Hines L, Link T, Peschel C, et al. Positron emission tomography in non-small-cell lung cancer: prediction of response to chemotherapy by quantitative assessment of glucose use. Journal of clinical oncology : official journal of the American Society of Clinical Oncology. 2003;21(14):2651-7.
11. de Geus-Oei LF, van der Heijden HF, Visser EP, Hermsen R, van Hoorn BA, Timmer-Bonte JN, et al. Chemotherapy response evaluation with 18F-FDG PET in

patients with non-small cell lung cancer. Journal of nuclear medicine : official publication, Society of Nuclear Medicine. 2007;48(10):1592-8.

12. Lodge MA, Chaudhry MA, Wahl RL. Noise considerations for PET quantification using maximum and peak standardized uptake value. Journal of nuclear medicine : official publication, Society of Nuclear Medicine. 2012;53(7):1041-7.
13. Weber WA, Gatsonis CA, Mozley PD, Hanna LG, Shields AF, Aberle DR, et al. Repeatability of 18F-FDG PET/CT in Advanced Non-Small Cell Lung Cancer: Prospective Assessment in 2 Multicenter Trials. Journal of nuclear medicine : official publication, Society of Nuclear Medicine. 2015;56(8):1137-43.
14. Keramida G, Hunter J, Dizdarevic S, Peters AM. The appropriate whole-body index on which to base standardized uptake value in 2-deoxy-2-[(18)F]fludeoxyglucose PET. The British journal of radiology. 2015;88(1052):20140520.
15. Hoang JK, Hoagland LF, Coleman RE, Coan AD, Herndon JE, 2nd, Patz EF, Jr. Prognostic value of fluorine-18 fluorodeoxyglucose positron emission tomography imaging in patients with advanced-stage non-small-cell lung carcinoma. Journal of clinical oncology : official journal of the American Society of Clinical Oncology. 2008;26(9):1459-64.
16. Im HJ, Zhang Y, Wu H, Wu J, Daw NC, Navid F, et al. Prognostic Value of Metabolic and Volumetric Parameters of FDG PET in Pediatric Osteosarcoma: A Hypothesis-generating Study. Radiology. 2018;287(1):303-12.
17. Incerti E, Broggi S, Fodor A, Cuzzocrea M, Samanes Gajate AM, Mapelli P, et al. FDG PET-derived parameters as prognostic tool in progressive malignant pleural mesothelioma treated patients. European journal of nuclear medicine and molecular imaging. 2018.
18. Kitajima K, Doi H, Kuribayashi K, Hashimoto M, Tsuchitani T, Tanooka M, et al. Prognostic value of pretreatment volume-based quantitative (18)F-FDG PET/CT parameters in patients with malignant pleural mesothelioma. European journal of radiology. 2017;86:176-83.
19. Pak K, Cheon GJ, Nam HY, Kim SJ, Kang KW, Chung JK, et al. Prognostic value of metabolic tumor volume and total lesion glycolysis in head and neck cancer: a systematic review and meta-analysis. Journal of nuclear medicine : official publication, Society of Nuclear Medicine. 2014;55(6):884-90.
20. McDonald JE, Kessler MM, Gardner MW, Buros AF, Ntambi JA, Waheed S, et al. Assessment of Total Lesion Glycolysis by (18)F FDG PET/CT Significantly Improves Prognostic Value of GEP and ISS in Myeloma. Clinical cancer research : an official journal of the American Association for Cancer Research. 2017;23(8):1981-7.
21. Garcia-Vicente AM, Perez-Beteta J, Amo-Salas M, Molina D, Jimenez-Londono GA, Soriano-Castrejon AM, et al. Predictive and prognostic potential of volume-based

metabolic variables obtained by a baseline (18)F-FDG PET/CT in breast cancer with neoadjuvant chemotherapy indication. Rev Esp Med Nucl Imagen Mol. 2018;37(2):73-9.

22. I HS, Kim SJ, Kim IJ, Kim K. Predictive value of metabolic tumor volume measured by 18F-FDG PET for regional lymph node status in patients with esophageal cancer. Clinical nuclear medicine. 2012;37(5):442-6.
23. Wahl RL, Jacene H, Kasamon Y, Lodge MA. From RECIST to PERCIST: Evolving Considerations for PET response criteria in solid tumors. Journal of nuclear medicine : official publication, Society of Nuclear Medicine. 2009;50 Suppl 1:122S-50S.
24. O JH, Jacene H, Luber B, Wang H, Huynh MH, Leal JP, et al. Quantitation of Cancer Treatment Response by (18)F-FDG PET/CT: Multicenter Assessment of Measurement Variability. Journal of nuclear medicine : official publication, Society of Nuclear Medicine. 2017;58(9):1429-34.
25. Nahmias C, Hanna WT, Wahl LM, Long MJ, Hubner KF, Townsend DW. Time course of early response to chemotherapy in non-small cell lung cancer patients with 18F-FDG PET/CT. Journal of nuclear medicine : official publication, Society of Nuclear Medicine. 2007;48(5):744-51.
26. van Elmpt W, Ollers M, Dingemans AM, Lambin P, De Ruysscher D. Response assessment using 18F-FDG PET early in the course of radiotherapy correlates with survival in advanced-stage non-small cell lung cancer. Journal of nuclear medicine : official publication, Society of Nuclear Medicine. 2012;53(10):1514-20.
27. de Jong EE, van Elmpt W, Leijenaar RT, Hoekstra OS, Groen HJ, Smit EF, et al. [18F]FDG PET/CT-based response assessment of stage IV non-small cell lung cancer treated with paclitaxel-carboplatin-bevacizumab with or without nitroglycerin patches. European journal of nuclear medicine and molecular imaging. 2017;44(1):8-16.
28. Jain RK. Normalizing tumor vasculature with anti-angiogenic therapy: a new paradigm for combination therapy. Nat Med. 2001;7(9):987-9.
29. Van der Veldt AA, Lubberink M, Bahce I, Walraven M, de Boer MP, Greuter HN, et al. Rapid decrease in delivery of chemotherapy to tumors after anti-VEGF therapy: implications for scheduling of anti-angiogenic drugs. Cancer cell. 2012;21(1):82-91.
30. Edet-Sanson A, Dubray B, Doyeux K, Back A, Hapdey S, Modzelewski R, et al. Serial assessment of FDG-PET FDG uptake and functional volume during radiotherapy (RT) in patients with non-small cell lung cancer (NSCLC). Radiotherapy and oncology : journal of the European Society for Therapeutic Radiology and Oncology. 2012;102(2):251-7.
31. Calais J, Thureau S, Dubray B, Modzelewski R, Thiberville L, Gardin I, et al. Areas of high 18F-FDG uptake on preradiotherapy PET/CT identify preferential sites of local

relapse after chemoradiotherapy for non-small cell lung cancer. Journal of nuclear medicine : official publication, Society of Nuclear Medicine. 2015;56(2):196-203.

32. Grootjans W, de Geus-Oei LF, Meeuwis AP, van der Vos CS, Gotthardt M, Oyen WJ, et al. Amplitude-based optimal respiratory gating in positron emission tomography in patients with primary lung cancer. European radiology. 2014;24(12):3242-50.
33. van der Vos CS, Meeuwis APW, Grootjans W, de Geus-Oei LF, Visser EP. Improving the spatial alignment in PET/CT using amplitude-based respiratory-gated PET and patient-specific breathing-instructed CT. Journal of nuclear medicine technology. 2018.
34. Wijsman R, Grootjans W, Troost EG, van der Heijden EH, Visser EP, de Geus-Oei LF, et al. Evaluating the use of optimally respiratory gated 18F-FDG-PET in target volume delineation and its influence on radiation doses to the organs at risk in non-small-cell lung cancer patients. Nuclear medicine communications. 2016;37(1):66-73.
35. Boellaard R, O'Doherty MJ, Weber WA, Mottaghy FM, Lonsdale MN, Stroobants SG, et al. FDG PET and PET/CT: EANM procedure guidelines for tumour PET imaging: version 1.0. European journal of nuclear medicine and molecular imaging. 2010;37(1):181-200.
36. Shankar LK, Hoffman JM, Bacharach S, Graham MM, Karp J, Lammertsma AA, et al. Consensus recommendations for the use of 18F-FDG PET as an indicator of therapeutic response in patients in National Cancer Institute Trials. Journal of nuclear medicine : official publication, Society of Nuclear Medicine. 2006;47(6):1059-66.
37. Chaft JE, Dunphy M, Naidoo J, Travis WD, Hellmann M, Woo K, et al. Adaptive Neoadjuvant Chemotherapy Guided by (18)F-FDG PET in Resectable Non-Small Cell Lung Cancers: The NEOSCAN Trial. Journal of thoracic oncology : official publication of the International Association for the Study of Lung Cancer. 2016;11(4):537-44.
38. Fledelius J, Winther-Larsen A, Khalil AA, Hjorthaug K, Frokiaer J, Meldgaard P. Assessment of very early response evaluation with (18)F-FDG-PET/CT predicts survival in erlotinib treated NSCLC patients-A comparison of methods. Am J Nucl Med Mol Imaging. 2018;8(1):50-61.
39. Kanazu M, Maruyama K, Ando M, Asami K, Ishii M, Uehira K, et al. Early pharmacodynamic assessment using (1)(8)F-fluorodeoxyglucose positron-emission tomography on molecular targeted therapy and cytotoxic chemotherapy for clinical outcome prediction. Clinical lung cancer. 2014;15(3):182-7.
40. Ho KC, Fang YD, Chung HW, Liu YC, Chang JW, Hou MM, et al. TLG-S criteria are superior to both EORTC and PERCIST for predicting outcomes in patients with metastatic lung adenocarcinoma treated with erlotinib. European journal of nuclear medicine and molecular imaging. 2016;43(12):2155-65.

41. Winther-Larsen A, Fledelius J, Demuth C, Bylov CM, Meldgaard P, Sorensen BS. Early Change in FDG-PET Signal and Plasma Cell-Free DNA Level Predicts Erlotinib Response in EGFR Wild-Type NSCLC Patients. Translational oncology. 2016;9(6):505-11.
42. van Gool MH, Aukema TS, Schaake EE, Rijna H, Codrington HE, Valdes Olmos RA, et al. (18)F-fluorodeoxyglucose positron emission tomography versus computed tomography in predicting histopathological response to epidermal growth factor receptor-tyrosine kinase inhibitor treatment in resectable non-small cell lung cancer. Annals of surgical oncology. 2014;21(9):2831-7.
43. Kaira K, Higuchi T, Naruse I, Arisaka Y, Tokue A, Altan B, et al. Metabolic activity by (18)F-FDG-PET/CT is predictive of early response after nivolumab in previously treated NSCLC. European journal of nuclear medicine and molecular imaging. 2018;45(1):56-66.
44. Everitt SJ, Ball DL, Hicks RJ, Callahan J, Plumridge N, Collins M, et al. Differential 18F-FDG and 18F-FLT Uptake on Serial PET/CT Imaging Before and During Definitive Chemoradiation for Non-Small Cell Lung Cancer. Journal of nuclear medicine : official publication, Society of Nuclear Medicine. 2014;55(7):1069-74.
45. Kim DH, Jung JH, Son SH, Kim CY, Hong CM, Oh JR, et al. Prognostic Significance of Intratumoral Metabolic Heterogeneity on 18F-FDG PET/CT in Pathological N0 Non-Small Cell Lung Cancer. Clinical nuclear medicine. 2015;40(9):708-14.
46. Aerts HJ, Velazquez ER, Leijenaar RT, Parmar C, Grossmann P, Carvalho S, et al. Decoding tumour phenotype by noninvasive imaging using a quantitative radiomics approach. Nat Commun. 2014;5:4006.
47. Pinto JA, Vallejos CS, Raez LE, Mas LA, Ruiz R, Torres-Roman JS, et al. Gender and outcomes in non-small cell lung cancer: an old prognostic variable comes back for targeted therapy and immunotherapy? ESMO Open. 2018;3(3):e000344.
48. Hosny A, Parmar C, Coroller TP, Grossmann P, Zeleznik R, Kumar A, et al. Deep learning for lung cancer prognostication: A retrospective multi-cohort radiomics study. PLoS Med. 2018;15(11):e1002711.
49. Hoekstra CJ, Stroobants SG, Smit EF, Vansteenkiste J, van Tinteren H, Postmus PE, et al. Prognostic relevance of response evaluation using [18F]-2-fluoro-2-deoxy-D-glucose positron emission tomography in patients with locally advanced non-small-cell lung cancer. Journal of clinical oncology : official journal of the American Society of Clinical Oncology. 2005;23(33):8362-70.
50. van Baardwijk A, Bosmans G, Dekker A, van Kroonenburgh M, Boersma L, Wanders S, et al. Time trends in the maximal uptake of FDG on PET scan during thoracic radiotherapy. A prospective study in locally advanced non-small cell lung cancer

(NSCLC) patients. Radiotherapy and oncology : journal of the European Society for Therapeutic Radiology and Oncology. 2007;82(2):145-52.

51. Lee DH, Kim SK, Lee HY, Lee SY, Park SH, Kim HY, et al. Early prediction of response to first-line therapy using integrated 18F-FDG PET/CT for patients with advanced/metastatic non-small cell lung cancer. Journal of thoracic oncology : official publication of the International Association for the Study of Lung Cancer. 2009;4(7):816-21.
52. Zhang HQ, Yu JM, Meng X, Yue JB, Feng R, Ma L. Prognostic value of serial [18F]fluorodeoxyglucose PET-CT uptake in stage III patients with non-small cell lung cancer treated by concurrent chemoradiotherapy. European journal of radiology. 2011;77(1):92-6.
53. Massaccesi M, Calcagni ML, Spitilli MG, Cocciolillo F, Pelligro F, Bonomo L, et al. 18 F-FDG PET-CT during chemo-radiotherapy in patients with non-small cell lung cancer: the early metabolic response correlates with the delivered radiation dose. Radiat Oncol. 2012;7(1):106.
54. Novello S, Vavala T, Levra MG, Solitro F, Pelosi E, Veltri A, et al. Early response to chemotherapy in patients with non-small-cell lung cancer assessed by [18F]-fluoro-deoxy-D-glucose positron emission tomography and computed tomography. Clinical lung cancer. 2013;14(3):230-7.
55. Usmanij EA, de Geus-Oei LF, Troost EG, Peters-Bax L, van der Heijden EH, Kaanders JH, et al. 18F-FDG PET early response evaluation of locally advanced non-small cell lung cancer treated with concomitant chemoradiotherapy. Journal of nuclear medicine : official publication, Society of Nuclear Medicine. 2013;54(9):1528-34.
56. Moon SH, Cho SH, Park LC, Ji JH, Sun JM, Ahn JS, et al. Metabolic response evaluated by 18F-FDG PET/CT as a potential screening tool in identifying a subgroup of patients with advanced non-small cell lung cancer for immediate maintenance therapy after first-line chemotherapy. European journal of nuclear medicine and molecular imaging. 2013;40(7):1005-13.
57. Huang W, Fan M, Liu B, Fu Z, Zhou T, Zhang Z, et al. Value of metabolic tumor volume on repeated 18F-FDG PET/CT for early prediction of survival in locally advanced non-small cell lung cancer treated with concurrent chemoradiotherapy. Journal of nuclear medicine : official publication, Society of Nuclear Medicine. 2014;55(10):1584-90.
58. Wang J, Wong KK, Piert M, Stanton P, Frey KA, Kong FS. Metabolic response assessment with (18)F-FDG PET/CT: inter-method comparison and prognostic significance for patients with non-small cell lung cancer. J Radiat Oncol. 2015;4(3):249-56.

59. Yossi S, Krhili S, Muratet JP, Septans AL, Campion L, Denis F. Early Assessment of Metabolic Response by 18F-FDG PET During Concomitant Radiochemotherapy of Non-Small Cell Lung Carcinoma Is Associated With Survival: A Retrospective Single-Center Study. Clinical nuclear medicine. 2014.
60. Dong X, Sun X, Sun L, Maxim PG, Xing L, Huang Y, et al. Early Change in Metabolic Tumor Heterogeneity during Chemoradiotherapy and Its Prognostic Value for Patients with Locally Advanced Non-Small Cell Lung Cancer. PloS one. 2016;11(6):e0157836.
61. Shang J, Ling X, Zhang L, Tang Y, Xiao Z, Cheng Y, et al. Comparison of RECIST, EORTC criteria and PERCIST for evaluation of early response to chemotherapy in patients with non-small-cell lung cancer. European journal of nuclear medicine and molecular imaging. 2016.
62. Fledelius J, Khalil AA, Hjorthaug K, Frokiaer J. Using positron emission tomography (PET) response criteria in solid tumours (PERCIST) 1.0 for evaluation of 2'-deoxy-2'-[18F] fluoro-D-glucose-PET/CT scans to predict survival early during treatment of locally advanced non-small cell lung cancer (NSCLC). Journal of medical imaging and radiation oncology. 2016;60(2):231-8.
63. Mattoli MV, Massaccesi M, Castelluccia A, Scolozzi V, Mantini G, Calcagni ML. The predictive value of (18)F-FDG PET-CT for assessing the clinical outcomes in locally advanced NSCLC patients after a new induction treatment: low-dose fractionated radiotherapy with concurrent chemotherapy. Radiat Oncol. 2017;12(1):4.

9

CHAPTER X

SUMMARY

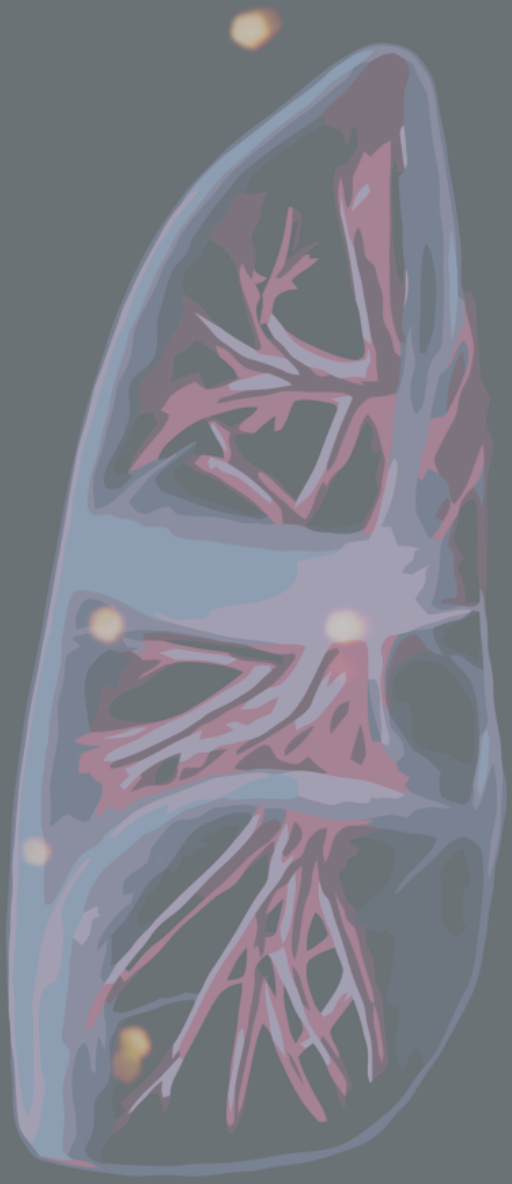

Lung cancer is a common type of cancer and it represents a substantial social and economic burden. Despite intensive efforts for lung cancer screening and follow-up, it is still the leading cause of cancer-related death. With intensive systemic treatment with chemotherapy, overall response rates are far from optimal and patients experience significant treatment-related toxicity. In order to identify non-responders, molecular imaging with ^{18}F-fluoro-deoxy-glucose positron emission tomography/computed tomography (FDG-PET/CT) can be used. In this thesis, the results of FDG-PET/CT for early in-treatment response in non-small cell lung cancer (NSCLC) are described. For delineation of metabolic active tumour, different methods are explored. With modern radiotherapy techniques, it is possible to direct a dose escalation to tumour subvolumes with increased metabolism, without a significant increase in treatment toxicity. Finally, gender-specific and histopathological differences in NSCLC are addressed in a nationwide autopsy study.

Role of FDG-PET/CT in characterisation and staging NSCLC

In **Chapter II** the current role of FDG-PET/CT in NSCLC is discussed. In vivo measurement of glucose metabolism with FDG-PET/CT is currently advised in clinical guidelines for characterisation of malignancy in pulmonary nodules. While in a majority of cases nodules are benign, FDG-PET/CT is useful for intermediate risk lesions as it can help to distinguish between benignity and malignancy with high accuracy. However, in endemic regions with pulmonary infections, the false positive rate with FDG-PET/CT is high. Apart from characterisation, FDG-PET/CT has a prominent role in staging. The introduction of FDG-PET/CT resulted in a significant number of management changes due to the detection of locoregional FDG-avid lymph node metastases and unexpected distant metastases. As a consequence, FDG-PET/CT reduces futile thoracotomies and reduce associated morbidity. For patients with FDG-avid lymphadenopathy, mediastinal staging by means of mediastinoscopy, endobronchial ultrasound-guided transbronchial needle aspiration or endoscopic ultrasound fine needle aspiration, is required. Only in patients with an FDG-avid primary tumour without FDG-avid lymph nodes in hilar or mediastinal lymph nodes, invasive pathologic examination of the mediastinum can be omitted.

FDG-PET/CT response prediction

This thesis focussed on the application of FDG-PET/CT as a predictive biomarker. These markers can be used to define early sensitivity to treatment and response. Treatment-induced changes in FDG-PET/CT early during chemotherapy (after the first treatment course) correlate with patient outcome. **Chapter III** described the clinical outcome in patients treated with concomitant chemo-radiotherapy evaluated with early in-treatment FDG-PET/CT. Twenty-eight patients with locally advanced (stage IIIA-IIIB) non-small cell lung cancer were included. A whole-body FDG-PET/CT was performed and, for response measurements, standardised uptake value (SUV) and total lesion glycolysis (TLG) were determined. Baseline FDG-PET/CT before treatment start and in-treatment FDG-PET/CT was performed. Pre-treatment TLG and a percentage change from baseline for each patient (ΔTLG) and correlated with outcome with a Cox-proportional Hazards analysis. Median cut-off of ΔTLG was a decrease of 45% on the in-treatment scan. These results showed that early in-treatment FDG-PET/CT was predictive of outcome in NSCLC patients treated with concomitant chemoradiotherapy. The volumetric parameter TLG, therefore, seems promising as a predictive and prognostic biomarker. In **Chapter IV** we briefly discuss the predictive value of FDG-PET/CT for neoadjuvant therapy and the importance of early in-treatment assessments. With early in-treatment FDG-PET/CT, image-guided treatment algorithms can be designed, to adjust treatment to the individual patient, minimising treatment toxicity of ineffective treatment and enabling fast switching to effective treatment.

For the definition of early metabolic response, it is important to realise that (apart from biological and patient-related factors) technical factors could have a significant influence on semiquantitative measurement with FDG-PET/CT. Apart from the choice of the semi-quantitative measurement (SUV_{max}, SUV_{peak}, SUV_{mean}, MTV and TLG), the method of delineation of the metabolic active tumour volume has a significant effect on the absolute FDG-uptake measurement and on the percentage change on the in-treatment scan. In **Chapter V** different semi-automatic methods for segmentation of the target lesions (primary tumour and metastatic lymph nodes) on early response FDG-PET/CT were studied. Also, the aggregation process, with or without the inclusion of the metastatic lymph nodes was assessed. Different segmentation methods were used: fixed threshold methods (40- 50% of SUV_{max}), relative threshold methods (signal-to-background method, relative-threshold-method) and adaptive methods (fuzzy locally advanced Bayesian). From a clinical perspective, the differences between segmentation methods were small, however, from a practical point of view the signal-to-background method resulted in more successful (semi)automatic segmentation of the primary tumour and affected lymph nodes. Especially

difficulties on the in-treatment scan emerged due to lymph node segmentation failures for fixed and adaptive delineation methods, due to the low signal-to-background ratio.

FDG-PET/CT and radiotherapy planning

In radiotherapy planning, FDG-PET/CT can assist the radiation oncologist for optimal dose delivery to the tumour, while sparing healthy tissues. FDG-PET/CT improves target accuracy for nodal radiation and has an advantage over CT in borderline sized nodes. For radiotherapy planning, FDG-PET/CT has the potential to allow radiation-dose escalation without increasing the dose to the organs at risk. Specifically, for locally advanced NSCLC the number of patients with local recurrence is significant, despite intensive concurrent treatment. In **Chapter VI** a PET-based planning study was performed in these patients with an early in-treatment metabolic non-response to explore the feasibility of radiation dose escalation and the effect on organs at risk. Ten patients, with a TLG decrease lower than 45% on the in-treatment scan, were selected for this planning study. A stereotactic boost was planned to the most radioresistant subvolumes of the primary tumour, on both pre-treatment FDG-PET/CT and in-treatment evaluation before the second cycle of treatment. A significant dose escalation was achievable while meeting strict dose constraints on organs at risk. In five patients the boost planned tumour volume (PTV_{boost}) was 9-40% smaller compared to the PTV_{boost} based on the pre-treatment FDG-PET/CT.

Response assessment in locally advanced (inoperable) NSCLC and metastatic NSCLC

The majority of patients who present with NSCLC have inoperable stage IIIB and IV disease. While chemotherapy is still the cornerstone of treatment, different targeted treatment strategies have been introduced. For example, vascular endothelial growth factor (VEGF) is an important mediator in tumour angiogenesis, which plays a vital role in cancer cell survival, local tumour growth and the development of distant metastases. In **Chapter VII** patients with newly diagnosed non-squamous NSCLC were treated with first-line chemotherapy (carboplatin and paclitaxel) in combination with bevacizumab, a monoclonal antibody against vascular endothelial growth factor. Twenty-six patients were treated and received a baseline FDG-PET/CT and an in-treatment FDG-PET/CT between 13-20 days, always before the second cycle of treatment. For response criteria, predefined criteria (PERCIST) were used. Early in-treatment FDG-PET was predictive of progression-free survival and overall survival, already after two weeks of therapy.

Distribution of NSCLC metastasis

Chapter VIII demonstrates the results of a nationwide autopsy study in NSCLC, showing different metastatic patterns between the two major histological subtypes, adenocarcinoma (AC) and squamous cell carcinoma (SCC). Patients with AC more frequently developed metastases (50% versus 25% in SCC, $P < 0.001$) and had metastases at multiple sites more often (77% versus 67%, $P = 0.004$). AC showed significantly more metastases in adrenal glands and bone, while SCC showed more kidney metastases. In women with AC, liver and lung metastases are more frequently present, compared to men. As biological differences in lung cancer between men and women are increasingly being recognised, knowledge of these factors is particularly important because of the continuing rise in the incidence of lung cancer in women. Knowledge of the distribution of metastatic patterns based on different prognostic factors could possibly improve the clinical assessment of unclear clinical findings.

Final remarks

The predictive performance of FDG-PET/CT is increasingly being recognised. In the general discussion different methodological considerations are presented for early response measurement. Differences in the quantification methods of metabolic active tumour volume and differences in quantitative parameters in current response monitoring studies are addressed. The primary challenge for early response monitoring is that the proper timing of FDG-PET/CT during treatment is crucial and it should depend on the treatment schedule and regimen. As there are numerous methods for defining metabolic response post-hoc, the use of prospectively defined criteria is of importance to avoid bias in interpretation. Moreover, for clinical implementation, harmonisation of response prediction methods is crucial. With the increasing treatment options, advances in targeted treatment and the promise of personalised treatment, the selection of effective treatment is becoming increasingly important.

SAMENVATTING

In Nederland is longkanker een veel voorkomende vorm van kanker met een incidentie van circa 13.300 in 2018. Hierdoor heeft het een aanzienlijke impact op de zorg en de totale kosten van oncologische zorg. Een groot gedeelte van deze patiënten presenteert zich met lokaal uitgebreide of gemetastaseerde ziekte en dit gaat gepaard met een slechte prognose. Bij lokaal uitgebreide ziekte is met intensieve systemische therapie zoals chemotherapie, al dan niet gecombineerd met radiotherapie, het percentage dat reageert op de behandeling relatief beperkt. Bovendien ervaren patiënten een significante toxiciteit van deze behandelingen. Om patiënten die mogelijk geen baat hebben van de behandeling zo vroeg mogelijk op te sporen, kunnen veranderingen in het glucosemetabolisme worden geanalyseerd middels moleculaire beeldvorming met ^{18}F-fluor-deoxy-glucose positron emissie tomografie/computer tomografie (FDG-PET/CT). In dit proefschrift worden de resultaten van FDG-PET/CT voor vroege response evaluatie bij niet-kleincellig longcarcinoom (NSCLC) beschreven bij stadium III en IV patiënten. Voor de kwantificatie van metabole respons worden verschillende kwantificatie methoden onderzocht. Verder wordt de rol van vroege response evaluatie FDG-PET/CT onderzocht voor beeld gestuurde radiotherapie. Hierbij is het mogelijk om een dosisverhoging te bereiken op therapieresistente gebieden in de tumor met een verhoogd glucosemetabolisme. Deze dosis verhoging is mogelijk, zonder een toename van de radiatie geïnduceerde toxiciteit. Ten slotte worden genderspecifieke en histopathologische verschillen in metastasen bij NSCLC bekeken in een landelijke obductie studie.

De rol van FDG-PET/CT in karakterisatie en stadering van NSCLC

In **Hoofdstuk II** wordt de huidige rol van FDG-PET/CT in NSCLC besproken. FDG-PET/CT speelt een belangrijke rol in het karakteriseren van een pulmonale nodus. Hoewel nodi in de meeste gevallen goedaardig zijn, is FDG-PET/CT nuttig voor aspecifieke laesies, waarbij op basis van FDG-opname een onderscheid is te maken tussen benigniteit en maligniteit, met een hoge nauwkeurigheid. Alleen in endemische regio's met veel longinfecties is het aantal vals-positieve uitslagen van FDG-PET/CT relatief hoog. Naast karakterisering van pulmonale nodi speelt FDG-PET/CT een prominente rol bij de stadiering. Door de introductie van FDG-PET/CT is er een betere detectie (t.o.v. diagnostische contrast CT) van locoregionale lymfekliermetastasen en metastasen op afstand, wat uiteindelijk een significante verandering in de besluitvorming tot gevolg kan hebben voor de patiënt. FDG-PET/CT vermindert het aantal onnodige thoracotomieën en vermindert daarmee ook geassocieerde morbiditeit. Voor patiënten met FDG-avide lymfeklieren wordt mediastinale stadiëring door middel van mediastinoscopie,

endobronchiale ultrasound geleide transbronchiale naaldaspiratie of endoscopische ultrasone fijne naaldaspiratie geadviseerd. Alleen bij patiënten met een FDG-avide primaire tumor zonder FDG-avide lymfeklieren in hilaire of mediastinale lymfeklieren, kan (invasief) pathologisch onderzoek van het mediastinum achterwege worden gelaten.

FDG-PET/CT respons predictie

Dit proefschrift onderzoekt de toepassing van FDG-PET/CT als een predictieve biomarker om vroege respons of non-respons op de behandeling vast te stellen. Vroeg tijdens het behandeltraject (na de eerste behandelingskuur) kan met een FDG-PET/CT de therapie geïnduceerde verandering worden bekeken. Deze metingen worden vervolgens gecorreleerd met de (progressie vrije) overleving van de patiënt. **Hoofdstuk III** beschrijft de klinische uitkomst van patiënten die zijn behandeld met concomitante chemo-radiotherapie. Deze patiënten werden geëvalueerd met een vroege FDG-PET/CT verricht 2 weken na start van de behandeling. Achtentwintig patiënten met lokaal uitgebreid (stadium IIIA-IIIB) niet-kleincellige longcarcinoom werden geïncludeerd. Een FDG-PET/CT van het lichaam werd uitgevoerd voor beoordeling van de respons. Hiervoor werd tijdens de behandeling gestandaardiseerde parameters zoals *standardised uptake value* (SUV) en *total lesion glycolysis* (TLG) gemeten. De FDG-PET/CT vóór aanvang van de behandeling en FDG-PET/CT vroeg in het behandeltraject werden met elkaar gecorreleerd. Baseline TLG en een procentuele verandering ten opzichte van de uitgangswaarde voor elke patiënt (ΔTLG) werd statistisch gecorreleerd aan progressie vrije overleving. De mediane afkapwaarde van ΔTLG was een afname van 45% op de vroege respons FDG-PET/CT. De analyses toonden aan dat vroege FDG-PET/CT-behandeling in de behandeling voorspellend was voor de uitkomst bij NSCLC-patiënten die werden behandeld met concomitante chemoradiotherapie. In dit onderzoek is de parameter TLG zowel een predictieve en prognostische biomarker. In **Hoofdstuk IV** bespreken we de voorspellende waarde van FDG-PET/CT bij neoadjuvante therapie en het belang van vroege evaluaties. Met de vroege FDG-PET/CT-behandeling kunnen beeldgeleide behandelingsalgoritmen worden ontworpen om de behandeling aan de individuele patiënt aan te passen, de behandelingstoxiciteit van niet-effectieve behandeling te minimaliseren en een snelle switch naar een effectieve behandeling mogelijk te maken.

Voor het definiëren van vroege metabole respons is het belangrijk om te realiseren dat naast biologische en patiënt gerelateerde factoren, ook technische factoren een significante invloed kunnen hebben op de semi-kwantitatieve metingen van FDG-PET/CT. Afgezien van de keuze van de semi-kwantitatieve meting (SUV_{max}, SUV_{peak}, SUV_{mean}, MTV en TLG), heeft de methode voor segmentatie van het metabole actieve tumorvolume een significant

effect op de hoogte van gemiddelde SUV (SUV_{mean}). Indirect heeft het ook een effect op de procentuele veranderingen in de parameter die worden berekend tijdens de vroege response evaluatie FDG-PET/CT. In **Hoofdstuk V** werden verschillende semi-automatische segmentatie methoden van de aangedane laesies (primaire tumor en FDG-avide lymfeklieren) op de vroege respons FDG-PET/CT geanalyseerd. Ook werd het aggregatieproces, de berekening met of zonder de inclusie van FDG-avide lymfeklieren, beoordeeld. Verschillende segmentatiemethoden werden gebruikt: vaste drempelwaarden (*fixed threshold* 40-50% SUV_{max}), relatieve drempelwaarden (*signal-to-background*, *relative threshold method*) en adaptieve methoden (*fuzzy locally adaptive Bayesian method*). Vanuit een klinisch perspectief waren de verschillen tussen de segmentatiemethoden klein als het gaat om de exacte verschillen in predictieve waarde, maar vanuit een praktisch oogpunt resulteerde de signaal-tot-achtergrond methode in meer succesvolle (semi)automatische segmentaties van de primaire tumor en de aangedane lymfeklieren. De meeste segmentatie problemen ontstonden als gevolg van segmentatie fouten bij vaste en adaptieve drempelwaarden op de vroege respons evaluatie FDG-PET/CT, vanwege de lage signaal-achtergrond door een lage FDG opname in de primaire tumor en/of aangedane lymfeklieren.

FDG-PET/CT en radiotherapie planning

Bij radiotherapieplanning kan FDG-PET/CT de radiotherapeut ondersteunen om enerzijds een optimale dosisafgifte in de tumor te bereiken en anderzijds zoveel mogelijk toxiciteit te besparen door radiatie op gezonde weefsels zoveel mogelijk te beperken. FDG-PET/CT verbetert de doelnauwkeurigheid voor bestraling van aangedane lymfeklieren en heeft hierdoor een zeker voordeel ten opzichte van CT bij lymfeklieren die niet-pathologisch vergroot zijn. Ten behoeve van de radiotherapieplanning kan FDG-PET/CT worden gebruikt om hoge stralingsdosis mogelijk te maken op actieve gebieden in de tumor, zonder een duidelijke toename te geven in de te verwachten toxiciteit op het aangrenzende gezonde weefsel. Dit is met name van belang voor patiënten met lokaal uitgebreid niet-kleincellig longcarcinoom waarbij het aantal patiënten met uiteindelijk een lokaal recidief significant is, ondanks de introductie van concomitante chemoradiatie. In **Hoofdstuk VI** werd een op FDG-PET/CT gebaseerd planningsonderzoek uitgevoerd bij patiënten die een metabole non-respons vertoonden op de vroege FDG-PET/CT. Het doel van deze studie was om de haalbaarheid van dosisescalatie en het effect hiervan op toxiciteit te onderzoeken. Tien patiënten, met een TLG-daling minder dan 45% op de vroege evaluatie scan, werden geselecteerd voor deze planningsstudie. Er werd een stereotactische boost gepland op de meest radioresistente subvolumes van de primaire tumor (de meest FDG-avide gebieden in de primaire tumor), voor zowel de baseline FDG-PET/CT als de evaluatie FDG-PET/CT welke werd verricht vóór de tweede

behandelingscyclus. Een aanzienlijke dosisverhoging was haalbaar, terwijl tegelijkertijd ook aan strikte dosisbeperkingen voor het gezonde weefsel en organen werden voldaan. Bij vijf patiënten was het boost-geplande tumorvolume (PTV_{boost}) 9-40% kleiner in vergelijking met de PTV_{boost} op basis van de FDG-PET/CT-behandeling vóór de behandeling.

Response beoordeling bij lokaal uitgebreid (inoperabel) NSCLC en gemetastaseerd NSCLC

De meerderheid van de patiënten met NSCLC presenteert zich met inoperabele ziekte (stadium IIIB) of gemetastaseerde ziekte (stadium IV). Chemotherapie speelt nog steeds een belangrijke rol in de behandeling, ook na introductie van verschillende doelgerichte behandelingsstrategieën. Vasculaire endotheliale groeifactor (VEGF) is bijvoorbeeld een belangrijke mediator bij tumorangiogenese, en speelt een vitale rol de bij overleving van kankercellen, lokale tumorgroei en de ontwikkeling van metastasen op afstand. In **Hoofdstuk VII** worden patiënten met een nieuw gediagnosticeerd niet-squameuze NSCLC behandeld met eerstelijns chemotherapie (carboplatin en paclitaxel) in combinatie met bevacizumab, een monoklonaal antilichaam tegen vasculaire endotheliale groeifactor. Zesentwintig patiënten werden behandeld in deze studie. Ze ondergingen een baseline FDG-PET/CT en een vroege respons evaluatie FDG-PET/CT na 13 tot 20 dagen, voorafgaand aan de tweede behandelingscyclus. Voor het beoordelen van metabole respons werden vooraf gedefinieerde PET-criteria (PERCIST) gebruikt. In deze studie werd aangetoond dat FDG-PET/CT voorspellend was voor progressievrije overleving en totale overleving, al zeer vroeg tijdens de behandeling.

Patroon van metastasen bij NSCLC

Hoofdstuk VIII toonde de resultaten van een landelijke obductiestudie bij NSCLC, waarbij verschillende patronen van metastasen tussen de twee belangrijkste histologische subtypes, adenocarcinoom (AC) en plaveiselcelcarcinoom (SCC) werden onderzocht. Patiënten met AC ontwikkelden vaker metastasen (50% versus 25% in SCC, $P < 0.001$) en hadden vaker metastasen op meerdere plaatsen (77% versus 67%, $P = 0.004$). AC vertoonde significant meer metastasen in de bijnieren en bot, terwijl SCC meer nier-metastasen liet zien. Bij vrouwen met AC kwamen lever- en longmetastasen vaker voor dan mannen. Aangezien de biologische verschillen bij longkanker tussen mannen en vrouwen in toenemende mate worden erkend, is kennis van deze factoren belangrijk. Dit geldt des te meer gezien de stijging in het aantal gevallen van longkanker bij vrouwen. Kennis van de verdeling van metastase patronen op basis van verschillende prognostische factoren zou de klinische beoordeling van onduidelijke bevindingen kunnen verbeteren.

Slotopmerkingen

De predictieve waarde van FDG-PET/CT wordt steeds meer erkend. In de discussie in dit proefschrift worden verschillende methodologische overwegingen genoemd bij vroege respons evaluatie met FDG-PET/CT. Verschillen in de kwantificatie van metabole actieve tumorvolumes, de definitie van het metabool actieve tumorvolume en de verschillen in kwantitatieve parameters bij respons evaluatie worden behandeld. Een belangrijke uitdaging bij vroege respons evaluatie is dat de juiste timing van FDG-PET/CT tijdens de behandeling cruciaal is en dat de timing mede afhankelijk is van het gekozen behandelingsschema. Omdat er verscheidene methoden zijn om een metabole respons te definiëren, is het gebruik van gevalideerde metabole respons criteria van belang om bias in de interpretatie en de resultaten te voorkomen. Bovendien is voor de klinische implementatie een standaardisering van metabole respons methoden essentieel. Met de toenemende behandelingsopties, de vooruitgang in doelgerichte behandeling en de komst van therapie op maat, is een goede en nauwkeurige selectie van effectieve behandelingen in toenemende mate belangrijk. Het uiteindelijke doel is het verbeteren van de overleving en de kwaliteit van leven.

APPENDICES

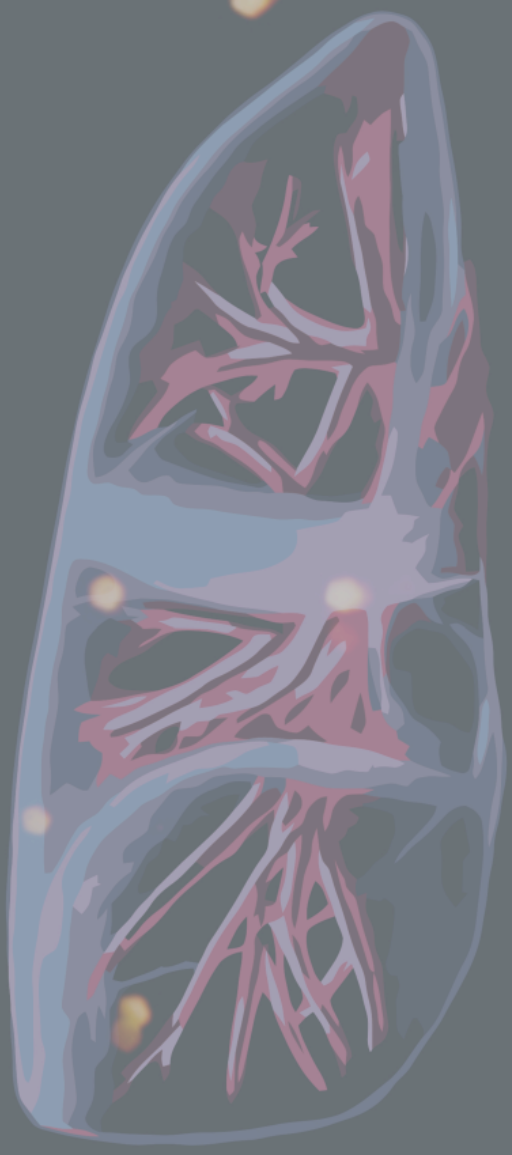

A

List of abbreviations

AC	adenocarcinoma
AS-NSCLC	advanced stage non-small cell lung cancer
ASCO	American Society of Clinical Oncology
AUC	area under the curve
BE	bevacizumab erlotinib
BED	biologically effective dose
BSA	body surface area (m^2)
BTV	biological target volume
CE	chemotherapy regimen consisting of cisplatin and etoposide
CI	confidence interval
CMR	complete metabolic response
CPB	carboplatin paclitaxel and bevacizumab
CP	carboplatin paclitaxel
CR	complete response
CRT	chemo-radiotherapy
CT	computed tomography
CTV	clinical target volume
CTx	chemotherapy
D_{max}	maximum dose within the planned target volume
EANM	European Association of Nuclear Medicine
EARL	EANM Research Limited
EBUS	endobronchial ultrasound
EGFR	epidermal growth factor receptor
EORTC	European Organization for Research and Treatment of Cancer
EQD_2	equivalent dose in 2 Gy fractions
ERM	early in-treatment response monitoring
ESMO	European Society for Medical Oncology
EUS	esophageal ultrasound
FAZA	^{18}F-fluoro-azomycin-arabinoside
FDG	^{18}F-fluoro-deoxy-glucose
FLAB	fuzzy locally adaptive Bayesian method
FLT	^{18}F-fluoro-thymidine
FMISO	^{18}F-fluoro-misonidazole
FWHM	full width at half maximum
GLUT	glucose-transporter
GTV	gross tumour volume
Gy	Gray
HR	hazard ratio
IGART	image guided adaptive radiotherapy
IMRT	intensity modulated radiotherapy treatment

IRB	institutional review board
IRW	Inveon Research Workplace
JI	Jaccard Index
k	Cohen k coefficient for agreement
LBM	lean body mass
LRFS	local recurrence free survival
MTV	metabolic tumour volume (cm^3)
MRI	magnetic resonance imaging
NE	not evaluable (response)
NSCLC	non-small cell lung cancer
OAR	organs at risk
ORG	optimally respiratory gating
OS	overall survival
OSEM	ordered subsets expectation maximization
OTT	overall treatment time
P	level of significance
PALGA	Pathologisch-Anatomisch Landelijk Geautomatiseerd Archief (Dutch pathology registry)
PD	progressive disease
PERCIST	PET response criteria in solid tumours
PET	positron emission computed tomography
PFS	progression-free survival
PMD	progressive metabolic disease
PMR	partial metabolic response
PR	partial response
PRV	planning organ at risk volumes
PTV	planned target volume
PVE	partial volume effect
ϱ	Spearman's non parametric rank correlation coefficient
R	Pearson
RCT	randomised controlled trail
RECIST	response evaluation criteria in solid tumours
ROC	receiver operating characteristic
ROI	region of interest
RT	radiotherapy
RTL	relative threshold level
RTOG	Radiation Therapy Oncology Group
SBR	signal to background ratio
SBRT	stereotactic body radiation therapy
SCC	squamous cell carcinoma
SD	stable disease
SIB	simultaneously integrated boost
SMD	stable metabolic disease

SPN	solitary pulmonary nodule
SPSS	statistical package for the social sciences
SUL	standardised uptake value corrected for lean body mass
SUL_{peak}	maximum average standardised uptake value corrected for lean body mass within a 1-cm^3 spherical volume
SUV	standardised uptake value (g . cm^{-3})
SUV_{peak}	maximum average standardised uptake value within a 1-cm^3 spherical volume
SUV_{max}	maximum voxel based on standardised uptake value
T40	segmentation theshold 40% of maximum standardised uptake value
T50	segmentation theshold 50% of maximum standardised uptake value
TBNA	transbronchial needle aspiration
TKI	tyrosine kinase inhibitor
TLG	total lesion glycolysis
ΔTLG	relative change in total lesion glycolysis (%)
TLG_{LN}	total lesion glycolysis of affected lymph nodes
TLG_S	summed total lesion glycolysis of both primary tumour and affected lymph nodes
TLG_T	total lesion glycolysis of primary tumour only
ToF	time-of-flight
TPI	total proliferation index
UICC	Union for International Cancer Control
VDT	volume doubling time
VEGF	vascular endothelial growth factor
VMAT	volumetric modulated arc therapy
VOI	volume of interest

ACKNOWLEGMENTS | DANKWOORD

Het onderzoek en dit proefschrift zouden niet tot stand zijn gekomen zonder de waardevolle bijdrage van velen. Allereerst wil ik alle patiënten bedanken, die ondanks hun ziekte, de toewijding hebben getoond om te participeren aan de klinische studies en kostbare tijd hebben vrijgemaakt om de medische wetenschap vooruit te helpen.
Enkele personen in het bijzonder wil ik nog graag bedanken voor hun bijdrage aan dit proefschrift.

Prof. dr. Lioe-Fee de Geus-Oei, beste Lioe-Fee, veel dank voor deze opportuniteit die ik van je heb gekregen. Naast vakinhoudelijke kennis van de nucleaire geneeskunde heb ik ook het doen van klinisch onderzoek van je aangeleerd. Ik waardeer het laagdrempelige overleg en je organisatie. Ondanks je drukke banen wist je wel altijd tijd vrij te maken voor begeleiding en sturing. Je was kritisch, rechtvaardig en complimenteus. Dank dat je altijd vertrouwen hebt uitgesproken, ook op momenten dat ik het misschien wat minder zag zitten. Promoveren was gelukkig veel meer dan het verdwaald raken in het bos van de wetenschap. Gelukkig kon ik door jou, Lioe-Fee, de weg altijd weer terugvinden.

Prof. dr. Johan Bussink, beste Jan. Je vurige passie voor wetenschap en tegelijkertijd de rust en het geduld wat je altijd uitstraalt zijn bewonderenswaardig. Fijn dat ik mocht meewerken aan een prachtig project voor m'n onderzoeksstage. Toen ik nog als coassistent een kijkje in de keuken mocht nemen op de afdeling Radiotherapie was ik dan ook meteen verkocht. Dank voor je vertrouwen en veel dank voor de prettige begeleiding en je immer kritische, maar ook zeer pragmatische aanpak.

Prof. dr. Wim Oyen, beste Wim. Je was altijd zeer betrokken als promotor. Ondanks dat we elkaar niet heel veel zagen, mede gezien je eerdere werkzaamheden in Londen, was het contact altijd zeer prettig en laagdrempelig. Het mailcontact was altijd snel en je antwoord zeer doelgericht. Je commentaar was altijd zeer waardevol en je besluiten doortastend. Verder wil ik nog veel bewondering uiten voor al je toonaangevende wetenschappelijke werk.

Dr. Eric Visser, dank voor al je uitleg en je geduld. Dank voor je wetenschappelijke inzichten en je altijd kritische blik op het schrijven. Ik kan mij nog het eerste moment herinneren dat wij elkaar spraken over segmentatie methoden, niet zozeer inhoudelijk (want daar begreep ik op dat moment eerlijk gezegd nog niet zoveel van!) maar wel je aanstekelijke passie voor de fysica en dat was zeer inspirerend.

Dr. Willem Grootjans, beste Willem, dank voor de prettige samenwerking tijdens ons onderzoek. Je manifesteerde je daadwerkelijk als de brug tussen de nucleaire geneeskunde

en de klinische fysica. Alle kostbare tijd en de noeste arbeid van het segmenteren (achter het IRW-station) …. Gedeelde smart is halve smart!

Dat moleculaire beeldvorming verder gaat dan alleen de afdeling Nucleaire geneeskunde, blijkt ook uit alle andere afdelingen die betrokken zijn geweest bij het huidige werk. Daarom wil ik ook alle betrokkenen vanuit de Radiologie, Longgeneeskunde, Radiotherapie en Pathologie bedanken voor de prettige samenwerking.

Prof. dr. Hans Kaanders, prof. dr. Esther Troost, dr. Tineke van der Zon-Meijer, dr. Robin Wijsman. Het is prachtig om te zien hoe de radiotherapie een sterke relatie heeft opgebouwd met de nucleaire geneeskunde. Jullie omarmen moleculaire beeldvorming om o.a. biologische mechanismen van radioresistentie te onderzoeken. Bedankt voor de prettige samenwerking! Dr. P. Span, beste Paul, dank dat je als vraagbaak wilde fungeren voor m'n statistiek. Altijd zeer behulpzaam was je als ik weer eens was verdwaald in de wondere wereld van SPSS.

Dr. Liesbeth P. Peters-Bax, beste Liesbeth, veel dank voor je begeleiding bij de respons beoordelingen op de CT-scans.

Dr. Olga Schuurbiers, beste Olga, dank voor je begeleiding tijdens de vroege fase van het student zijn en je input tijdens de onderzoeksstage die uiteindelijk hebben geleid tot m'n allereerste publicatie.

Dr. Miep van der Drift, dr. Erik H.F.M. van der Heijden, dr. Anja Timmer-Bonte, veel dank voor jullie tijd en inzet bij onder andere de inclusie van alle patiënten en het beoordelen van de manuscripten.

Prof. dr. Iris Nagtegaal, dank voor alle input bij de obductie studie.

Voor zover nog niet genoemd, wil ik alle overige co-auteurs van bedanken voor alle gedachtewisselingen, correcties, ideeën en input.

De leden van de manuscriptcommissie, prof. dr. C.M.L van Herpen, prof. dr. M. van der Heijden en prof dr. E.F.I. Comans, wil ik bedanken voor het beoordelen van dit proefschrift.

Opleiding en wetenschap gingen in de praktijk hand in hand. Aan alle stafleden van de Nucleaire geneeskunde, Marcel, Martin, Anne, James, Maartje, Fred, wil ik veel dank uitspreken voor alle begeleiding tijdens de opleiding. Prof. dr. M. Gotthardt, beste Martin, veel klinische vaardigheden heb ik van je aangeleerd, waarvoor dank, maar bovenal ook dank dat je mij hebt gered in Winterberg. Dr. M.J.R. Janssen, beste Marcel, zonder jou was ik wellicht niet eens zover gekomen. Het combineren van een opleiding en een promotie traject is niet altijd even makkelijk geweest. Onze gesprekken en je geduld hebben mij uiteindelijk ook geholpen om te komen op een plek waar ik nu sta in het leven en daarvoor ben ik je nog altijd dankbaar.

Verder wil ik ook alle laboranten van de nucleaire geneeskunde bedanken, Michel, Martin, Bernadette, Jurrian, Marie-Claire, Eddy, Marjo, Marga, Merijn (mogelijk ben ik nog een aantal anderen vergeten, bij deze excuus!), veel dank voor jullie ondersteuning en onuitputtelijke inzet op de nucleaire geneeskunde! De oud-AIOS, Christel, Sabine, Tom, Linda, Willemijn, Erik. In ons hart blijven wij altijd "Nijmegen". Dank voor de gezellige tijd op de werkvloer en daarbuiten.

Ook wil ik mijn huidige collegae, de afdeling Nucleaire geneeskunde te Dordrecht, de maten, Shiuw en Boudewijn bedanken. Dank voor jullie begrip en de steun die ik kreeg om onder andere ook deze laatste horde te nemen.

De familie, broers, aanhang, schoonfamilie, dank voor jullie oprechte interesse. Pa en ma, veel dank voor jullie onuitputtelijke steun, bemoedigende woorden en vertrouwen. Jullie hebben altijd klaargestaan en mij ook altijd op persoonlijk vlak bijgestaan.

Michael, brother for life. Weinig woorden zijn nodig. Patrick van de Camp, altijd oog voor detail en bovendien sparringpartner op het digitale slagveld. Dank dat jullie mijn paranimfen wilden zijn.

Lieve Ellen, de allerliefste, dit proefschrift zou niet compleet zijn zonder een ode aan jou. Behind every man's success is a woman. Jij zorgde voor de stabiele basis en gaf mij de ruimte en de tijd om aan dit proefschrift te werken. Jij stimuleerde en ondersteunde mij. Dank voor je geduld, je wijze raad, liefde en aandacht. Met dit proefschrift wordt een drukke periode afgesloten. Op ons volgende project samen!

Curriculum vitae

Edwin Usmanij werd op 29 juni 1988 geboren in Tiel, Gelderland. Hij groeide op in Oosterhout, Noord-Brabant. In 2006 behaalde hij zijn diploma aan het Sint-Oelbert gymnasium te Oosterhout, waarna hij geneeskunde ging studeren in Nijmegen. In 2012 rondde hij geneeskunde af met een wetenschappelijke stage op de afdeling Radiotherapie en Nucleaire geneeskunde van het Radboudumc Nijmegen. In 2013 startte hij met de opleiding nucleaire geneeskunde, eveneens aan het Radboudumc (opleiders prof. dr. W.J.G. Oyen en prof. dr. L.F. de Geus-Oei en later dr. M.J.R. Janssen). Het begin van de opleiding tot specialist werd gecombineerd met een promotieonderzoek wat heeft geleid tot dit proefschrift. Het promotieonderzoek naar vroege respons evaluatie met ^{18}F-fluorodeoxyglucose positron emissie tomografie (FDG-PET/CT) bij niet-kleincellig longcarcinoom werd verricht onder begeleiding van prof. dr. L.F. de Geus-Oei, prof. dr. J. Bussink en prof. dr. W.J.G. Oyen.

Na de opleiding te hebben afgerond is hij sinds februari 2018 werkzaam als nucleair geneeskundige in het Albert Schweitzer Ziekenhuis te Dordrecht.

PhD Portfolio E.A. Usmanij

Institute for Health Sciences
Radboudumc

PhD student: E.A. Usmanij **Department**: Radiation Oncology, Radiology and Nuclear Medicine Graduate school: Radboud Institute for Health Sciences	**PhD period**: 10-7-2012 until 31-12-2018 **Promotors**: prof. dr. L.F. de Geus-Oei, prof. dr. J. Bussink, prof. dr. W.J.G. Oyen

TRAINING ACTIVITIES	Year(s)	ECTS
a) Courses & Workshops		
- Coordinating radiation protection expert (formerly level 3), Radboud University	2016	20
b) Seminars & Lectures		
- * Dutch Society of Nuclear Medicine (NVNG), Scientific Symposium, Nijmegen, The Netherlands	2012	0.3
- * Landelijk platform voor Radiotherapie, Annual Meeting, Heelsum, The Netherlands	2014	0.3
- * Dutch Society of Nuclear Medicine (NVNG), Scientific Symposium, Amersfoort, The Netherlands	2016	0.3
c) International Symposia & Congresses		
- * Annual Congress of the European Association of Nuclear Medicine, Lyon, France.	2013	1.0
- * Annual Congress of the Society of Nuclear Medicine, San Diego, United States of America.	2016	1.0
- # Annual Congress of the European Association of Nuclear Medicine, Dusseldorf, Germany.	2016	1.0
- Annual Congress of the European Association of Nuclear Medicine, Vienna, Germany	2017	1.0
d) Other		
- Scientific meeting of the NVNG	2012-2019	2x year, 0.3

Oral (*) and poster presentations (#) are indicated with a * and # before the name of the activity, respectively.

Research Data Management

The research described in this thesis, based on the results of human studies, have been carried out in accordance with the national applicable rules concerning the review of research ethics committees and informed consent, in accordance with the principles of the Declaration of Helsinki by the World Medical Association of June 1964. The medical and ethical review board has given approval to the human studies in Chapter III, V, VII and VIII. All data retrieved have been collected and processed fully anonymised. The patient data for the analyses of these studies are stored in the Radiology and Nuclear Medicine trail bureau. Published data generated or analysed in this thesis are part of published articles and its additional files are available from the associated corresponding authors on reasonable request. Further use of these patient data in future research is only possible after a renewed permission by the patient as recorded in the informed consent.

The FAIR principles in research data management

A guideline to provide machine-readable data to allow for easy sharing of research data has recently been proposed as the FAIR-principles (1). These principles are guidelines to enable and improve Findability, Accessibility, Interoperability and Reuse of research data. The research data retrieved and stored in this thesis are not adapted to these proposed guidelines, since all data collection has been performed and stored before the FAIR guidelines were published. The anonymised study databases have been transferred to the research group for possible future research projects.

Reference

1. Wilkinson MD, Dumontier M, Aalbersberg IJ, et al. The FAIR Guiding Principles for scientific data management and stewardship. Scientific Data 2016; 2:160018.

LIST OF PUBLICATIONS

Publications included in this thesis are marked by an asterisk (*)

* **Usmanij EA**, de Geus-Oei LF, Troost EG, Peters-Bax L, van der Heijden EH, Kaanders JH, Oyen WJ, Schuurbiers OC, Bussink J. FDG-PET Early Response Evaluation of Locally Advanced Non-Small Cell Lung Cancer treated with Concomitant Chemo-Radiotherapy. *J Nucl Med. 2013 Sep;54(9):1528-34*

* **Usmanij EA**, Bussink J, de Geus-Oei LF. Lung cancer - Metabolic activity measured by FDG PET predicts pathological response in locally advanced superior sulcus NSCLC. *Lung Cancer. 2014 Dec;86(3):374*

Heijmen L, **Usmanij EA**, Brouwer C, Bulten BF, Janssen MJR. 131-Iodine uptake in metastatic gallbladder cancer. *Tijdschr Nucl Geneeskd, 2014; 36(3):1282- 4*

* **Usmanij EA**, de Geus-Oei LF, Bussink J, Oyen WJ. Update on FDG-PET/CT in Non-Small Cell Lung Cancer *Curr Opin Pulm Med. 2015 Jul;21(4):314-21*

* Grootjans W**, **Usmanij EA****, Oyen WJ, van der Heijden EH, Visser EP, Visvikis D, Hatt M, Bussink J, de Geus-Oei LF. Performance of automatic image segmentation algorithms for calculating total lesion glycolysis for early response monitoring in non-small cell lung cancer patients during concomitant chemoradiotherapy. *Radiother Oncol. 2016 Jun;119(3):473-9*

* **Usmanij EA**, Natroshvili T, Timmer-Bonte JNH, Oyen WJG, van der Drift MA, Bussink J, Geus-Oei LF. The predictive value of early in-treatment FDG-PET/CT response to chemotherapy in combination with bevacizumab in advanced non-squamous non-small cell lung cancer. *J Nucl Med 2017 Aug;58(8):1243-1248.*

van de Luitgaarden ACM, **Usmanij EA**, de Geus-Oei LF, de Rooy JWJ, Flucke UE, Kaal SEJ, Soomers VLMN, van Riel CAHP, Schreuder HWB, Oyen WJG. Interval from fist symptoms to diagnosis in high-grade primary osteosarcoma and Ewing sarcoma of bone in relation to metabolic activity on FDG-PET/CT. *(submitted)*

Usmanij EA, Meiss L, Senden PJ, de Klerk JMH. Myocardial ischaemia due to subclavian stenosis after coronary artery bypass graft: a case report, *Eur Heart J Case Rep. 2018;Jun 2;2(2)*

* Meijer TWH, Wijsman R, **Usmanij EA**, Schuurbiers OC, van Kollenburg P, Bouwmans L, Bussink J, de Geus-Oei LF. Stereotactic radiotherapy boost after definite chemoradiation for non-responding locally advanced NSCLC based on early response monitoring ^{18}F-FDG-PET/CT. *Phys Imag in Radiat Oncol 2018; Jul(7):16-22*

** equal authorship contribution